

Lateral Interactions and Receptive Field  
Structure of Lobula Plate Tangential Cells in  
the Blowfly

**Dissertation**

Zur Erlangung des Doktorgrades  
der Naturwissenschaften (Dr.rer.nat.)  
der Fakultät für Biologie  
der Ludwig-Maximilians-Universität München

Angefertigt am Max-Planck-Institut für Neurobiologie,  
Abteilung 'Neuronale Informationsverarbeitung'

Vorgelegt von  
Karl Farrow

München 2005

Hiermit erkläre ich, daß ich die vorliegende Dissertation selbständig und ohne unerlaubte Hilfe angefertigt habe. Sämtliche Experimente wurden von mir selbst durchgeführt, außer wenn explizit auf Dritte verwiesen wird. Ich habe weder anderweitig versucht, eine Dissertation oder Teile einer Dissertation einzureichen bzw. einer Prüfungskommission vorzulegen, noch eine Doktorprüfung durchzuführen.

München, den

1<sup>st</sup> Gutachter: Dr. Alexander Borst

2<sup>nd</sup> Gutachter: Dr. Tobias Bonhoeffer

Tag der mündlichen Prüfung 07.06.2005

# Table of Contents

---

<b>Table of Contents</b> .....	<b>i</b>
Figures and Tables.....	iii
Abbreviations.....	v
<b>Abstract</b> .....	<b>1</b>
<b>1 Introduction</b> .....	<b>4</b>
Orientation Behavior in the Fly.....	6
Mechanisms of Direction Selectivity .....	6
Anatomy of the Fly Visual System.....	10
Lobula Plate Tangential Cells .....	15
Complex Receptive Fields.....	20
Lobula Plate Circuitry .....	21
Goals .....	26
<b>2 Methods</b> .....	<b>27</b>
Preparation .....	27
Visual Stimulation.....	29
Electrical Recording.....	31
Laser Ablations .....	31



## Table of Contents

Data Analysis .....	32
Network Modeling .....	34
<b>3 Results .....</b>	<b>38</b>
Ablation Assessment.....	39
Input Circuitry to the HS- and CH-cells.....	41
Rotational Flow-Field Selectivity .....	45
Basis of the Broad Receptive Fields of VS-cells .....	60
Vertical-Horizontal Interaction.....	71
<b>4 Discussion .....</b>	<b>76</b>
Laser Ablation Technique.....	76
Building Receptive Fields .....	79
Input Structure to HS- and CH-Cells.....	80
Flow-Field Selectivity of H1- and H2-cells.....	83
Basis of the Broad Receptive Fields of VS-cells .....	86
Vertical-Horizontal Interactions .....	91
Summary .....	93
<b>5 References .....</b>	<b>95</b>
<b>Thanks &amp; Acknowledgements.....</b>	<b>104</b>
<b>Curriculum Vitae.....</b>	<b>105</b>



## Table of Contents

---

### Figures and Tables

#### Introduction

<b>Figure 1.1:</b>	Optic Flow and Flow-Fields	5
<b>Figure 1.2:</b>	Motion Detector	8
<b>Figure 1.3</b>	Retina and the Origins of Retinotopy	11
<b>Figure 1.4</b>	Pathways from the Retina to the Lobula Plate	13
<b>Figure 1.5</b>	Retinotopy in the Fly Visual System	14
<b>Figure 1.6</b>	Lobula Plate Tangential Cells	17
<b>Figure 1.7</b>	Response Properties of LPTCs	18
<b>Figure 1.8</b>	Complex Receptive Fields	19
<b>Figure 1.9</b>	Bilateral Horizontal Interactions	22
<b>Figure 1.10</b>	VS-Cell Network	23
<b>Figure 1.11</b>	Horizontal-Vertical Interactions	25

#### Methods

<b>Figure 2.1</b>	Visual Stimulus Setup	28
<b>Figure 2.2</b>	Creating a Peristimulus Histogram	33
<b>Table 2.1</b>	Compartmental Model Hodgkin-Huxley Parameters	36
<b>Table 2.2</b>	Compartmental Model Synaptic Weight Table	37

#### Results

<b>Figure 3.1</b>	Ablation Assessment	39
<b>Figure 3.2</b>	Firing Rate Control	40
<b>Figure 3.3</b>	Possible Input Circuitry to HS- and CH-cells	41
<b>Figure 3.4</b>	Response Similarities Between HS- and CH-cells	42
<b>Figure 3.5</b>	HS-cell Ablations	43
<b>Figure 3.6</b>	CH-cell Ablations	44
<b>Figure 3.7</b>	Contrast Dependent Flow-Field Selectivity	46



## Table of Contents

<b>Figure 3.8</b>	H1 Flow-Field Selectivity to White Noise Stimulus	47
<b>Figure 3.9</b>	Single HS- and CH-Cell Ablations	48
<b>Figure 3.10</b>	Double CH-Cell Ablations	50
<b>Figure 3.11</b>	Analytical Lobula Plate	51
<b>Figure 3.12</b>	Current Flow Rectification Between CH- and H1-cells	53
<b>Figure 3.13</b>	Signals Driving H2-cell Flow-Filed Selectivity	54
<b>Figure 3.14</b>	Model Network Response to Rotation	55
<b>Figure 3.15</b>	Model Network Response to Translation	56
<b>Figure 3.16</b>	Model Network Response to Ipsilateral Motion	57
<b>Figure 3.17</b>	Flow-Field Selectivity of Model H1 - and H2-Cells	58
<b>Figure 3.18</b>	Current Injections into Model CH-cell	59
<b>Figure 3.19</b>	Neural Identification	61
<b>Figure 3.20</b>	VS-cell Network and Receptive Fields	62
<b>Figure 3.21</b>	Proximal Cell Ablations	63
<b>Figure 3.22</b>	VS4-cell's Deficit after the Ablation of Frontal Viewing VS-cells	65
<b>Figure 3.23</b>	Distal Ablation	66
<b>Figure 3.24</b>	Summary of Ablations	67
<b>Figure 3.25</b>	VS1- and Medial VS-Cell Receptive Fields	68
<b>Figure 3.26</b>	VS1-Cell Ablations	69
<b>Figure 3.27</b>	Horizontal vs Vertical Response of H1- and H2-cells	72
<b>Figure 3.28</b>	Receptive Fields of H1 and the Frontally Viewing VS-Cells	73
<b>Figure 3.29</b>	Horizontal Vertical Interactions	74
<b>Figure 3.30</b>	VS1-cell Ablations	75

### Discussion

<b>Figure 4.1</b>	Schematic Diagram of Input-Output Pathways of HS- and CH-cells	80
<b>Figure 4.2</b>	Alternative Connectivity among the Horizontal Sensitive Cells	85



## Table of Contents

---

### Abbreviations

2-DG	2-Deoxy-Glucose	IDL	Interactive Data Language
A	Amperes	IPSP	Inhibitory Post Synaptic Potential
dCH	Dorsal Centrifugal Horizontal	KAc	Potassium Acetate
DS	Direction Selective	LPTC	Lobula Plate Tangential Cell
EPSP	Excitatory Post Synaptic Potential	ND	Null Direction
FD	Figure Detection	<i>ora</i>	Outer Rhabdomeres Absent
g	Conductance	PD	Preferred Direction
GABA	$\gamma$ -amino butyric acid	pH	Potential of Hydrogen
GUI	Graphic User Interface	PSTH	Peristimulus Histogram
H1	Horizontal One	<i>sev</i>	Sevenless
H2	Horizontal Two	V	Volts
HSE	Horizontal System Equatorial	vCH	Ventral Centrifugal Horizontal
HSN	Horizontal System Northern	V1	Vertical One
HSS	Horizontal System Southern	VS	Vertical Systems
Hu	Horizontal Unidentified	W	Watts
I	Current	$\Omega$	Ohms







## Abstract

---

As a fly flies around in the world the visual scene moves constantly across its eyes. Depending on its path, this elicits a particular large-field motion pattern called 'flow field'. Since the flow-fields are characteristic for particular flight trajectories they can be used to guide behavior, in particular to control the course of the fly. In the blowfly, these visual motion cues are mediated by a set of 60 motion-sensitive neurons called lobula plate tangential cells (LPTCs). The directionally selective response of the LPTCs has been ascribed to the integration of local motion information across their extensive dendritic trees. As the lobula plate is organized retinotopically the receptive fields of the tangential cells ought to be determined by their dendritic architecture. This appears not always to be the case. Recent experiments have revealed many lateral connections among tangential cells that appear to mediate their often complex receptive fields. Here single cells were ablated in order to determine which lateral connections are functionally important. I found that the ablation of a single cell, or class of cells revealed that the lateral connections among LPTCs can be the source of their local motion input, or augment the feedforward input from local motion elements through either dendro-dendritic and axonal-axonal connections. Other connections between LPTCs were found to have no discernable functional significance and suggest that the lobula plate circuitry is yet to be fully revealed. The specific projects are outlined below.

### Input Circuitry to the HS- and CH-cells

A single class of the lobula plate tangential cells the CH (centrifugal horizontal) neurons, play an important role in two pathways: figure-ground discrimination and flow-field selectivity. As was recently found, the dendrites of CH-cells are electrically coupled to the dendritic tree of another class of neurons sensitive to horizontal image motion, the



## Abstract

horizontal system cells (HS). However, whether motion information arrives independently at both of these cells or is passed from one to the other is not known. Here I examine the ipsilateral input circuitry to HS and CH neurons by selective laser ablation of individual interneurons. I find that the response of CH neurons to motion presented in front of the ipsilateral eye is entirely abolished after the ablation of HS-cells. In contrast the motion response of HS-cells persists after the ablation of CH-cells. I conclude that HS-cells receive direct motion input from local motion elements, whereas CH-cells do not; their motion response is driven by HS-cells. This connection scheme is discussed with reference as to how the dendritic networks involved in figure-ground detection and flow-field selectivity might operate.

### Rotational Flow-Field Selectivity

The group of neurons that processes horizontal motion forms a symmetric bilateral network that is able to combine information about motion presented in front of both eyes. Here I consider a group of 16 neurons whose connections have been explicitly identified. Each of these neurons has a large dendritic tree receiving information about ipsilateral local motion events that is spatially pooled to produce a directionally selective response. In addition, some of the lobula plate neurons are also sensitive to motion cues in front of the other eye. This information is carried by the spiking neurons H1, H2 and Hu that send their axons to the other side of the brain, where the H1- and H2-cells synapse onto 2 of the 3 HS-cells, and all three contralaterally projecting cell provide input to both CH-cells. The CH-cells are known to provide inhibitory input to the H1- and H2-cells. These network interactions appear to amplify the response to rotational stimuli and reduce the response to translation. I ablate either single HS-cells or both CH-cells in order to break the path whereby information about the opposite eye reaches the H1- and H2-cell. I did not find that these ablations affected the flow-field selectivity of either H1- and H2-cells. Network modeling showed that although the described circuitry does support rotational flow-field selectivity for the HS- and CH-cells, the model H2-cell does not show the expected flow-field selectivity. This suggests that the circuitry or cellular mechanisms underlying the response properties of the H2-cell are not completely understood.

### Basis of the Broad Receptive Field of VS-cells

As the lobula plate is organized retinotopically the receptive fields of the tangential cells



## Abstract

ought to be determined by their dendritic architecture. This appears not always to be the case. One compelling example is the exceptionally wide receptive fields of the vertical system (VS) tangential cells. Using dual intracellular recordings Haag and Borst (2004) found VS-cells to be mutually coupled in such a way that each VS-cell is connected exclusively to its immediate neighbours. This coupling may form the basis of the broad receptive fields of VS-cells. Here I tested this hypothesis directly by photo-ablating individual VS-cells. The receptive field width of VS-cells indeed narrowed after the ablation of single VS-cells, specifically depending on whether the receptive field of the ablated cell was more frontal or more posterior to the recorded cell. In particular, the responses changed as if the neuron lost access to visual information from the ablated neuron and those VS-cells more distal than it from the recorded neuron. These experiments provide compelling evidence that the lateral connections amongst VS-cells are a crucial component in the mechanism underlying their complex receptive fields, augmenting the direct columnar input to their dendrites.

### Vertical-Horizontal Interactions

Two heterolaterally spiking cells, the H1- and H2-cells have been shown to be sensitive to vertical motion presented in the frontal portion of their receptive fields. Receptive field measurements performed here show that the H1-, VS1- and VS2-cells all respond to vertical downward motion across an almost completely overlapping portion of the frontal visual field. Using dual intracellular recordings Haag and Borst (2003) demonstrated that the VS1-cell but not the VS2-cell supplies input to both these cells. Through current injections into different compartments of the VS1-and VS2-cells I have provided physiological evidence that the output of VS1-cell near its dendritic arbors is the likely site of its input to the H1-cell. This coupling may form the basis of the vertical sensitivity of the H1- and H2-cell. I tested this hypothesis directly by recording the sensitivity of the H1-cell to horizontal and vertical motion in the frontal visual field both before and after the ablation of single VS1-cells. After the ablation of the VS1-cell the response of the H1-cell to vertical motion disappeared but its response to horizontal motion remained robust. These experiments demonstrate that the VS1-cell provides the input to the H1-cell that makes it sensitive to vertical motion in the frontal visual field likely through connections in their dendritic trees.



## 1 Introduction

---

The ability of animals to navigate in the world relies heavily on the processing of visual information. Whenever an animal moves through its environment or an object moves past it the visual system is challenged with motion. By examining large sections of the changing retinal image it is possible to make good estimates of ones self motion in comparison to both the landscape and moving objects of interest (Fig 1.1). Two fantastic examples that highlight the speed and sophistication of visually guided behavior in insects involve pursuit maneuvers. First, when in pursuit of flying conspecifics, it takes as little as 30 ms for a fly to execute a corrective turn once its target has changed course (Collett and Land, 1975), and second, dragonflies actively use motion camouflage to disguise themselves during aerial pursuit (Mizutani et al., 2003). The optic flow information needed to execute these behaviors is not explicitly represented in the two-dimensional brightness patterns of the retinal image. This information needs to be computed from the temporal brightness changes in the retina. This raises an interesting question for visual neuroscientists: how is the brain organized to analyze visual patterns and extract the relevant motion information that is used to guide behavior?

In flies, the processing of large field motion starts in the retina. From here the time varying brightness patterns, detected by the array of photoreceptors, are passed through 3 retinotopically arranged neuropile layers, including the lamina, medulla and the lobula complex. In these layers information about motion is extracted (Buchner et al., 1984; Strausfeld, 1984; Bausenwein and Fischbach, 1992). In a subdivision of the lobula complex, the lobula plate, there exist a set of large field motion sensitive cells that are only a few synapses away from both the retina and the muscles responsible for head and body movements. These cells, the lobula plate tangential cells (LPTCs), are ideally placed to guide behavior.



## Introduction

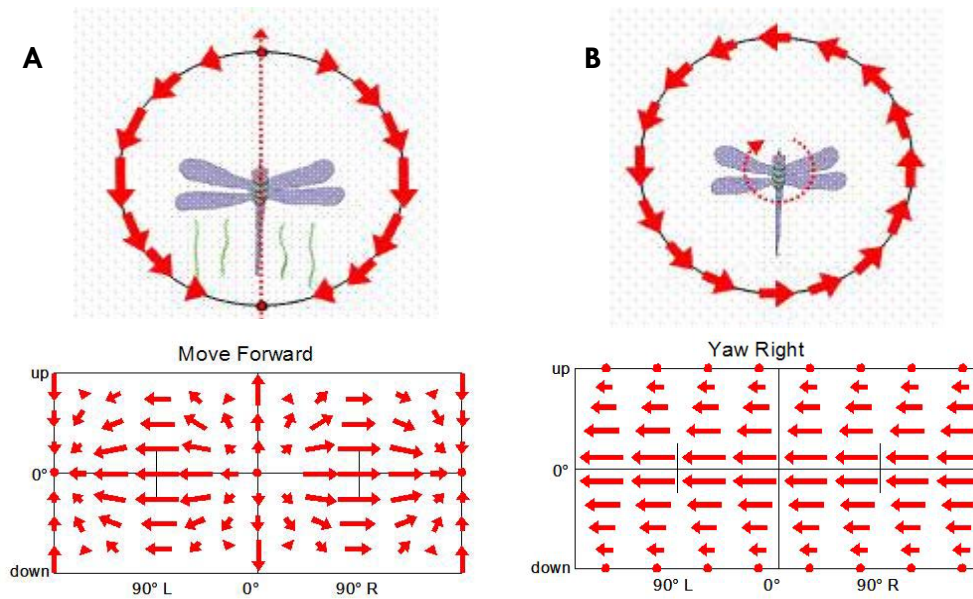


**Figure 1.1: Optic Flow and Flow Fields.** The top row shows the view from above as an insect moves forward (A) or turns to the right (B). The bottom row is from the point of view of the insect, with the 360 degree field of view flattened onto the page. **A)** Insect traveling forward. The optic flow travels from the forward to backward direction, and is generally faster on the left and right than in the front or back. The optic flow diverges in the frontal visual field and contracts in the rear **B)** Insect rotating to the right. Here the optic flow is to the left in all directions and at every point in the visual world. If the insect were flying a curved path, the optic flow patterns would be a combination of these two patterns. Figure adapted from [www.centeye.com](http://www.centeye.com).

In general, LPTCs are sensitive to visual motion in a direction selective (DS) way. They are excited by motion in one direction, their preferred direction (PD), and inhibited by motion in the opposite direction, their null direction (ND). Based on a combination of ablation experiments (Heisenberg et al., 1978; Geiger and Nüssel, 1981; Geiger and Nüssel, 1982; Hausen and Wehrhahn, 1983; Hausen and Wehrhahn, 1990), as well as the similarities between the LPTCs response properties and various types of motion-driven response behavior of flies (Borst and Bahde, 1988; Borst, 1991) it has been concluded that LPTCs are involved in the fly's visual course control. Here I investigate what role the lateral connections among LPTCs have in shaping their receptive field structures to extract relevant optic flow information.

Below I will first describe the most basic computation necessary to start extracting direction selective motion information from the brightness patterns on the retina. This discussion will describe some of the behavioral, neurophysiological and theoretical experiments that have been performed to determine the form this computation likely takes. Second, I will describe



## Introduction

the basic anatomy of the fly visual system with particular focus on the lobula plate and its tangential cells. Finally, I will describe the connections among the lobula plate tangential cells and the complex receptive fields that they putatively mediate.

---

### Orientation Behavior in the Fly

Generally, during locomotion ones visual system is subjected to continuous changes of the retinal images termed 'optic flow'. In order to get an initial understanding of how flies respond to different optic flow patterns behavioral experiments have concentrated on compensatory optomotor behavior in response to the movement of large vertically or horizontally striped backgrounds. When the background is oscillated during tethered flight, where the fly cannot actually move, the fly attempts to turn, both its body and head, in order to follow the background (Fermi and Reichardt, 1963; Götz, 1964; Reichardt, 1969; Poggio and Reichardt, 1976; Reichardt and Poggio, 1976; Hengstenberg, 1984; Hengstenberg et al., 1986; Egelhaaf and Borst, 1993). During free flight these movements would act to reduce retinal slip and serve to help the fly maintain a straight course by compensating for undesired deviations: a gust of wind that causes the fly to veer to the left would create a rightward image motion in the eyes and cause the insect to generate a compensatory turn to the right. Investigations of this optomotor response have unveiled some of the characteristics of motion perception by the fly's visual system (Reichardt, 1969).

---

### Mechanisms of Direction Selectivity

The most significant aspect of the optomotor response and its mediating cells, the LPTCs, is their directionally selective response to visual motion. In contrast the initial sensory cells, the photoreceptors, respond to a moving grating with modulations in accordance with the number of stripes passing by per second. It is only when a minimum of two photoreceptor signals, displaced along the path of image motion are considered that the direction of motion be derived. The most successful theories developed to account for motion selectivity are based on a delay and compare principal that was first proposed by Exner (1894). A formal algorithm to compute the direction of motion from time varying brightness patterns



## Introduction

was developed after observing the optomotor behavior in the *Chlorophanus* beetle by Reichardt and Hassenstein (Reichardt, 1961). This model has become known as the correlation type motion detector (Reichardt, 1961; Reichardt, 1987; for review see: Borst and Egelhaaf, 1993; Clifford and Ibbotson, 2003).

### Theory

The Reichardt motion detector model consists of two arms that perform two essential operations, including:

1. Asymmetric temporal filtering that acts to delay the signal in one arm as compared to the other.
2. A non-linear interaction where a low-pass filtered (delayed) signal is multiplied with a high-pass filtered (non-delayed) from a neighbouring image location.

The difference between the output signals of both subunits results in the final detector response. It is the combination of a temporal delay and a multiplication allows this type of detector to measure the degree of coincidence between its input channels. This process is on average a spatio-temporal crosscorrelation.

Generally, when a pattern passes the detector from left to right, bright features in the pattern activate the left input channel before the right input channel (Fig 1.2). The time interval between activation depends both on the velocity of the object and the distance between the two inputs. If one delays the left input signal correctly, then both signals will arrive simultaneously at the multiplication stage of the left subunit, resulting in a large response (Fig 1.2D). For the right subunit, the asymmetric temporal filtering increases the time-shift between the input signals, leading to a smaller detector response (Fig 1.2D). After subtracting the output signals of both subunits, the final output response is obtained. In the example shown here pattern motion from left to right is called the PD of the motion detector, while motion in the opposite direction will result in a sign-inverted response. This is called the ND of the detector.



## Introduction

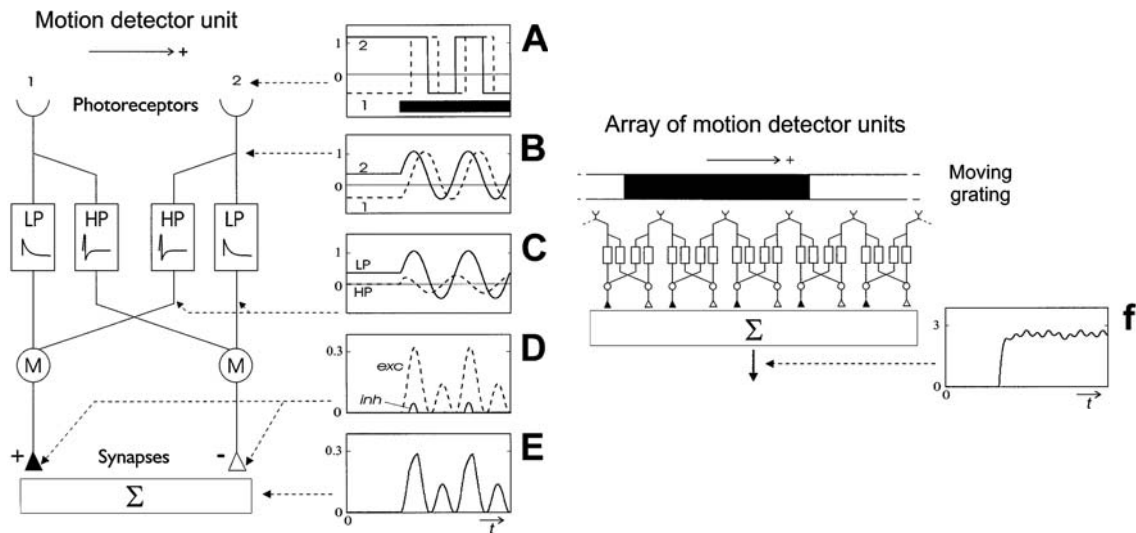


**Figure 1.2: Motion Detector. Left Side.** Elaborated version of the correlation-type motion detector with its component responses (A–E) to a square wave grating that moves with a constant velocity in the PD. The time of stimulation is indicated by the solid bar in A. Note that M is the nonlinear combination, multiplying the delayed/low-pass filtered signal from the high-pass/instantaneous signal from neighbouring photoreceptors. **Right Side.** An array of detectors is used to simulate the neural layers between the photoreceptors and tangential cells. The amplitude of the summed responses of all synapses reflects the pattern velocity (f). Adapted from Haag et al. (1999).

## Experimental Evidence

There are key 2 characteristics of an animal or cell that produce its directionally selective response by integrating input from an array of correlation type motion detectors that include:

1. The mean response amplitude should depend on the structure of the pattern. For a moving grating pattern the response will depend on the spatial wavelength, its contrast and overall brightness. In particular, the velocity leading to a maximum response should increase with the spatial wavelength of the pattern, such that the ratio of the spatial wavelength and velocity are constant, i.e. at the same temporal frequency.
2. The structure of the pattern should be visible in the response if there is insufficient integration across the spatial pattern. For a moving grating oscillation should be apparent, where the modulation frequency is equal to the temporal frequency of





## Introduction

the stimulus.

The predicted pattern dependant changes in the optimal velocity have been recorded not only in LPTCs but also in the optomotor behavior of flies. Optomotor behavior has been shown to follow a temporal frequency, i.e. the velocity (deg/s) divided by the spatial frequency (deg), tuning rather than the pure velocity of the pattern (Fermi and Reichardt, 1963; Götz, 1964; Buchner, 1976). To summarize, when a fly is placed in a large drum covered with vertical stripes the strength of the optomotor response has been found to vary on a variety of stimulus parameters. If the angular period of the stripes is kept constant and the rotational speed of the drum is varied, the strength of the optomotor behavior varies in a bell-shaped curve with a velocity peak. If the angular period is double and the rotational speed of drum again varied one finds again the bell shaped response, except now the peak response occurs at a velocity twice as high. The optomotor response of flies is actually tuned to the temporal frequency of the stimulus. Analogous results have been observed for the mediating interneurons in the lobula plate (Haag et al., 2004).

In addition, optical and electrophysiological recordings from LPTCs have confirmed that during motion stimulus there are indeed oscillations in the neural response reflecting the spatial structure of the stimulus pattern. These oscillations are visible only when a neuron has insufficiently large stimulus to allow spatial integration across many local motion inputs to cancel them out, or if one specifically looks at the consequence of the local motion input in a cell's dendrites. Indeed, oscillations in the membrane potential of HS-cells (Egelhaaf and Borst, 1989) have been noted that depend on the temporal frequency of the stimulus when presented through a thin slit. Also, calcium concentration oscillations have been seen in the dendrites of LPTCs, before spatial integration takes place (Single and Borst, 1998; Haag et al., 2004). These oscillations increase with the contrast level and do not disappear as the light intensity increases (Haag et al., 2004).

Further evidence for the correlation-type of motion detector also comes from apparent motion experiments where, instead of actually moving a grating pattern, local luminance was changed in a stepwise manner in neighbouring areas of the H1-cell's receptive field. These studies used sophisticated optics to sequentially stimulate single ommatidia (Schuling et al., 1989) or even single photoreceptors within an ommatidium (Riehle and Franceschini,



## Introduction

1984; Franceschini et al., 1989). These studies revealed that successive stimulation of photoreceptors R1 and R6 within one ommatidium is sufficient to elicit directionally selective responses in H1 (Riehle and Franceschini, 1984; Franceschini et al., 1989). In addition, interactions between ommatidia separated by up to eight times the inter-ommatidial angle were shown to contribute to the response of the neuron (Schuling et al., 1989; Egelhaaf and Borst, 1992).

It has also been demonstrated that when an LPTC is presented with a random velocity distribution with a mean of zero it alters the input-output relationship to maximize information transfer based on the width of the distribution (Brenner et al., 2000; Fairhall et al., 2001; Borst, 2003b). This property has been demonstrated to be inherent in the structure of the correlation type motion detector (Borst et al., in press).

How the motion detector is implemented is currently an intense focus of research. However, it is thought that there exist at least four separate units at each point in the visual world with four distinctly orientated preferred directions: up, down, right and left. Each LPTC is thought to receive input from two such units, with opposite preferred directions, one provided by excitatory the other by inhibitory input, at each point in the retinotopic map on to their dendrites. It has been shown that by integrating across a large number of these units many of the response properties of LPTCs and visually guided behavior can be explained (Fig 1.2). Below the circuitry of the visual system of the fly is described focusing on pathways that have been shown to be activated during motion stimulation and thus are likely involved in motion detection.

---

## Anatomy of the Fly Visual System

The first stage of visual processing starts with the sensation of brightness by light sensitive cells in the eye. In flies, this structure is built from an array of facets or ommatidia. Each ommatidium possesses its own lens and set of photoreceptors. The photoreceptors send their axons to a set of brain structures, the 'visual ganglia', devoted exclusively to image processing. These visual ganglia are organized into columns that retinotopically represent positions in the world. This means that in each neural layer the neighborhood relationships between image points are conserved. The different neuropile are called the lamina,



## Introduction

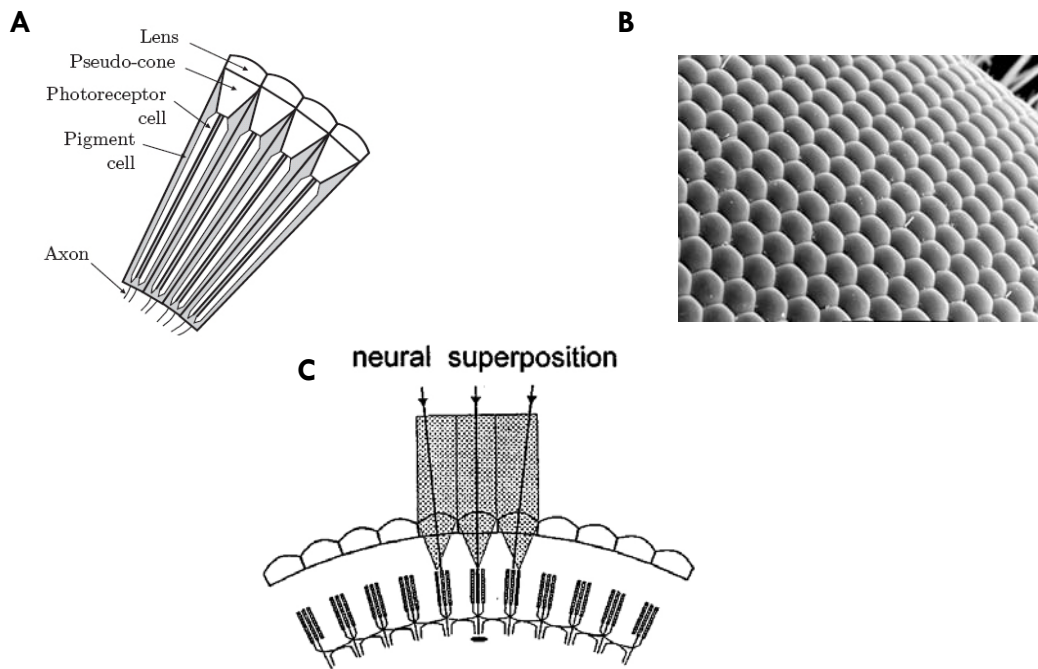


**Figure 1.3: Retina and the Origins of Retinotopy.** **A.** A schematic of the fly retina illustrates the basic structure of the light capturing device of a fly. **B.** An electron micrograph of the faceted eye of a blowfly at a magnification of  $\sim 375$ . **C.** Schematic of how light from different facets is combined in single columns of neurons in the fly. Figure A adapted from Hardie (1984). Figure B from [www.bath.ac.uk/ceos/Insects1](http://www.bath.ac.uk/ceos/Insects1). Figure C adapted from Land (1997).

medulla and lobula complex. The latter can be divided into the lobula and the lobula plate. Each column of these layers is formed by a group of stereotyped set of neurons that are repeated throughout the layer. These columnar elements have been anatomically described in *Calliphora*, *Musca* and *Drosophila*.

### The Retina

The initial sensation of the visual world is by light sensitive cells. In blowflies the eye is constructed from a vast array of  $\sim 5000$  hexagonal ommatidia (Hardie, 1984). The spatial resolution of light detected by the retina is about 100 times poorer than ours. This is because the resolution of each lens is limited by diffraction to  $\sim 1^\circ$  (Land and Eckert, 1985; For review see: Land, 1997). In addition visual acuity is not uniform across the whole retina. In the female blowfly *Calliphora* the spatial resolution is about twice as high in the frontal visual field as in the lateral part (Petrowitz et al., 2000). The orientation of



## Introduction

the ommatidial rows along the eye lattice varies in a characteristic that has been suggested to be an adaptation for efficient evaluation of optic flow induced by self-motion (Land, 1997; Petrowitz et al., 2000).

Each ommatidium is a functional unit consisting of an inert cornea and a pseudocone that together makes up the lens that focuses light onto a group of eight photoreceptors, R1-R8 (Fig 1.3). The photoreceptors R1-R6 are arranged around the outside of the ommatidia, while R7 and R8 lay centrally one above the other. The output of photoreceptors R1-6 project to the lamina, while photoreceptor cells R7 and R8 project to the medulla (layers M6 and M3 respectively). After precisely measuring the receptive fields of individual rhabdomeres (Kirschfeld, 1967) and anatomical mapping of retinula cell axons (Braitenberg, 1967) it was realized that the projection of photoreceptors R1-R6 to the lamina is such that 6 photoreceptors from neighbouring ommatidia that view the same point in space converge onto a single column in the lamina (Fig 1.3c) (For review see: Hardie, 1984). This maximizes photon capture and improves signal-to-noise ratio (Kirschfeld, 1967; for review see: Laughlin, 1981). In order to achieve this projection pattern the photoreceptor axons have to twist  $180^\circ$ , which exactly counteracts the image inversion produced by the facet lens.

Evidence suggesting that it is the information passed on by R1-R6 that is important for motion detection has come from the *Drosophila* mutants *sev* (sevenless) and *ora* (outer rhabdomere absent) (Harris et al., 1976; Heisenberg and Buchner, 1977). They report that the *Drosophila* mutant *sev*, which has its R7 destroyed, exhibits qualitatively normal behavior during optomotor behavior (Heisenberg and Buchner, 1977). On the other hand, in the *ora* mutant, which has R1-R6 destroyed, the optomotor behavior is severely affected (Heisenberg and Buchner, 1977). Hence, it has been presumed that circuitry involved in motion detection starts with light detection by R1-R6.



## Introduction

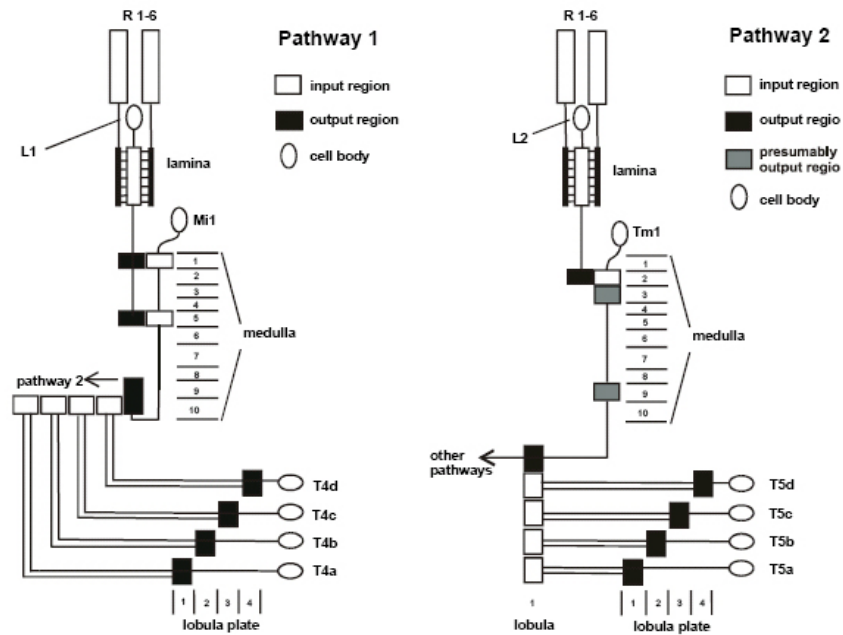


**Figure 1.4: Pathways from the Retina to the Lobula Plate.** Two different pathways leading from photoreceptors R1-6 to the lobula plate tangential cells. Both pathways pass through the lamina and medulla. Pathway one finishes with projection directly from layer 10 of the medulla to the lobula plate. Pathway 2 continues to layer 1 of the lobula and then projects to the lobula plate. Figure modified from Bausenwein et al. (1992).

### The Lamina

This neuropile is very regularly structured. For each point in the visual world there is one column comprising of 5 laminar monopolar cells (L1-L5). Each column is encapsulated by glia cells and hence each group has been termed a 'cartridge'. Each optic cartridge receives one input from single R1, R2, R3, R4, R5 and R6 photoreceptors that view the same point in the visual world but arrive from neighbouring ommatidia. Photoreceptors R1-R6 make synaptic contact with laminar monopolar cells (L1 and L2).

The lamina monopolar cells (L1/L2-type) have been shown to amplify signals arriving from photoreceptors, have narrow dynamic ranges at single mean intensity levels that shift quickly according to the mean luminance and, in general act as high pass filters that extract information about contrast (Laughlin, 1981). The receptive fields of laminar monopolar cells have been shown to have single narrow peaked receptive fields like those of the photoreceptors (Järvilehto and Zettler, 1973; Dubs, 1982). The L1 and L2 monopolar cells project to different layers within the medulla. The L1-cell projects to both



## Introduction

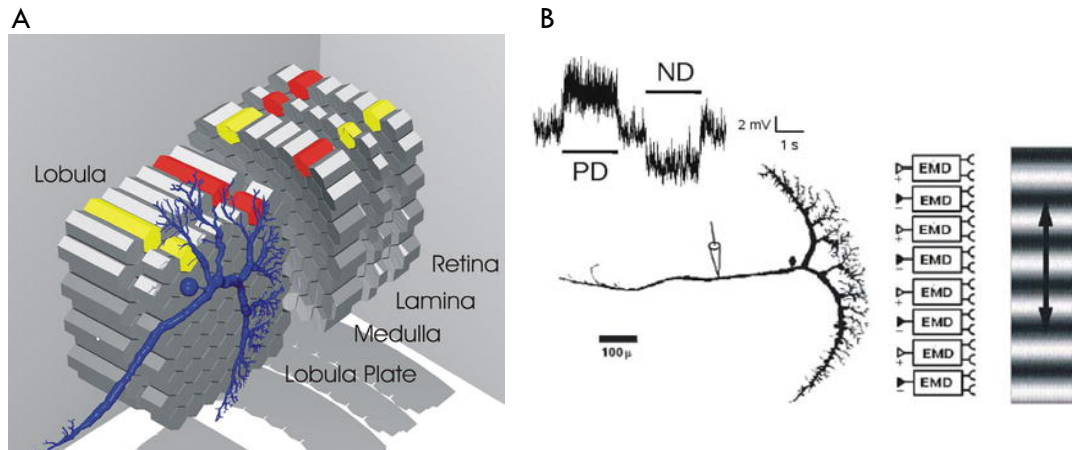


**Figure 1.5: Retinotopy in the Fly Visual System.** Schematic of the retinotopic pathway from the retina, through the optic lobes to a tangential cell in the lobula plate. **A)** Visual information from the eyes is processed in three successive layers called the lamina, the medulla, and the lobula complex, the latter being divided into an anterior lobula and a posterior lobula plate. Each layer is divided into a series of columns. The columns in each layer can be seen to represent the facets of the retina in a one-to-one fashion leading to a retinotopic projection of the visual scene onto the dendrites of an LPTC. **B)** In the lobula plate, large tangential cells spatially integrate the output of local motion-sensitive elements and produce an increase in activity for PD motion and decrease in activity to ND motion. Here the graded membrane potential of a VS3-cell is shown. Figure A courtesy of Cuntz and Borst. Figure B adapted from Single et al. (1997).

layer M1 and M5 of the medulla, while the L2-cell project to layer M2 (Bausenwein et al., 1992). The L1- and L2-cells are the beginning of two separate motion sensitive pathways that provide input to the lobula plate (fig 1.4).

### The Medulla

The medulla surrounds the lobula complex and can be divided into 10 layers. In the medulla the motion sensitive pathways are continued. Using the 2-Deoxy-Glucose (2-DG) method it has been shown that specific layers are labeled during motion stimulation (Bausenwein et al., 1992; Bausenwein and Fischbach, 1992). Generally, the pathways carrying motion information can be divided in two: one initiated by input from L1-cells and the other by L2-cells. The input to the medulla from L1 monopolar cells synapses on the intrinsic medulla neurons Mi1, in layer M1 and M5, which in turn synapse on medullary output T4-cells in layer M10 that project directly to the lobula plate. The second important pathway passing through the medulla arrives in layer M2 from L2-cells. Here, the L2-cells connect to the trans-medulla Tm1-cell that connects to the most posterior stratum of the lobula.



## Introduction

### The Lobula

Like the medulla the lobula is made up of many layers, in this case 6 (Fischbach and Dittrich, 1989). During motion stimulus 3 layers within the lobula are labeled using the 2-DG method (Buchner et al., 1984). The most posterior layer is where trans-medulla (Tm1) cells terminate. This layer also contains the T5-cell arborizations. T5-cells come in four flavours depending to which layer of the lobula plate they project (Fischbach and Dittrich, 1989). The layer where they terminate corresponds to the four preferred direction of motion of the lobula plate tangential cells.

### The Lobula Plate

The lobula plate can be divided, in addition to the retinotopic organization present throughout the visual ganglia, by the preferred direction of motion of its composite cells. Using the 2-DG method four separate layers can be distinguished depending on the direction of motion presented to the fly (Buchner et al., 1984; Bausenwein et al., 1992; Bausenwein and Fischbach, 1992). This has also been seen using a combined electrophysiological and light microscope investigation (Hausen, unpublished). These layers correspond to horizontal motion (anterior two strata) and vertical motion (posterior two strata). Anatomical investigations have revealed that the neurons that putatively supply input to the LPTCs, the T4- and T5-cells also terminate in each of the four strata of the lobula plate (Strausfeld and Lee, 1991). Additionally, the LPTCs extend their dendrites to the four different strata of the lobula plate according to their preferred direction (Hausen et al., 1980; Eckert, 1982; Hausen, 1982; Hengstenberg et al., 1982; Hausen, 1984; Krapp et al., 1998).

---

### Lobula Plate Tangential Cells

The lobula plate contains approximately 60 tangential cells that extend their dendrites across many columns. Generally, LPTCs can be grouped according to their response characteristics and anatomy. Each class of cells has a specific combination of the following characteristics:

1. Preferred orientation: whether they respond primarily to horizontal or vertical



## Introduction

image motion.

2. Prevalent electrical response mode: whether they respond to image motion with a graded shift of membrane potential, a change in firing rate or a mixture of both (Fig 1.7).
3. Projection area: whether the neurons send their axons to the contralateral brain hemisphere (heterolateral LPTCs), the ipsilateral side (ipsilateral LPTCs), or both.
4. Spatial integration properties: whether their response increases with visual pattern size, or whether they are tuned to small moving patterns.

When the LPTCs are grouped according to preferred orientation one can find two groups: horizontally and vertically sensitive cells. These two groups can be further divided.

### Horizontal System (HS) Cells

In each lobula plate there are three horizontal system (HS) cells (Hausen, 1982), the northern (HSN), equatorial (HSE) and southern (HSS) cells. These three cells view the upper, middle and lower parts of the visual field respectively. The dendritic tree of each cell covers approximately 1/3 of the lobula plate, such that the HSN covers the dorsal third, the HSE the middle third and the HSS the ventral third (Fig 1.6). Each HS-cell responds to front-to-back motion in front of the ipsilateral eye with a graded depolarization in membrane potential decorated with high frequency events called spikelets. Additionally, back-to-front motion presented in front of the contralateral eye causes an increase in the EPSP activity recorded in the HSN- and HSE-cells but not the HSS-cell. During spatially restricted motion stimulation presented in front of the ipsilateral eye local calcium accumulation occurs in their dendritic trees (Borst and Egelhaaf, 1992; Egelhaaf et al., 1993; Dürr and Egelhaaf, 1999; Haag and Borst, 2002).





## Introduction

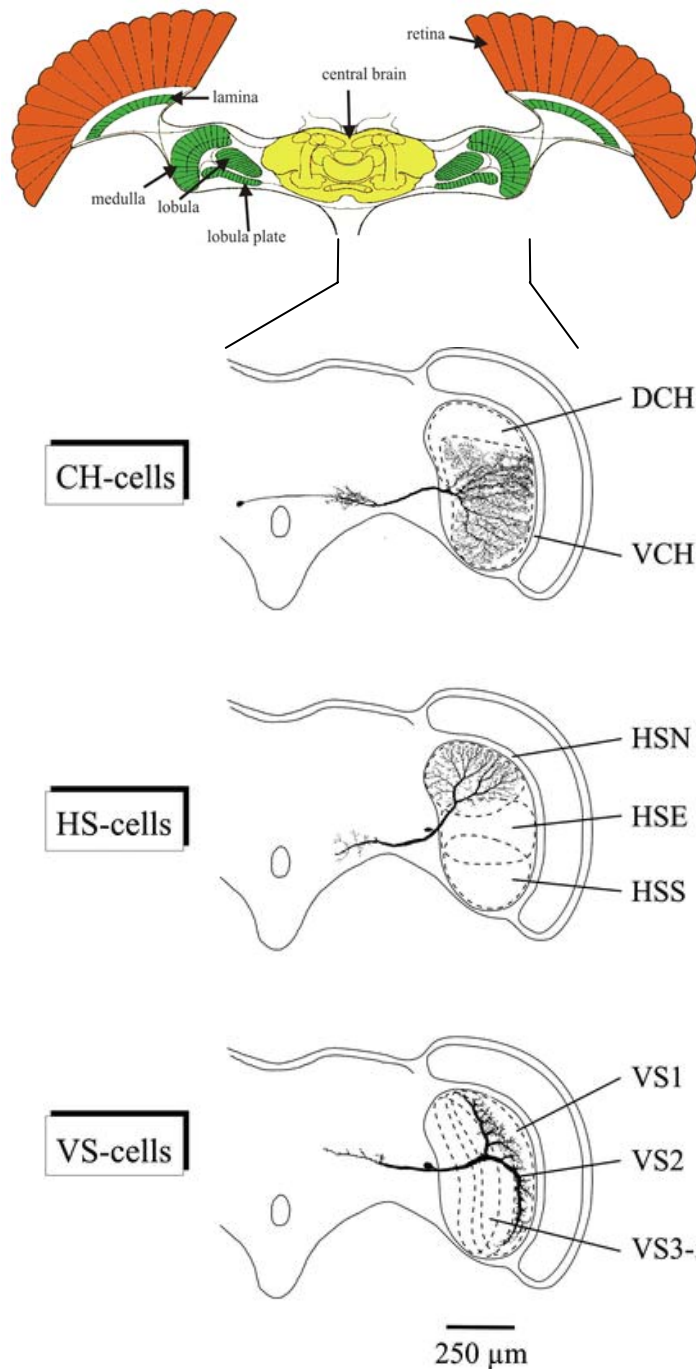


**Figure 1.6: Lobula Plate Tangential Cells.** Top. Schematic outline of a horizontal section through the fly's head highlighting the visual ganglia.

Below. Enlarged frontal view of fly brain highlighting the position of different LPTCs within the lobula plate. The dotted lines indicate the dendritic extent of the different LPTCs. Figure adapted from Borst and Haag (1996).

### Centrifugal Horizontal (CH) Cells

The lobula plate contains two CH-cells per hemisphere. The dorsal (dCH) and ventral (vCH) cells have large arborizations covering the dorsal and ventral halves of the lobula plate respectively. Consequently the dCH-cell views the upper visual field while the vCH-cell views the lower visual field. These cells are so named as it has been demonstrated that they have input synapses at what would normally be thought of as their axon terminal and



## Introduction

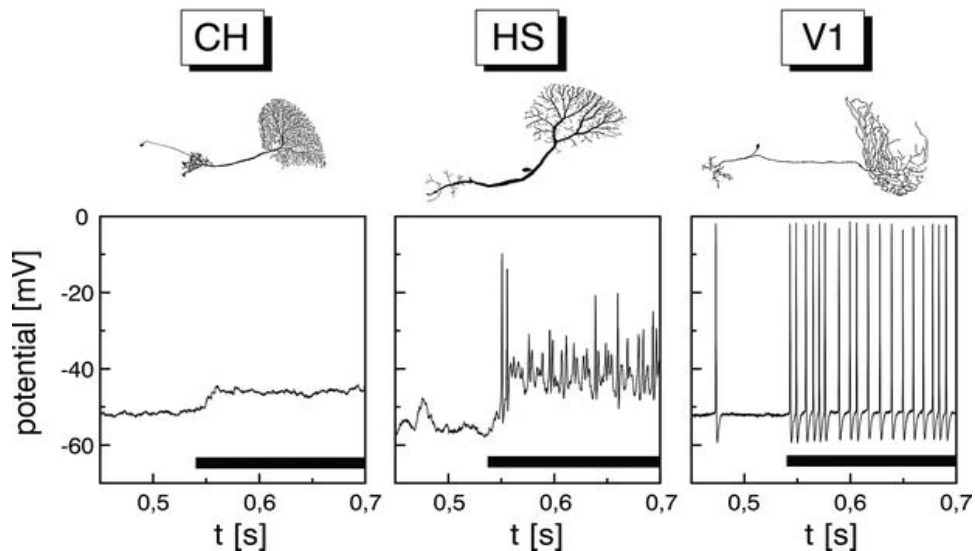


**Figure 1.7: Response Properties of LPTCs.** LPTCs respond to motion stimuli presented in the ipsilateral visual field in three distinct modes: pure graded depolarization (CH-cells), a mixed depolarization superimposed with spikelets (HS- and VS-cells) or with an increase in spiking frequency (V1-, H1-, H2- and the FD-cells). Figure adapted from Borst and Haag (2003).

both input and output synapses in their extensive 'dendritic' trees (Gauck et al., 1997). CH-cells are selectively activated by front-to-back motion presented in front of the ipsilateral eye that elicits a graded depolarization of the membrane potential. Like the HS-cells, back-to-front motion presented in front of the contralateral eye causes an increase in the EPSP activity. Also, during spatially restricted motion stimulation presented in front of the ipsilateral eye local calcium accumulation occurs in the dendritic trees of CH-cells (Borst and Egelhaaf, 1992; Egelhaaf et al., 1993; Dürr and Egelhaaf, 1999; Haag and Borst, 2002) that covers a larger extent of its dendritic tree than in the HS-cell (Haag and Borst, 2002).

### Vertical System (VS) Cells

There are at least 10 VS-cells in each lobula plate (Hengstenberg et al., 1982; Krapp et al., 1998), but an eleventh may exist medial to the VS10-cell (Hengstenberg et al., 1982). Each VS-cell is characterized by its bifurcating axon resulting in a dorsal and ventral main dendrite. They all respond maximally to downward motion, presented at a particular frontal-posterior position, with a graded depolarization of the membrane potential (Hengstenberg, 1982; Haag et al., 1997; Krapp et al., 1998). Generally, the more medial a cell's dendritic tree, the more posterior the slice of the visual world it views. From



## Introduction

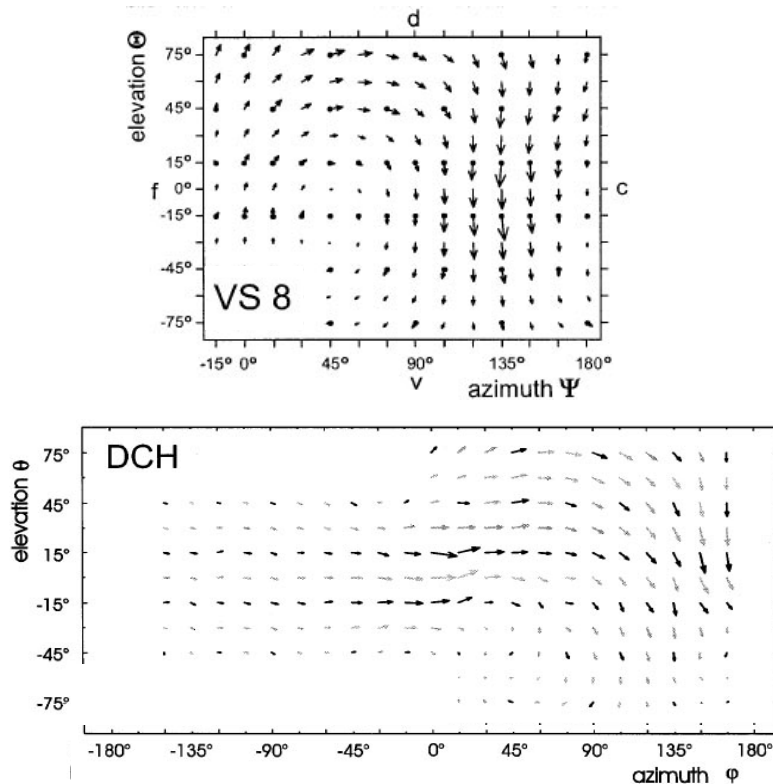


**Figure 1.8: Complex Receptive Fields.** Shown is the receptive fields of a VS8- (**Top**) or dCH-cell (**Bottom**) as measured using a local motion stimulus presented at many points within the visual world. Each arrow represents the PD, indicated by its direction, and its relative strength, by its length. Figures adapted from Krapp et al. (1998) and Krapp et al. (2001).

the area of the lobula plate that each cell's dendrites cover, 12-29% for VS2-VS9 (Hengstenberg et al., 1982), the expected width of the receptive field should amount to about 30°-40°.

### Heterolateral Spiking Cells

There are a number of LPTCs that connect the two lobula plates. These cells respond to motion invariantly with modulations in firing rate. Of these there is a minimum of 6 cells that prefer large field horizontal motion, H1-H6 (Hausen, unpublished; Douglass and Strausfeld, 1996) and two cells that prefer vertical motion, V1-V2 (Hausen, unpublished; Hausen, 1984). Of these cells, the H1-, H2- and V1-cells have all been shown to have complex receptive fields. The H1- and H2-cells respond, in addition to back-to-front horizontal motion, to downward motion in the frontal receptive fields (Haag and Borst, 2003), while the V1-cell is sensitive to horizontal motion in its upper visual field (Karmeier et al., 2003).



## Introduction

### Figure-Detection Cells

In addition to the large-field motion cells there exists a set of cells, which are also spiking interneurons, but prefer motion of small fields. These cells were first described by Egelhaaf (1985). He identified a set of 4 cells (FD1-FD4) that each respond much better to motion of relatively small targets as compared to extended patterns. In addition each FD-cell was found to be inhibited by motion in front of the contralateral eye (Egelhaaf, 1985). Another set of small field selective neurons have been described that are also inhibited by motion in front of the contralateral eye; contralateral inhibited, CI-cells (Gauck and Borst, 1999). These cells are also selective for small targets.

---

### Complex Receptive Fields

During free flight the entire retinal image is continuously shifted. This optic flow, which guides orientation behavior, depends in a characteristic way on the trajectory of the animal and the three-dimensional structure of the environment it is moving through (Koenderink, 1986). For example, the optic flow induced by an object is dependent on both the direction and distance of that object from the subject. If an insect doubles its speed, the magnitude of the optic flow it sees will double. Similarly, if an object is brought twice as close the magnitude of the optic flow will again double. Optic flow also depends on the angle of orientation between an insect's direction of flight and the object it is looking at. If a fly is flying in a straight line, the optic flow is fastest when the object is perpendicular orientated, i.e. 90 degrees to one's side, or directly above or below the fly. If the object is brought closer to the forward or backward direction, the optic flow will be less, while an object directly to the front will have no optic flow and appear to stand still. The useful information needed to guide behavior cannot be discerned by examining small areas of the visual field, but rather one must determine its global features. This means that the neurons that mediate orientation behaviors need to combine measurements of local motion across large areas of the visual field. In addition, it is helpful to combine information arriving on both eyes. This is particularly useful when attempting to distinguish between rotational and translational flow-fields. Rotational flow-fields are made up of local motion cues that point in the same direction on both eyes, while translational flow-fields contain motion signals that are orientated in opposite directions (Fig 1.1). Not surprisingly, the LPTCs in flies have complex receptive fields that not only extend across



## Introduction

wide swaths of the ipsilateral visual field but also often include input from the opposite eye as well.

It has long been noted that some LPTCs combine information arriving from both eyes. However, each LPTCs' receptive field has only recently been mapped in detail (Krapp and Hengstenberg, 1996; Krapp et al., 1998; Haag and Borst, 2001; Krapp et al., 2001; Haag and Borst, 2003; Karmeier et al., 2003). They have been found to be quite complex, often containing different PD in different parts of their receptive fields and extending across extremely wide areas of the visual field (Fig 1.8). In particular, the set of VS-cells has surprisingly extensive receptive field that often extent across the whole ipsilateral visual field. For example, the VS8-cell has a preferred response to downward motion in the posterior visual field, back-to-front motion in the upper lateral visual field and upward motion in the frontal visual field (Krapp et al., 1998). In addition, a set of primarily horizontally sensitive cells, the HS- and CH-cells, combine information arriving on both eyes such that they are selective for rotational stimuli as compared to stimuli simulating a translational movement. The neural interactions that allow these cells to combine information from disparate parts of the visual field rely on a combination of local motion information arriving on the dendritic trees of each LPTC from outside the lobula plate and network connections among the LPTCs themselves.

---

## Lobula Plate Circuitry

As previously described each LPTC has a large dendritic tree that receives information about ipsilateral local motion events. There, local motion cues are spatially pooled such that each neuron produces a directionally selective response to motion presented in front of the ipsilateral eye. The circuitry that connects LPTCs to each other has been revealed to be surprisingly complex: consisting both of bilateral elements that allow each lobula plate to talk to one another, as well as intra lobula plate connections. The intra lobula plate connections can either be axon-axonal or dendro-dendritic. The lobula plate connections have been implicated in the building of complex receptive fields of individual LPTCs.



## Introduction

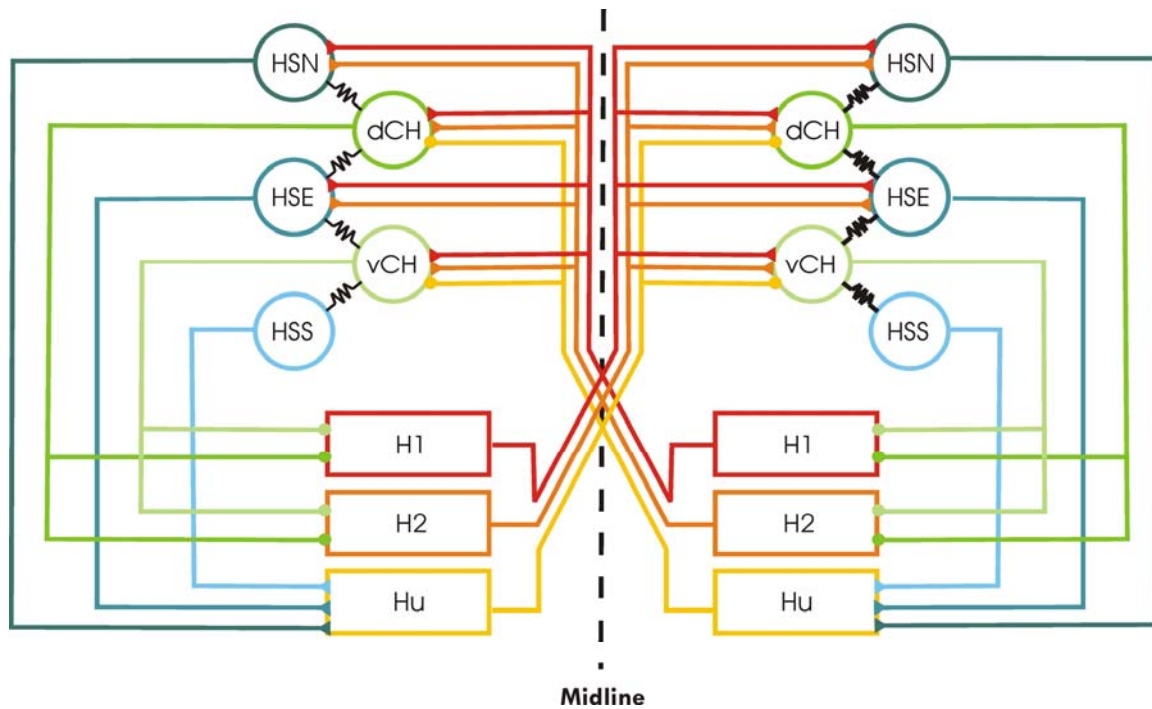


**Figure 1.9: Bilateral Horizontal Interactions.** Circuit diagram of the interactions among LPTCs on both sides of the brain. The connectivity between a group of 16 tangential cells sensitive to horizontal image motion is shown. Excitatory and inhibitory connections are displayed as triangles and circles, respectively. Electrical coupling between cells is indicated by black resistors. Adapted from Haag and Borst (unpublished)

### Interactions of Horizontal Sensitive Cells

The groups of neurons that process horizontal motion form a symmetric bilateral network that is able to combine information about motion presented in front of both eyes. Here I consider a group of 16 neurons whose connections have been explicitly identified (Haag and Borst, 2001; Haag and Borst, 2002). It has been demonstrated that some of the lobula plate neurons are sensitive to motion cues in front of both eyes. The information arriving from the contralateral eye is carried by the spiking neurons H1, H2 and Hu that send their axons to the opposite hemisphere, where they synapse onto 2 of the 3 HS-cells (Horstmann et al., 2000; Haag and Borst, 2001) and both centrifugal horizontal (CH) neurons (Haag and Borst, 2001). These network interactions appear to amplify the response to rotational stimuli and reduce the response to translation. The nature of the input from Hu is likely through GABAergic synapses (Gauck et al., 1997). However, the nature of the input of H1, and H2 input to CH- and HS-cells may be either through chemical input synapses (Gauck et al., 1997) or via electrical coupling.



## Introduction

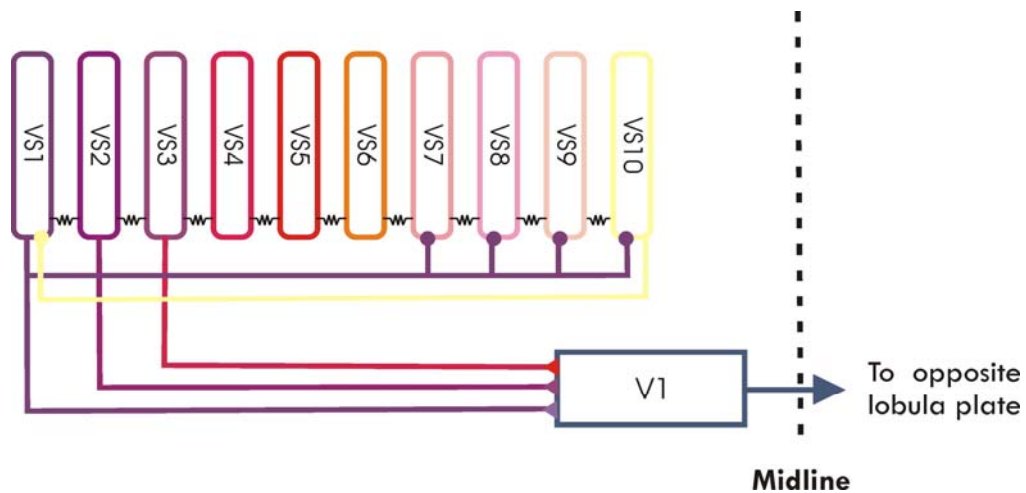


**Figure 1.10: VS-Cell Network.** Each VS-cell is connected to its neighbour via electrical synapses. This putatively results in a broad vertical sensitivity for downward motion. In addition the medial VS-cell (VS7, 8, 9 and 10) receives inhibitory input from VS1 which itself is excited by downward motion in the frontal visual field. This may cause the upward sensitivity found in VS8-, VS9- and VS10-cells. One of the medial cells also sends an inhibitory connection to the VS1-cell. In addition, the VS1-, VS2- and VS3-cells synapse onto the V1-cell which provides input to the opposite lobula plate. Adapted from Cuntz (2004)

Within a single lobula plate the extensive arborizations of CH-cells are the site of both input and output synapses. One of the inputs to CH-cells occurs via an electrical coupling with the overlapping dendritic trees of HS (horizontal system) cells (Haag and Borst, 2002). CH-cells also possess GABAergic output synapses that are spread across their extensive lobula plate arborization (Gauck et al., 1997). This inhibitory output is involved in separate computations that contribute to the detection of objects, via FD (figure-detection) cells (Egelhaaf, 1985; Warzecha et al., 1993f; Haag and Borst, 2002; Cuntz et al., 2003) and flow-field selectivity, via H1 and H2 neurons (Haag and Borst, 2001).

In regard to this circuit's involvement in flow-field selectivity, the H2-cell exhibits a non-linear combination of motion presented in front of the different eyes. Specifically, it is not responsive to motion presented in front of the contralateral eye on its own, but its response to ipsilateral motion is influenced by contralateral stimuli, such that its response to rotation is larger than its response to translation (Haag and Borst, 2001). The H2-cell putatively receives ipsilateral information directly from local motion detectors. In addition, it has been shown that the H2-cell receives inhibitory input from ipsilateral CH-cells, such that injections of positive current inhibit the activity of the H2-cell (Haag and Borst, 2001). As the CH-



## Introduction

cells receive synaptic input from contralaterally projecting spiking H1-, H2- and Hu-cells, they may provide a pathway for information from the other brain hemisphere to influence the activity of the H2-cell (Fig 1.9). The contralaterally projecting H2-cell and Hu-cell synapse on the CH-cell in the protocerebrum while the H1-cell provides input via its large axonal arborizations in the lobula plate. The CH-cells then make dendro-dendritic connections with the H1- and H2-cells.

### Vertical-Vertical Interactions

A recent dual intra-cellular recording study has demonstrated that within a single lobula plate VS-cells are electrically connected, putatively via their overlapping axons (Haag and Borst, 2004). Haag and Borst (2004) demonstrated that each VS-cell is connected to the VS1-cell, such that the strength of the connection diminished as the cells move further apart, actually becoming negative for the most separated cells. This implies that each VS-cell is connected exclusively to its immediate neighbours; forming a row of cells starting with the VS1-cell whose dendrites reach the lateral edge of the lobula plate and moving to the VS10-cell at the medial edge and including at least one inhibitory loop linking the medial and lateral cells. This connection scheme has been proposed to be responsible for the extremely wide receptive fields of VS-cells and the responsiveness of the medial VS-cells to frontal visual stimuli.

### Horizontal-Vertical Interactions

Some of the VS-cells' dendritic trees, VS1, VS7, VS8, VS9 and VS10, stratify in more than one layer of the lobula plate (Eckert, 1982; Hengstenberg et al., 1982). Not coincidentally these cells, in addition to being sensitive to vertical downward motion, are also sensitive to horizontal front-to-back motion (Krapp et al., 1998). The source of this sensitivity to horizontal motion is not clear. It may arise from direct input from horizontally orientated local motion detectors or from the network connection among LPTCs. For VS7- and VS8-cells the source of horizontal sensitivity in the dorsal visual field likely arises from input from the HSN-cell. Current injections into the HSN-cell, of both positive and negative current, are positively correlated with the EPSP frequency of VS7- and VS8-cells (Haag and Borst, 2004). It is not just cells of the vertical system that demonstrate a sensitivity to motion in more than one direction.





## Introduction

The heterolaterally spiking cells H1 and H2 also demonstrate this property. It has been found that the H1- and H2-cells show a strong response to downward motion presented in the frontal receptive field (Haag and Borst, 2003). Current injections into the VS1-cell, which also responds to downward motion in the frontal visual field, are positively correlated with the firing rate of both the H1- and H2-cells (Haag and Borst, 2003).

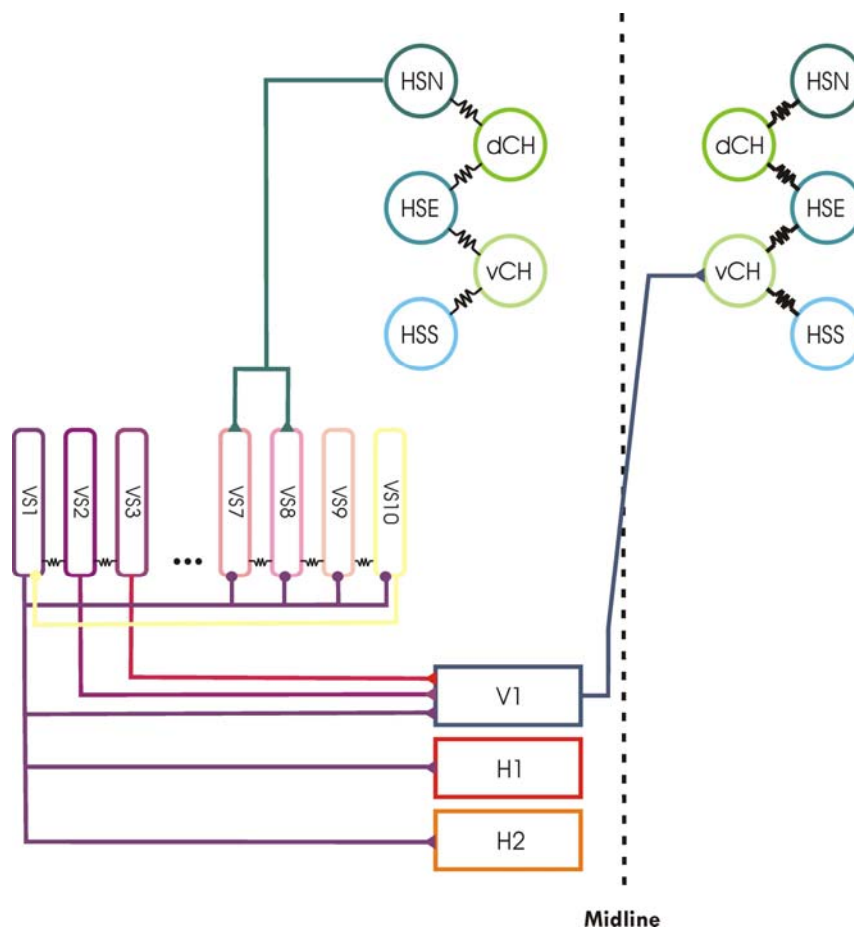


**Figure 1.11: Horizontal-Vertical Interactions.** A circuit diagram highlighting the interactions between tangential cells where one is primarily horizontally sensitive and the other vertically. The HSN-cell provides indirect excitatory input to the VS7- and VS8-cells via a spiking cell. The VS1-cell provides excitatory input to both the H1- and H2-cell. Finally, the V1-cell provides excitatory input to the vCH-cell in the opposite lobula plate.



### Goals

Here I use a single cell ablation technique to investigate the role of the interactions among LPTCs in processing optic flow information. I will focus on 6 of the connections described above. Single cells, or classes of cells, are ablated to determine if particular cells play a role in shaping the receptive fields of other LPTCs. First, the role of the dendro-dendritic electric coupling between HS- and CH-cells will be investigated. These experiments will attempt to determine whether HS-cells, CH-cells or both receive direct input from local motion detectors. Second, I will attempt to determine if the dendro-dendritic inhibitory input of CH-cells to H2-cells is indeed responsible for their flow-field selectivity. Next, the role of coupling between neighbouring VS-cells will be examined. In particular, single VS-cells will be ablated to determine if the electrical coupling between neighbouring VS-cells forms the basis of their wide receptive fields. In addition, by ablating the VS1-cell I will attempt to resolve whether the inhibitory input of this cell is responsible for the upward sensitivity of the medial VS-cells (VS8, 9 and 10) in the frontal visual field. Finally, the input of the VS1-cell to H1-cell will be dissected in order to determine if the VS1-cell is responsible for the H1-cell's sensitivity to vertical motion in the frontal visual field.



## 2 Methods

---

### Preparation

---

Female blowflies, *Calliphora Vicina*, were briefly anesthetized with CO<sub>2</sub> and mounted ventral side up with wax on a small platform. Generally flies were 1-10 days old. Younger flies, 2-5 days old, were used for experiments where no extra cellular recordings were made, while older flies, 4-10 days old, when experiments involving extra cellular recordings were performed. In order to get access to the back of the flies head their head was bent forward and waxed to its thorax. The head capsule was then opened from behind and the trachea and air-sacs that normally cover the lobula plate were removed. The head capsule was filled with Case-Ringers solution of pH 7.2 (NaCl 110 mM, KCl 5.4 mM, CaCl<sub>2</sub>·H<sub>2</sub>O 1.9 mM, MaHCO<sub>3</sub> 20 mM, TRIS/HCl 15 mM, Glucose 13.9 mM, Sucrose 73.7 mM and Fructose 23 mM). To reduce movements of the brain caused by peristaltic contractions of the esophagus either one or both of the following was performed:

1. The abdominal cavity was pressed flat and waxed to the glass, and/or,
2. The proboscis of the animal was cut away and the gut was pulled out.

The second procedure was only performed for experiments describing the input circuitry to HS and CH-cells. It was found that for prolonged extracellular recordings the removal of the gut was followed by a marked increase in the firing rate of both H1, and H2-cells. By leaving the gut in the firing rates of these neurons remained stable for much longer. In cases where the proboscis and gut were not removed the proboscis was pulled taut and waxed to the thorax. For additional recording stability the antennae were removed and underlying tissue waxed. This preparation allowed for stable intracellular recordings of up



## Methods

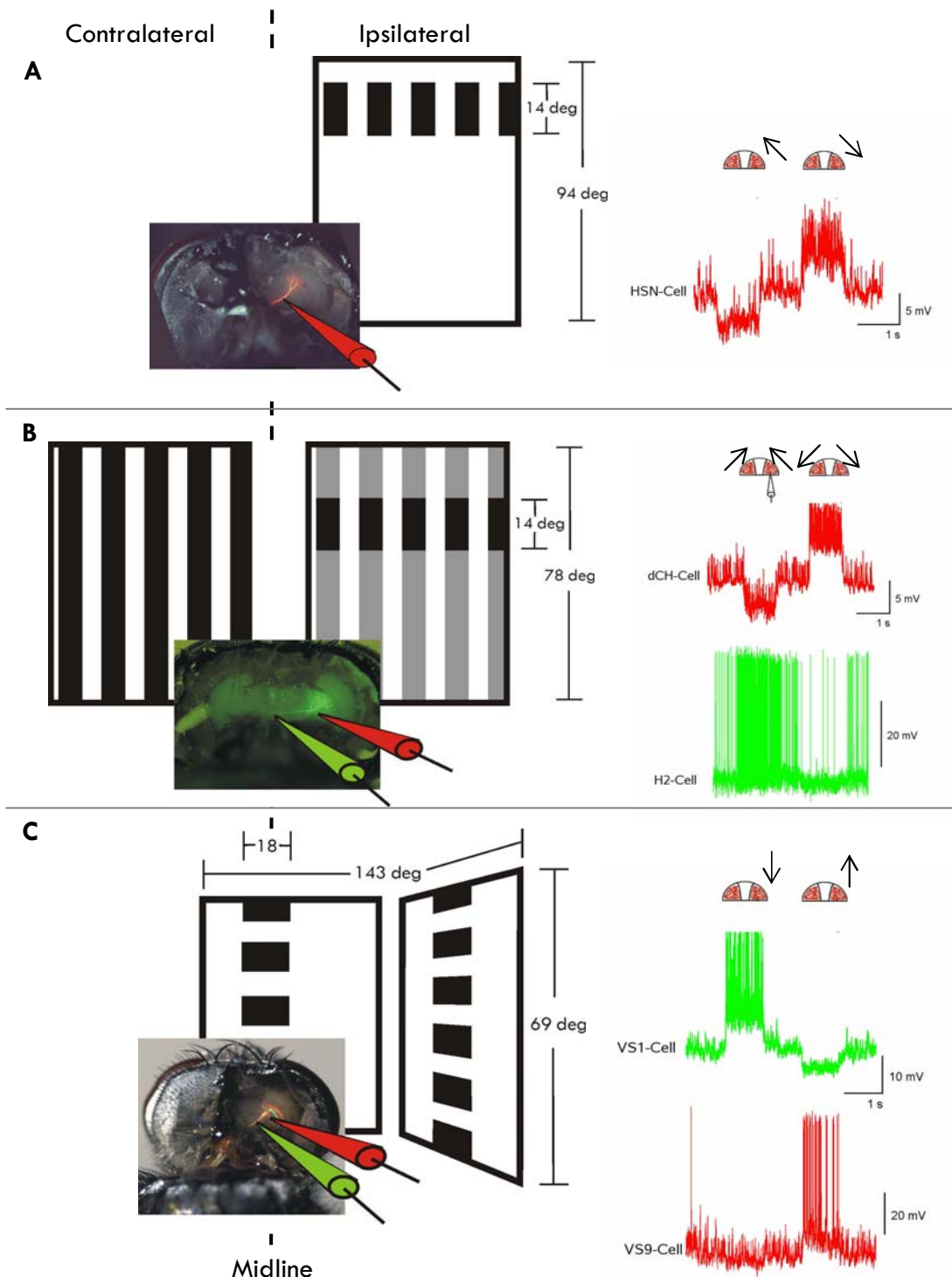


**Figure 2.1: Visual Stimulus Setup.** Shown is a fly looking at the visual stimulus for the different experiments. The cuticle has been removed to gain access to the lobula plate. All cells recorded received their local motion input from the right eye. To the right of each screen is a sample recording from each type of experiment. **A)** Input circuitry to HS- and CH-cells. Recording is of a HS-cell to ipsilateral motion. Recording of HSN-cell to ipsilateral motion. **B)** Flow Field Selectivity of Horizontally Sensitive Cells. Recording of a dCH-cell and H2-cell (shown in picture) to a rotational stimulus. The vertical extent of the ipsilateral stimulus was either restricted (black) or full screen (grey) **C)** Vertical Receptive Fields. Recording of a VS1-cell (top) and a VS9-cell (bottom) to downward motion then upward motion in the frontal visual field. Recording from the same fly. Pictures of fly heads in A and C are courtesy of Jürgen Haag.



## Methods

to 45 minutes and extracellular recordings of 2-3 hours.

The flies were then mounted in an upright position on a heavy recording table facing one or two monitors that displayed grating patterns, which could be moved in various directions. The flies were aligned in reference to their deep pseudopupile.

---

### Visual Stimulation

Visual stimuli were presented on Tektronix CRT monitors (width: 10 cm, height: 13 cm). The images presented consisted of a square grating where the spatial frequency, spatial extent, contrast, brightness and orientation were all controlled by an image synthesizer (Picasso, Innisfree Inc., USA) at a frame rate of 200 Hz. The image synthesizer was controlled by a Pentium III PC via a DAS16/12 board (Computer Boards, Inc.) such that various velocity patterns (e.g. white noise, velocity steps ...) could be used. The stimulation software was written in Delphi (Borland) by Jürgen Haag. The details of the visual stimuli used for each project are described below (Fig 2.1).

### Ipsilateral Motion for Input Circuitry Analysis

The monitor was located 6 cm in front of the fly. The centre of the screen was at  $0^\circ$  elevation from the equator of the fly's eyes and orientated  $55^\circ$  lateral from the midline. As seen by the fly, the monitor had a horizontal angular extent of  $79^\circ$  and a vertical extent of  $94^\circ$ . The pattern consisted of a square wave grating with a spatial wavelength of  $28^\circ$ . The pattern presented was a constant velocity pulse of 1s that moved at a temporal frequency of 1.7 Hz, which is defined as the angular velocity of the pattern divided by its spatial wavelength. The pattern contrast was 96 %. The mean luminance of the pattern amounted to 12 cd/m<sup>2</sup>.

### Horizontal Rotation and Translational Flow Fields

Here two stimulation monitors were used, one stimulating the ipsilateral and the other the contralateral eye. The centre of each screen was situated 8 cm from the fly eye  $55^\circ$  to the left or right of the fly's midline. The screens had a horizontal angular extent of  $64^\circ$  and a



## Methods

vertical extent of  $78^\circ$ . The pattern consisted of a square wave grating with a spatial wavelength of  $21^\circ$ . The pattern was moved with either a constant velocity for 1, 1.5 or 2s at a temporal frequency of 1.6 Hz, or with a white noise velocity profile. The white noise stimulus consisted of sweeps 9 s long. The patterns had either a contrast of 95% or 5%. The mean luminance of the pattern was  $12 \text{ cd/m}^2$ .

### Vertical Receptive Field Analysis

Visual stimuli were presented on two Tektronix CRT monitor located 9.5 cm in front of the fly. The center of each screen was at  $0^\circ$  elevation from the equator of the fly's eyes. As seen by the fly, the monitor had a horizontal angular extent of  $143^\circ$  ( $-30^\circ$  frontally to  $113^\circ$  laterally) and a vertical extent of  $69^\circ$ . The pattern consisted of a square wave grating with a spatial wavelength of  $18^\circ$ , produced by an image synthesizer (Picasso, Innisfree Inc., USA) at a frame rate of 200 Hz. The pattern moved at a temporal frequency of 1.5 Hz, which is defined as the angular velocity of the pattern divided by its spatial wavelength. The pattern contrast was 96 %. The mean luminance of the pattern amounted to  $12 \text{ cd/m}^2$ . The stimulation and acquisition software was written in Delphi (Borland).

While recording a single cell the pattern was presented at 10 different locations moving from left to right. The stripes were  $18.5^\circ$  wide on the front screen and  $18^\circ$  wide on the side screen. At each location the pattern moved vertically. This setup allowed us to stimulate the full primary receptive fields' of VS1-6 robustly. In addition I could test the response of VS7-10 in their frontal receptive field: their complete primary receptive fields were not in the range of our monitors.

### Horizontal-Vertical Interactions

The Tektronix CRT monitors were located 7.5 cm from the fly eye. One was centered  $25^\circ$  right of the fly, stimulating the flies ipsilateral frontal visual field. A second monitor was positioned at  $90^\circ$ . The vertical extent of each screen was  $82^\circ$ , while the horizontal extent was  $67^\circ$ . The pattern consisted of a square grating that was moved either horizontally or vertically at 1.7 Hz and had a spatial wavelength of  $23^\circ$ . The pattern contrast was 94 % with a mean luminance of  $11 \text{ cd/m}^2$ .



---

### Electrical Recording

For data analysis the output signals of the amplifiers (NPI-SEL10 in case of intra-cellular recordings, or threshold device in case of extracellular recordings) were fed to a PIII PC via a 12-bit A/D converter (DAS-1602/12, Computerboards, Middleboro, Mass., USA) at a sampling rate of 1 kHz, during white noise stimuli, or, 5 kHz during velocity steps and double recording, and stored to hard disc.

### Intra-Cellular

Glass electrodes were pulled on a Brown-Flaming micropipette puller (P-97) using thin-wall glass capillaries with an outer diameter of 1 mm (Science Products GMBH, Hofheimer, Germany). The tip of the electrode was filled with either 10 mM Alexa 568 (Alexa Fluor 568 hydrazide; Molecular Probes, Eugene, OR) or 6-carboxy-flourescein (Flourescein; Molecular Probes). Alexa 568 and 6-carboxy-flourescein fluoresce as red and green respectively, allowing us to identify more than one cell at time. The shaft of the electrode was filled with 2 M KAc plus 0.5 M KCl. Electrodes had resistances of either 10-15 M $\Omega$  or 15-20 M $\Omega$  for Alexa and 6-carboxy-flourescein filled electrodes respectively. Recorded signals were amplified using an SEL10 amplifier (NPI Electronics, Tamm, Germany). All recordings were made in the main thick branches of the neurons.

### Extra-Cellular

Extracellular recordings were used to record from both H1 and H2-cells. I used standard tungsten electrodes with a resistance of about 1 M $\Omega$ . Extracellular signals were amplified; band pass filtered and subsequently processed by a threshold device delivering a 100-mV pulse of 1 ms duration as each spike was detected (Workshop of MPI Tübingen).

---

### Laser Ablations

The selective ablation of single neurons was performed by laser illumination of the lobula plate with a 15-30 mW blue (488 nm) laser (Spectra Physics, 163-E11) for 90-120 secs. The cell to be ablated was filled with a saturated solution of 6-carboxy-flourescein in 1 M potassium acetate (-2 to -10 nA; 1-15 min). The neuron to be recorded was filled with



## Methods

Alexa 568 or recorded extracellularly. This allowed for the selective ablation of the Fluorescein filled neuron as, unlike 6-carboxy-fluorescein, Alexa 568 is only weakly excited by blue light (488 nm) and therefore is not toxic to the neuron while it fluoresces. This procedure was first developed for single cell ablation in the lobster (Miller and Selverston, 1979; Selverston and Miller, 1980; Selverston et al., 1985) and was later successfully applied in the auditory system of crickets (Selverston et al., 1985; Jacobs and Miller, 1985) as well as the visual system of the blowfly (Warzecha et al., 1992; Warzecha et al., 1993).

---

## Data Analysis

### Measurement of Neural Responses

All data were analyzed off line using a custom built GUI in MATLAB 6.5. The GUI allowed one to load and sort through the various sweeps in a data set. It also allowed the calculation of graded potential and firing rate responses with mean and standard deviation calculations over selected time divisions. In addition, one could extract the EPSPs, IPSPs from the response and also prefilter the signals with low-, high or band-pass filters. The EPSP extraction was aided by a program written by Hermann Cuntz that picked out local maxima and minima in a one dimensional array.

### Graded Neural Response

Graded neural responses were calculated by taking an average of the steady-state portion of the response minus the baseline. The steady-state portion of the response was determined to begin 0.5 s after the application of the stimulus. Typically during the first 0.5 s the response experiences an overshoot, whose amplitude depends on the characteristics of the stimulus, such as contrast and speed (Reisenman et al., 2003).

### Spiking Neural Response

The response of spiking neurons to velocity steps stimuli was calculated by counting the average number of spikes present during the stimulus and then divided by the length of the stimulus. This was accomplished by first constructing a peristimulus time histogram (Fig





## Methods

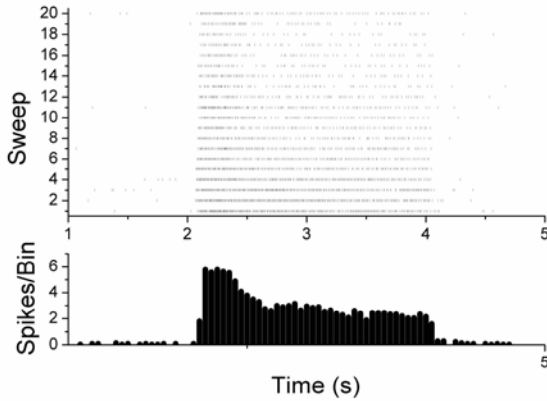


**Figure 2.2: Creating a Peristimulus Histogram.** Recording of an H1-cell to ipsilateral PD motion starting at 2s for a duration of 2 seconds. **Top)** Each dash represents a spike recorded at a particular time. Each row represents one sweep or presentation of the stimulus. **Bottom)** The number of spike recorded in each 10 s bin were averaged across sweeps.

2.2).

### Information Theory

In order to test the response of the neurons to a richer stimulus than velocity steps, white noise velocity profiles were presented to the flies. From these it was possible to measure an information rate. For spiking neurons this was not done to the raw data but to a matrix of data where each element was a 1 or 0, representing the presence or absence of a spike in that time bin respectfully. Each row of the matrix represented single sweeps, while each column represented time bins of 1 ms. This data was converted to an information rate using the direct method (Strong et al., 1998; Borst and Theunissen, 1999) The basic equations tell us that the information contained in the response (R) about the stimulus (S),  $I(R,S)$  can be calculated in three ways:

$$I(R,S) = H(R) - H(R|S)$$

$$I(R,S) = H(S) - H(S|R)$$

$$I(R,S) = H(R) + H(S) - H(R,S)$$

Here the first equation was used to calculate the information rates. This equation states that the information contained in the response about the stimulus is equal to the total entropy (H) of the response minus the entropy in each response given the specific stimulus.

The entropy is calculate as:

$$H(R) = -\sum_i p(r_i) \log_2(r_i)$$

where  $p(r_i)$  is the probability of word  $r_i$  occurring in the data set. Words are sequential sets of response in the data. Since our data was initially represented as a series of 0's and



## Methods

l's sequential sets of values were represented by their binary value.

In order to avoid overestimating the entropy rate from slow signal dynamics long words were used. This becomes difficult because the number of possible words grows exponentially with the word length, leading to insufficiently filled probability density distributions (Treves and Panzeri, 1995; Panzeri and Treves, 1996). Here I used a dual extrapolation method to get account for this problem (Strong et al., 1998), where for a given temporal resolution and word length the total and noise distributions are built using subsets of the dataset. When the entropy rate is plotted as a function of the fraction of the data sample used the entropy rate for infinitely large data samples at a given word length can be read off from the graphs Y-intercept. This procedure is repeated for increasing word lengths, by plotting the information rates as a function of the inverse word length and extrapolating the rate to infinitely long words. In summary, when the information is considered as a function of the, wordlength  $l$  and sample size  $j$ , i.e.  $I = f(l, j)$  the procedure consists in finding:

$$I = \lim_{l \rightarrow \infty} (\lim_{j \rightarrow \infty} (I(l, j))).$$

Seven different lengths of response strings were chosen:  $l = 4, 5, 6, 7, 8, 9$  and  $10$ . Thus, the response strings used for the extrapolation to infinitely long responses were between  $4$  and  $10$  msec long. To extrapolate to infinitely long words, the calculations were based on data fractions of  $1/5, 1/4, 1/3, 1/2$  and  $1$  of the original sample size. These were picked randomly from all samples. The program to calculate the information rate was written in MATLAB 6.5.

---

## Network Modeling

In order to better understand how the interactions between network elements affect their response properties I have constructed a network of single compartment elements in Matlab 6.5. This work was initiated by Alexander Borst. I modified code he created in IDL as the starting point of the model shown here. In particular, the integration routine, general appearance of the GUI, summed motion detector response and method for calculating the steady-state properties of the individual cells were integrated into my version of the



## Methods

model from Alexander Borst's IDL code.

The network model uses the experimentally determined characteristics of voltage- and ion-gated currents in LPTCs, these currents were incorporated into single compartmental models of the respective cells. The starting point for determining the parameters were taken from previously constructed multi-compartmental models of the HS- and CH-cell either in isolation (Borst and Haag, 1996; Haag et al., 1997; Haag et al., 1999) or connected in a dendritic network (Cuntz et al., 2003). Following the formalism of Hodgkin and Huxley (1952) each current was treated as a combination of subunits that denoted the activation and inactivation characteristics. The synaptic connections among the LPTCs were taken from double recording experiments (Haag and Borst, 2001; Haag and Borst, 2002).

The HS-cell was modeled with an inward sodium ( $I_{Na}$ ), outward potassium ( $I_K$ ) and outward potassium dependent sodium current ( $I_{Na,K}$ ). The CH-cell was modeled as a passive compartment with no active currents, while the spiking cells contained an inward sodium current ( $I_{Na}$ ) and an outward potassium ( $I_K$ ). The active currents took the following forms:

- $I_{Na}(t) = (V(t) - E_{rev}) \cdot g_{max} \cdot m^3 h$ ;  $g_{max}^{HS} = 4$ ,  $g_{max}^{Sp} = 100$ ;  $E_{rev} = 100$
- $I_K(t) = (V(t) - E_{rev}) \cdot g_{max} \cdot n^4$ ;  $g_{max}^{HS} = 1$ ,  $g_{max}^{Sp} = 40$ ;  $E_{rev}^{HS} = -30$ ,  $E_{rev}^{Sp} = -30$
- $I_{Na,K}(t) = (V(t) - E_{rev}) \cdot g_{max} \cdot m^3 h$ ;  $g_{max}^{HS} = 2$ ;  $E_{rev} = -25$

Where  $g_{max}$  is the maximum conductance,  $E_{rev}$  is the reversible potential,  $m$  and  $n$  are activation variables,  $h$  is an inactivation variable and  $V(t)$  is the time varying membrane potential. The resting membrane potential for each cell was 0. The activation and inactivation variables were set to change with the membrane potential with the dynamics of a first order low-pass filter:

- $\frac{dx(t)}{dt} = \frac{x_{\infty} - x(t)}{\tau_x}$ ;  $\tau_m = 1ms$ ,  $\tau_h = 2ms$ ,  $\tau_n = 3ms$

Where the steady-state response of  $m$ ,  $n$  and  $h$  are of the form:

- $f(x) = \frac{1}{1 + e^{(MidV-x) \cdot slope}}$ ; see Table 2.1.

In order to model the resting firing rates of the spiking neurons Gaussian white noise was added to the membrane potential of varying levels. This allowed the H1-cells to have a baseline firing rate of  $\sim 20$  Hz and the Hu- and H2-cell to firing spontaneously at  $\sim 5$  Hz.



## Methods

The individual cells were given the appropriate inputs according to the connections deduced through double recordings and the ablation experiments in section 3.1 (Haag and Borst, 2001; Haag and Borst, 2002). The electrical synapses were modeled as linear first-order low-pass filters with time constants of 50 ms. This time constant takes into account the low-pass filter characteristics of signals being passed from the axon of the HS-cell to the axon of the CH-cell (Haag and Borst, 2002; Cuntz et al., 2003). The driving force was the voltage gradient between the two cells, such that if the membrane potential

		MidV (mV)	Slope (mV)	$\tau$ (ms)
<i>HS</i>	<i>m</i>	-1	6	1
	<i>h</i>	-11	-8	4
	<i>n</i>	14	11	15
<i>CH</i>	<i>m</i>	11	8	7
	<i>h</i>	-3	-10	10
	<i>n</i>	8	16	10
<i>Hx</i>	<i>m</i>	8	35	1
	<i>h</i>	-3	-15	2
	<i>n</i>	8	15	3

**Table 2.1:** Variables defining the steady-state responses of the activation and inactivation variable for the HS-, CH- and the spiking cells (Hx).

in the HS-cell was higher than in the CH-cell current would flow into the CH-cell and vice versa. The PSP input to CH- and HS-cells from spiking cells was modeled as a current injection (duration=1 ms, decay time constant=2 ms) whenever a spike occurred in the relevant neuron. A table of the synaptic weights is shown below (Table 2.2). The input from HS- and CH-cells to H1-, H2- and Hu-cells was also modeled as a current injection. The magnitude of the current was the membrane potential of the HS- or CH-cell multiplied by the synaptic weight. For the CH-cell, current was only passed if the CH-cells membrane potential was above rest, 0 mV.

The ipsilateral visual input to the cells was supplied through an array of motion detectors. The summed output of which was fed into the one compartment cells with a sign denoting their PD. The simulated visual stimulus represented a spatial sine grating that was moved with step velocities of 2 Hz with a time resolution of 1 ms. At each time step, I modeled photon noise by contaminating the grating with Gaussian white noise. This pattern



## Methods

stimulated an array

	HSL	HSR	CHR	CHL	H1L	H1R	H2L	H2R	HuL	HuR
HSL		0	2	0	0	1	0	2	0	0
HSR	0		0	2	1	0	2	0	0	0
CHL	2	0			0	1.5	0	3	0	-1
CHR	0	2	0		1.5	0	3	0	-1	0
H1L	0	0	-0.3	0		0	0	0	0	0
H1R	0	0	0	-0.3	0		0	0	0	0
H2L	0	0	-0.3	0	0	0		0	0	0
H2R	0	0	0	-0.3	0	0	0		0	0
HuL	0.5	0	0	0	0	0	0	0		0
HuR	0	0.5	0	0	0	0	0	0	0	

**Table 2.2:** The weights of the connections between the various model neurons.

of 5 motion detectors. The motion detectors consisted of two mirror-symmetrical subunits. In each subunit, the local luminance level at one image location was filtered by a first-order low-pass (time constant 20 msec) and subsequently multiplied with the high-pass filtered luminance of the neighboring location (time constant 50 msec). The signals from the subunits were subtracted, and the output of all five motion detectors was summated. The whole network was simulated at 1 ms time steps. At each time step the currents and membrane potential in each model cell was calculated. The network model simulations were written in MatLab 6.5.



### 3 Results

---

The lobula plate tangential cells respond to motion presented to the ipsilateral eye with either a graded shift in membrane potential superimposed with high frequency events or a modulation in firing. The basic directionally selective response of each LPTC can be attributed to the integration of local motion information arriving on their dendrites. The response of each cell to such stimuli results in a primary response. However, it is clear that the responses of most LPTCs are more complex than this and respond to motion presented both outside their expected receptive fields, as predicted by their dendritic extent, and in directions different from the preferred direction of motion arriving on their dendrites. These receptive field properties are likely a consequence of the dendritic architecture of each LPTC but to a larger degree it appears that network interactions among the LPTCs play a significant role. Below a set of experiments is described where a single LPTC or single class of LPTCs is ablated in order to determine whether its/their input helps augment the primary receptive field of connected cells.



## Ablation Assessment

The ablation technique employed here takes advantage of the fact that Fluorescein but not Alexa568 is toxic to cells when illuminated by a powerful blue light. Individual neurons were filled with either Fluorescein or Alexa568. The affect of ablating the Fluorescein filled cell/s on the response properties of the Alexa568 filled cell was probed. In order to assess the effectiveness and specificity of our ablation technique on the visual response to PD motion, membrane potential and input resistance of a neuron, filled with either 6-carboxy-fluorescein or Alexa568, was measured before and after exposure of the neuron to laser illumination (15 mW, 488 nm) for periods of 30s. Between exposure periods I waited 1 minute before testing the input resistance and visual response of the neuron. I found that after 4 epochs of laser exposure, i.e. a total of 120 seconds, the input resistance of an HSE neuron filled with 6-carboxy-flourescein was reduced from  $\sim 4$  to 1  $M\Omega$  (Fig 3.1C, green line), while its resting membrane potential increased from  $-49$  to  $-15$  mV (Fig 3.1A , green line). In addition the visual response of the HSE neuron fell from 3.5 to 0.2 mV (Fig 3.1B, green line). Similar results were found in HSS-, dCH-, VS4-, and VS2-cells.

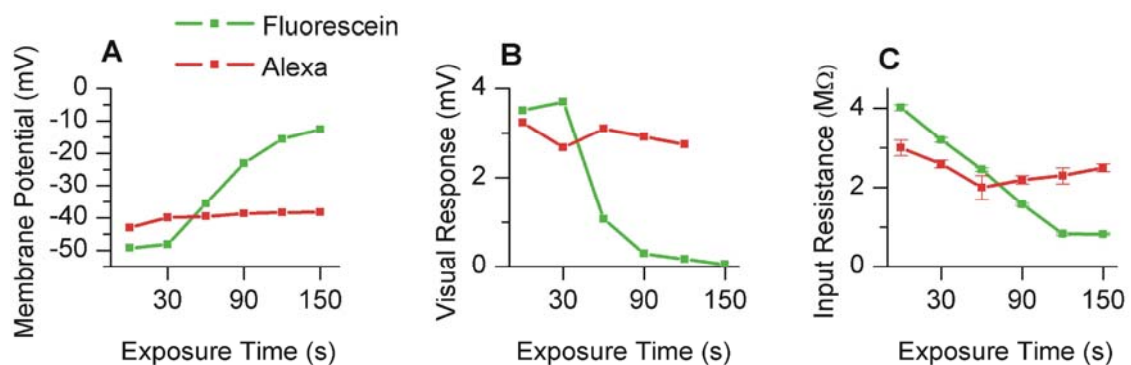


**Figure 3.1: Ablation Assessment.** Response of an HSE neuron, filled with Fluorescein (black line), or a dCH neuron, filled with Alexa568 (gray line), after illumination with a 15 mW laser for periods of 30 seconds. These cells were recorded separately in different flies. The input resistance (A), membrane potential (B) and visual response to ipsilaterally presented PD motion (C) of each neuron was measured 1 minute after each epoch of laser illumination. Each point is the mean  $\pm$  SEM.



## Results

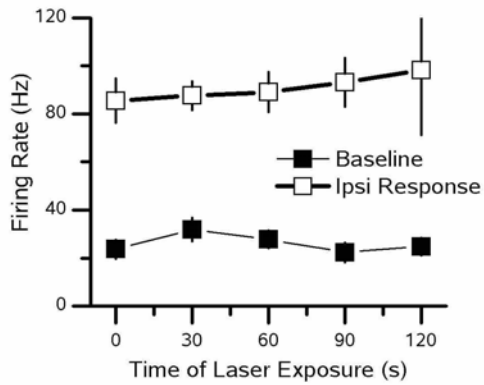


**Figure 3.2: Firing Rate Controls.** The response of H1-cells ( $n=5$ ) was measured after 30 s epochs of 15 mW laser illumination. After each epoch both the baseline firing rate (black squares) and response to ipsilateral back-to-front-motion was measured. No differences were seen after 4 exposures, or a total of 120s.

When a dCH neuron was filled with Alexa568, instead of Fluorescein, the input resistance, visual response and resting membrane potential remained constant for as long as I were able to hold the neuron (Fig 3.1, red line). This was also true in one other CH-cell tested as well as a VS3-cell filled with Alexa488. In addition extracellularly recorded cells did not show any significant changes after exposure to the 15 mW laser for up to 120 s. When H1-cells were recorded in response to ipsilateral PD motion their baseline firing rate and response magnitude remained unperturbed (Fig 3.2).

In general, I was only able to ablate cells densely filled with Fluorescein. Unfilled cells, or cells filled with Alexa568 or Alexa488 were unaffected by laser irradiation of up to 300 seconds. The above experiments demonstrate that I can selectively ablate single neurons.





## Input Circuitry to the HS- and CH-cells

HS and CH neurons not only share many visual response properties but are also electrically connected (Haag and Borst, 2002). Each CH-cell has a dendritic field that overlaps with two of the three HS-cells. The dCH-cell receives input from HSN and HSE neurons via their overlapping dendritic trees, whereas the vCH-cell is connected to HSE and HSS neurons (Haag and Borst, 2002. see also Fig 1.9). The responses of HS- and CH-cells to preferred direction (PD) motion presented in front of the ipsilateral eye are similar. Each neuron responds with a graded shift in membrane potential (Eckert and Dvorak, 1983). In Figure 3.4, the response of an HSE and vCH neuron to ipsilaterally presented PD motion is shown. Here, a square wave grating, with its vertical extent restricted to the receptive field of the HSE neuron, was moved in the PD during which the neurons responded with a graded shift in average membrane potential of 7mV (HSE) or 4mV (vCH). In addition, the HS-cell also produced small action potential-like events, called spikelets (Hengstenberg, 1977; Haag and Borst, 1996; Haag et al., 1997). The high-frequency events seen in the vCH trace are EPSPs caused by input from contralateral H1 and H2 cells. During spatially restricted motion stimulation local calcium accumulation occurs in the dendritic trees of both HS- and CH-cells (Borst and Egelhaaf, 1992; Egelhaaf et al., 1993; Dürr and Egelhaaf, 1999; Haag and Borst, 2002). Hence, local motion

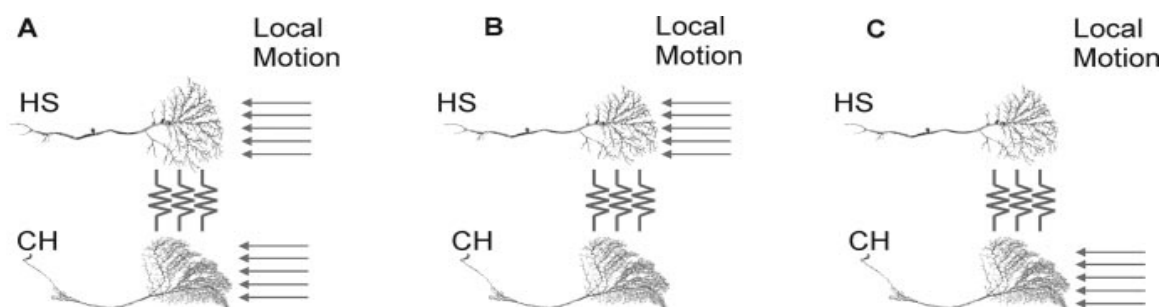


**Figure 3.3: Possible Input Circuitry to HS- and CH-cell.** Three possible connection schemes that can explain the response of both HS- and CH-cells to ipsilateral motion stimuli. **A)** Both HS and CH neurons might receive input from retinotopically arranged columnar motion-sensitive elements. **B)** Only HS neurons might receive motion input from columnar elements. **C)** Only CH neurons might receive input from local motion elements. The data presented here supports the scheme presented in B.



## Results

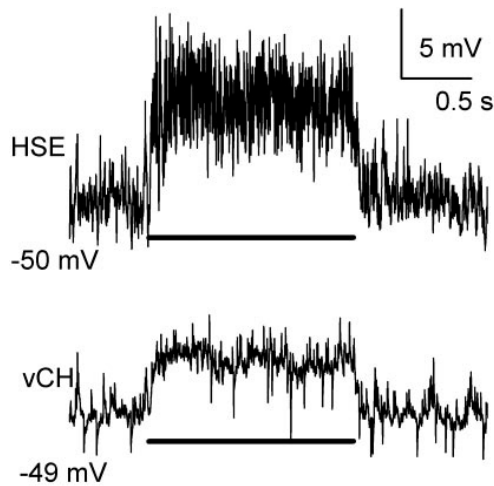


**Figure 3.4: Response Similarities Between HS- and CH-cells.** Response of simultaneously recorded HSE- and vCH-cells to an ipsilaterally presented motion stimulus in the preferred direction, i.e. from front to back. Both neurons responded with a graded membrane shift of either 7 mV (HSE) or 4 mV (vCH) superimposed by EPSPs. In addition the HSE-cells response appears noisier due to the active properties present in HS-cells. The bar underneath the response traces indicates stimulus period.

elements must either synapse directly on the dendritic trees of HS- and CH-cells or local motion information is passed between these neurons via an electrical coupling of their dendritic trees (Haag and Borst, 2002). The direct local motion input to HS neurons may arrive in part via chemical synaptic input from columnar T4-cells located in the medulla (Strausfeld and Lee, 1991). Chemical input synapses have also been found on the dendritic tree of CH-cells (Gauck et al., 1997). However, whether these synapses form the input pathway for local motion elements is not known. The experimental data available at present lead to three possible input schemes, outlined as both CH and HS-cells receive input from local motion elements and each other (Fig 3.3A), the motion response of CH-cells is due entirely to input from HS-cells (Fig 3.3B), or CH-cells drive the response of HS-cells (fig 3.3C). To investigate whether the response of CH-cells is solely attributable to input from HS-cells or a combination of HS-cell input and parallel input from columnar elements, a single HS neuron was selectively ablated while a CH-cell located in the same hemisphere, with an overlapping dendritic field was recorded by means of intracellular electrodes.

### HS-Cell Ablations

In figure 3.5A one can see the average response of a vCH neuron to a preferred direction (PD) motion stimulus both before (green line) and after (red line) the ablation of an HSE neuron. Here the HSE was filled with 6-carboxy-flourescein and the vCH with Alexa568. The average response of the vCH neuron to PD motion was  $3.0 \pm 0.2$  mV (mean  $\pm$  SEM) in the intact animal, while this response was reduced to  $0.4 \pm 0.1$  mV after the selective ablation of the HSE-cell (Fig 3.5B, third column). The visual stimulus was restricted



## Results

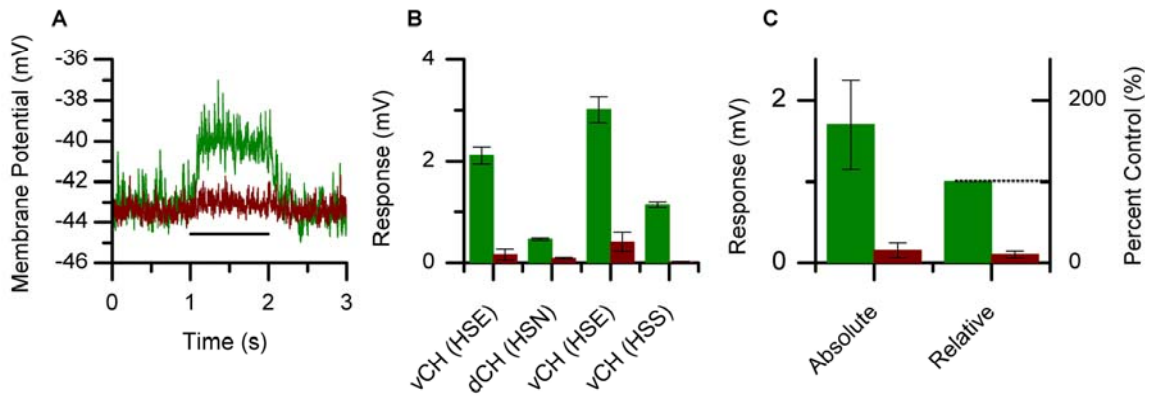


**Figure 3.5: HS-cell Ablations.** A) Average response of a vCH neuron to PD motion both before (black line) and after (gray line) the selective ablation of an HSE neuron. The bar underneath the response traces indicates stimulus period. The response dropped from  $3.01 \pm 0.15$  mV to  $0.42 \pm 0.1$  mV (mean  $\pm$  SEM). B) Average response of CH neurons before and after the selective ablation of single HS neurons. There are 2 examples of a vCH neuron before and after the ablation of an HSE neuron (columns 1 and 3). One example of a vCH-cell before and after a HSS neuron ablated (column 4). Also shown is the average response of a dCH-cell after the ablation of an HSN neuron (column 2). C) The average response of these 4 neurons went from  $1.69 \pm 0.56$  to  $0.17 \pm 0.09$  mV (mean  $\pm$  SEM) after the ablation of a single HS neuron, which corresponds to a reduction of  $89 \pm 4$  %.

to receptive field of the HSE neuron and had a vertical extent of 14.25 deg. After the ablation the response of the vCH neuron had not completely disappeared, which may be due to a residual response of the HSS neuron. Similar results were found in three other experiments (Fig 3.5B). In Figure 3.5B one can see the response of vCH-cells before and after the ablation of either the HSE or HSS-cell, as well as the effect of the ablation of an HSN-cell in the response of a dCH-cell. On average the response of the CH neurons fell to  $11 \pm 4$  % ( $\pm$  SEM,  $n=4$ ) of the pre ablation response (Fig 3.5C). The average response fell from  $1.69 \pm 0.56$  to  $0.17 \pm 0.09$  mV (mean  $\pm$  SEM,  $n=4$ ; Fig 3.5C).

### CH-Cell Ablations

In order to test whether HS-cells are driven directly by local motion elements or via input from CH-cells HS-cells were recorded both before and after the ablation of a single CH neuron. In figure 3.6A the average response of an HSN-cell is shown both before (green line) and after (red line) the selective ablation of a dCH neuron. Here the dCH was filled with 6-carboxy-flourescein and the HSN with Alexa568. The visual stimulus was again restricted to 14.25 deg. After the ablation of the dCH neuron the response of the HSN neuron did not change. Its response before the ablation of the dCH neuron was  $2.67 \pm 0.03$  mV; while after the ablation it was  $2.75 \pm 0.03$  mV (mean  $\pm$  SEM). Figure 3.6B



## Results

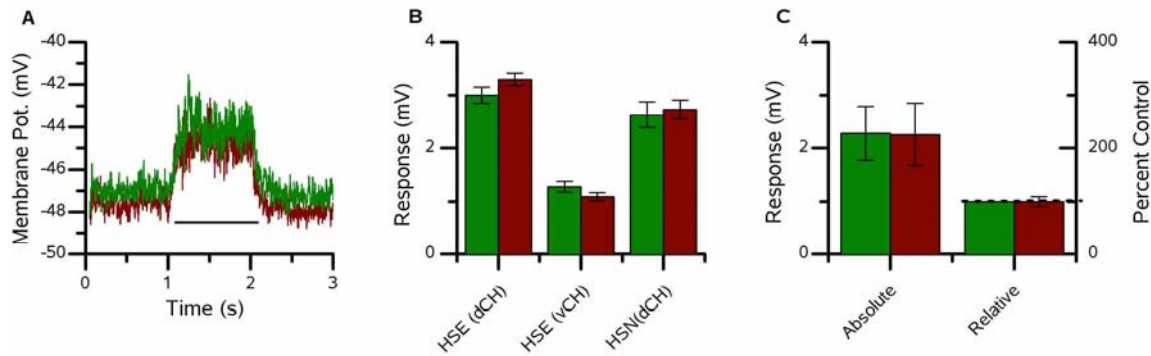


**Figure 3.6: CH-cell Ablations.** A) Average response of an HSN neuron both before (black line) and after (light grey line) the selective ablation of a dCH neuron. The bar underneath the response traces indicates the stimulus period. The response changed from  $2.63 \pm 0.03$  mV to  $2.73 \pm 0.03$  mV (mean  $\pm$  SEM) after ablating the dCH neuron. B) Average response of HS neurons before and after the selective ablation of single CH neurons. Two examples of an HSE-cell are shown with the ablation of either a dCH- (column 1) or a vCH-cell (column 2). In addition the mean response of an HSN-cell is shown both before and after the ablation of a dCH-cell (column 3). The error bars represent the standard error of the mean. C) The average response of these 3 neurons before the ablation was a graded shift in membrane potential of  $2.28 \pm 0.51$  (mean  $\pm$  SEM). The response after the selective ablation of a CH neuron was  $2.26 \pm 0.59$  (mean  $\pm$  SEM), which responds to a decrease of only  $0.66 \pm 10\%$ .

shows the response of a HSE-cell both before and after the ablation of either a dCH- or vCH-cell. Also shown is the effect of ablating a dCH-cell on the response of an HSN-cell. In Fig 3.6C the average response (mean  $\pm$  SEM) of 3 HS-cells to ipsilaterally presented PD motion is shown both before ( $2.28 \pm 0.51$  mV) and after ( $2.26 \pm 0.59$  mV) the ablation of a single CH neuron. This is a change of only 0.66 % as compared to a reduction of 89 % in the response of CH neurons after the ablation of HS neurons. The response of HS neurons appears to be independent of input from CH-cells.

## Conclusions

The above experiments demonstrate that the response of CH cells to visual motion presented in front of the ipsilateral eye is entirely dependent on input from electrically coupled HS-cells. In contrast, the response of HS cells turned out to be independent of input from CH cells. These two results provide convincing evidence that HS neurons receive local motion information directly from local motion elements and pass this information on to CH neurons. Such a connection scheme has implications for understanding the visual response properties of CH cells, including their spatial integration properties, dendritic calcium signals during null direction motion stimuli, and the spatial blurring of motion



signals on their dendrites.

---

### Rotational Flow-Field Selectivity

Within the lobula plate there are cells that respond to motion in front of both eyes, the basis of which includes both connections between the two lobula plates as well as interactions among LPTCs within the same lobula plate. This network of horizontal sensitive cells has been shown to comprise positive feedback loops such that the activity of a single cell reinforces its own activity after passing around the loop (Haag and Borst, 2001; Haag and Borst, 2002). Some of the LPTCs integrate binocular information in a non-linear manner. Here flow-field selectivity is defined as the non-linear combination of information from both eyes. One example of this is the flow-field selectivity demonstrated by the H2-cell. The H2-cell is not responsive to motion presented in front of the contralateral eye on its own. However, its response to ipsilateral motion is influenced by contralateral stimuli, such that its response to rotation is larger than its response to translation (Haag and Borst, 2001). Another heterolaterally projecting cell, the H1-cell, has the same network connectivity as the H2-cell (Haag and Borst, 2001). However unlike the H2-cell, its response to high-contrast velocity steps is not influenced by the contralateral stimuli. Both the H1- and H2-cells are spiking cells, and each receives information from the opposite hemisphere via CH-cells. This information is carried from the other brain hemisphere by the partner heterolateral spiking cells, H1, H2 and Hu. The H2-cell and Hu-cell synapse on the CH-cell in the protocerebrum while the H1-cell provides input via its large axonal arborizations in the lobula plate. The CH-cells then make dendro-dendritic inhibitory connections with the H1- and H2-cells (see Fig 1.9).

### Flow Field Selectivity of H1 and H2

In previous experiments it has been shown that H2-cells, but not H1-cells, are flow-field selective for rotation at high contrast (Haag and Borst, 2001). Here I show that the H1-cell is also selective for rotation when presented with a more diverse set of stimuli. First, the flow-field selectivity was tested with velocity steps at both high (95%) and low (5%) contrast (Fig 3.7). Second, the flow-field selectivity was examined using a white noise velocity profile (Fig 3.8).



## Results

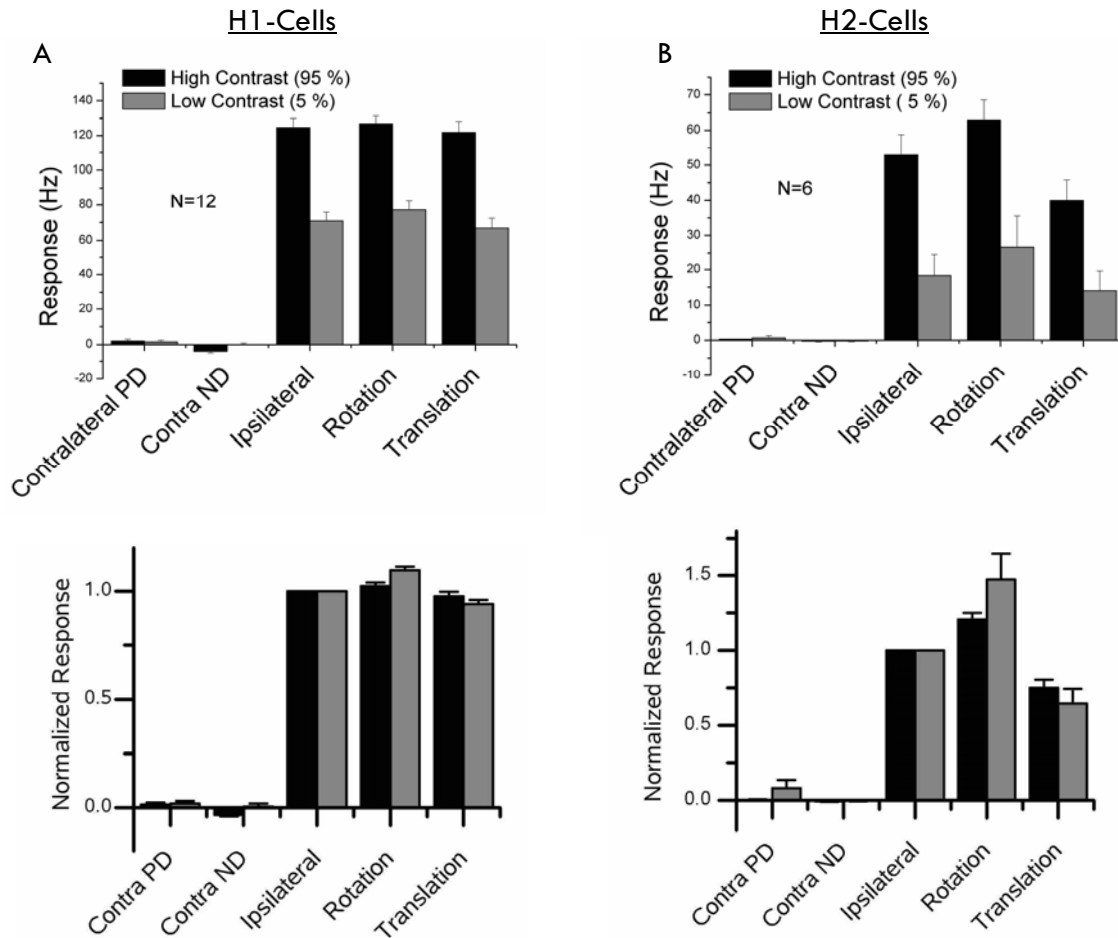


**Figure 3.7: Contrast Dependent Flow-Field Selectivity.** **A)** H1-cells do not show flow-field selectivity during velocity steps at high contrasts (dark bars). However, at low contrast (grey bars) the relative response during a translational stimulus is significantly smaller ( $p < 0.001$ ) than during rotational stimuli, although the affect is small. **B)** H2-cells, unlike H1-cells, show obvious flow-field selectivity during high contrast velocity steps (black bars). This selectivity is enhanced at low contrasts (grey bars).

In response to a high contrast velocity step, presented to the ipsilateral eye, the H1-cell responds with an increase in firing frequency of  $\sim 120$  Hz. On the other hand, the H1-cell does not respond to motion presented in front of the contralateral eye. When tested with high-contrast velocity steps that mimic a rotational flow-field the response remains the same as that of the ipsilateral response. This is also true for translational velocity steps from the front to the back in front of each eye; the response is 97% of the ipsilateral response. The difference between the response to rotation and translation was not statistically different ( $p > 0.2$ ). However, when the contrast of the stimulus is reduced to 5% the response of the H1-cell becomes selective, although only slightly, such that the response to rotation is significantly larger than that to translation ( $p < 0.001$ ). In addition, the H1-cell



## Results

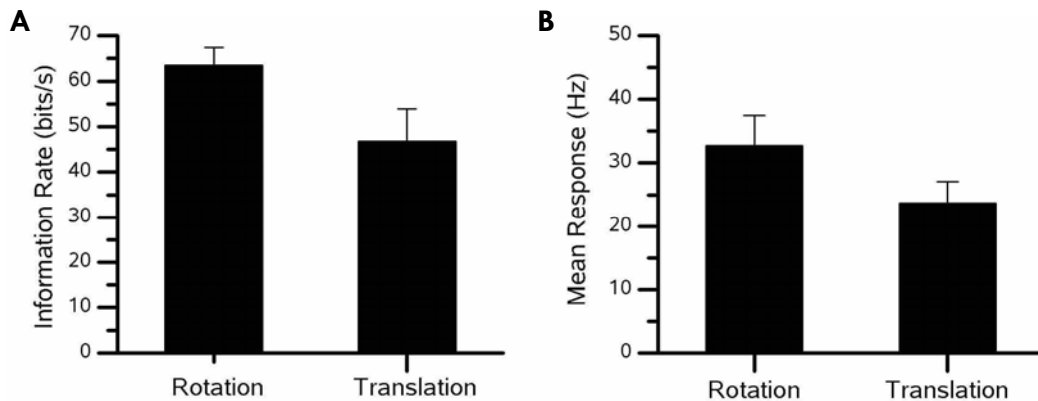


**Figure 3.8: H1 Flow-Field Selectivity to White Noise Stimulus.** Here each eye was presented with the identical white noise velocity profiles. The difference is that during translation the sign of the velocity is reversed in front of the contralateral eye. **A)** H1-cells ( $n=6$ ) show flow-field selectivity during white noise stimulus,  $p < 0.05$  (rotation  $>$  translation). **B)** The mean firing rate in the two circumstances drops from  $32.8 \pm 4.8$  and  $23.7 \pm 3.4$ , which by convention is not considered significant,  $p = 0.15$ . However, a trend is apparent.

is selective for rotation when stimulated with a white noise velocity profile. Here the response was measured as an information rate in bits/s. Each eye was stimulated with the same velocity profile, where rotation consisted of velocity profiles presented in phase on the two screens and translational of velocity profiles  $180^\circ$  out of phase. The response to rotational stimuli produced a response of 64 bits/s, while that to translation was 45 bits/s. The average firing rate during rotation and translation was 32.8 and 23.7 Hz respectively. These results show that although during simple high contrast stimuli the response of the H1-cell is unaffected by what the contralateral eye sees, during more challenging stimuli (low contrast or white noise velocity profiles) the H1-cell becomes flow-field selective, if only to a small degree.

Unlike the H1-cell, the H2-cell shows a highly non-linear summing response of inputs from both eyes that makes the H2-cell selective for rotational motion during high-contrast velocity steps (Haag and Borst, 2001). Although the H2-cell does not respond to motion presented exclusively in front of the contralateral eye, contralateral motion does modulate the response to ipsilateral stimulation (Haag and Borst, 2001). In 6 cells I found the same pattern for high contrast stimuli. The response to rotation and translation was 120.0 % and 75.1 % that to ipsilateral stimulation. In the same 6 cells the selectivity for rotation significantly increased in response to velocity steps when the contrast was low, 5%. Here the response to rotation was 147.3 % and 64.5 % that of the response to ipsilateral



## Results

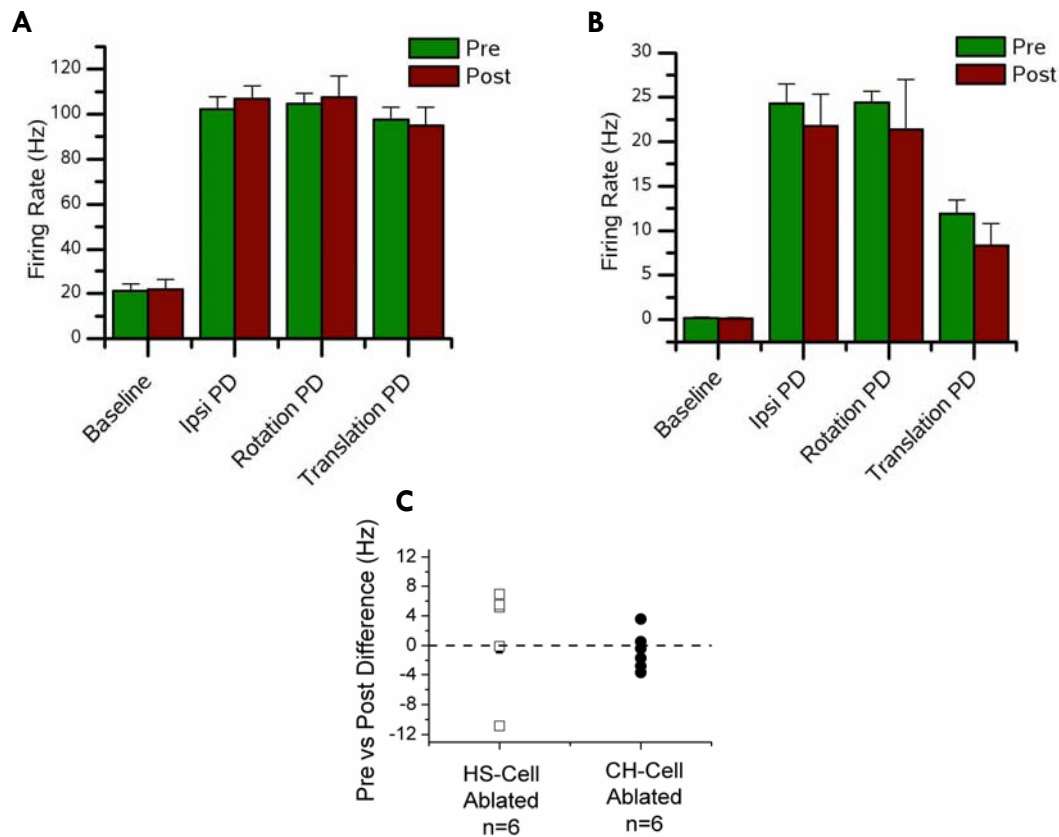


**Figure 3.9: Single HS- and CH-Cell Ablations.** The ablation of single HS- or CH-cells had no affect on the response of H1- or H2-cells. Here the ipsilateral stimulus was spatially restricted so as to only stimulate the HS- or CH-cell that was ablated. **A)** The ablation of CH-cell had no affect on the baseline firing rate or flow-field selectivity of H1-cell (n=6) to PD motion. The mean response to ipsilateral, rotational and translational PD motion remained the same after the ablation of a single HS-cell. **B)** This was also true of H2-cells. H2-cells remained flow-field selective after the ablation of single CH-cells. **C)** As HS- and CH-cell have opposite PD then the H1-cell and the CH-cell provides a rectifying input to the H1-cell that would only inhibit during back-to-front motion, ND for the H1-cell, I looked specifically at the ipsilateral ND response of the H1-cell at low contrast (5%). I found no difference in the ND of the H1-cell after single cell ablations of either HS- or CH-cells.

stimulation respectively.

It is evident that the heterolaterally projecting cells, H1 and H2, are both to some degree selective for rotational stimuli. The source of this selectivity has been proposed to be inhibitory input from CH-cells, via GABAergic output synapses, that carries information from the contralateral hemisphere (Haag and Borst, 2001). The activity of CH-cells contains both information from the opposite lobula plate, carried by contralaterally projecting H1-, H2-, and Hu-cells, and signals originating from dendritically linked HS-





## Results

cells. From coupled HS-cells, CH-cells receive local motion information with a PD opposite to that of ipsilateral H1- and H2-cells. This means that activity in HS-cells inhibits the H1- and H2-cells during front-to-back motion indirectly via CH-cells. Thus, CH-cells may play a role in both the rotational selectivity and ND response to ipsilaterally presented motion.

Here the function of this input scheme to H1- and H2-cells is tested either by ablating single HS- and CH-cells, or ablating both CH-cells.

### Firing Rate Control

CH-cells have GABAergic output synapses in their large lobula plate arborization that supplies inhibitory input to H1- and H2-cells that may contribute to their baseline firing rate. In order to make sure that ablating CH- or HS-cell did not affect the resting firing rate of post synaptic cells I ablated single HS- or CH-cells and measured the resting firing rate of the H1-cell. I found that the firing rate remained essentially the same after the ablation of either a HS- or CH-cell. After the ablation of an HS-cell the firing rate of H1 remained constant (Pre=17.8 +/- 3.4 Hz; Post=19.6 +/- 3.7 Hz (P=0.74, N=6). Similarly after the ablation of single CH-cells the firing rate of the H1-cells did not change (Pre=19.7 +/- 2.4 Hz; Post=20.2 +/- 3.2 Hz; P=0.90, N=6). These results imply that the CH-cell does not continuously release GABA under normal conditions that would keep the firing rate of the H1-cell low.

### Single Ipsilateral HS- and CH-Cell Ablations

Here I ask whether the inhibitory input from CH-cells plays a role in the ND response of the H1-cell. The CH-cells pass on information, received from ipsilateral HS-cells, to the H1- and H2-cells about ipsilateral motion. As the HS- and CH-cells have the opposite PD, front-to-back, to that of the H1- and H2-cells, back-to-front, the CH-cells depolarize and in turn release GABA during back-to-front motion, the ND for the H1- and H2-cells. Here, I test this proposal by ablating single HS- or CH-cells cells, which should result in a decrease response of H1- and H2-cells to front-to-back motion in front of the ipsilateral eye. The ablation of either single HS- or CH-cells was found to have no effect on the H1-cells response to ipsilaterally presented front-to-back velocity steps at high contrast. The pre vs post difference after the ablation of single HS-cells was found to be 0.98 +/- 2.7 Hz. The pre vs post difference after the ablation of single CH-cells was -0.75 +/- 1.1 Hz. Neither



## Results

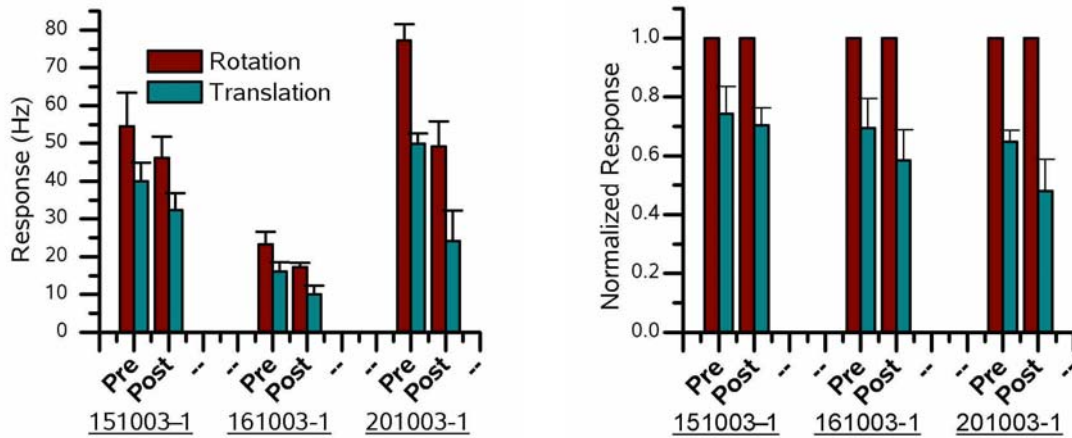


**Figure 3.10: Double CH-Cell Ablations.** H2-cells remained selective for rotational flow-fields after the ablation of both CH-cells. **A)** The response of the H2-cell to either rotational (red bars) or translational (blue bars) of 2 second long velocity steps. **B)** The normalized response of the the experiments shown in three. The flow-field selectivity did not change significantly after the ablation of both CH-cells. All values are mean  $\pm$  SEM.

of these changes were significantly different from zero, with  $P = 0.73$  and  $P = 0.53$  respectively (Fig 3.9C).

Similarly the flow-field selectivity of both H1- and H2-cells was unaffected by the ablation of single HS- or CH-cells (Fig 3.9A and B). In the case of HS-cells this is unsurprising as visual information from the contralateral eye need not pass through HS-cells to reach the spiking cells. For single CH-cells this result could be explained by the steep saturation of the spatial integration properties of H1-cells (Single et al., 1997). H1-cells are maximally responsive to all patterns with a horizontal extent of  $25^\circ$  wide and higher (Single et al., 1997). As a single CH-cell covers a much larger area than  $25^\circ$ , then the input from one CH-cell should have the same influence as the input from two.

### Double CH-Cell Ablations

As the spatial information from the opposite eye is collapsed into the spiking activity of the contralaterally projecting neurons that provide input to both CH-cells, and LPTCs have been found to have highly saturating spatial integration properties, I performed ablations of both ipsilateral CH-cells that provide synaptic input to the dendritic tree the H2-cell. These double ablations should completely break the path of information transferred from the contralateral eye and thus render the H2-cell unselective for rotation.



## Results

I managed to perform this experiment in three separate flies. In each case one of the CH-cells was recorded during the ablation and its death confirmed, while simultaneously recording the H2-cell. The average response in the intact fly to rotational stimulation was 51.6 Hz, while that to translation was 38.2 Hz. After the ablation of both CH-cells the response to both rotation and translation dropped to  $37.5 \pm 10.2$  and  $22.2 \pm 6.5$  Hz respectively. However, the H2-cells remained selective for rotation such that its response to translation was  $59.3 \pm 6.2\%$  that of its response to rotational stimuli. This selectivity was true for all three flies tested (fig 3.10). Contrary to our predictions, in each experiment the H2-cell remained selective for rotation after the ablation of both CH-cells.

### Modeling Horizontal Flow-Field Selectivity

In an attempt to better understand how the horizontal network described above functions, modeling work was initiated. This took two forms. First, a simple analytical model was constructed in order to understand how the basic circuitry operates to shape the response of the different cells at different positions within the network. Second, a more elaborate

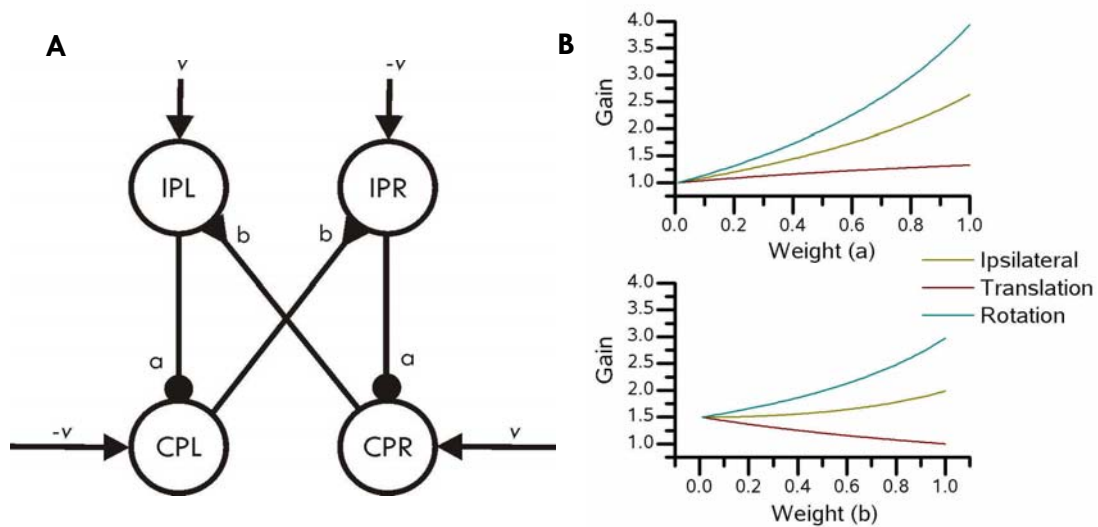


**Figure 3.11: Analytical Lobula Plate.** A simplified model of the lobula plate circuitry illustrates some of the basic behavior seen in the real neurons. **A)** Here the set of HS- and CH-cells were collapsed into single IP units, while the heterolaterally projecting H1-, H2-, and Hu-cell are represented by the CP units. The weights are signified by  $a$  and  $b$  and can range from 0 to 1.  $v$  represents the velocity input from each eye and the sign in front indicates whether the input prefers front-to-back or back-to-front. **B)** The gain of the network for the CPL unit. In the top graph the weight of  $a$  is increased from zero to 1 while  $b$  is held constant at 0.5. Below,  $a=0.5$  while  $b$  is increased from 0 to 1. Note in all cases that the gain for rotation is the largest and translation smallest. Also in all cases increasing  $a$  causes an increase in the gain, while increasing  $b$  causes a decrease in the gain during translation.



## Results

numerical model was built to see if a realistic connection scheme could account for the responses seen *in vivo*, and, in addition, check if the negative finding of the ablation experiments were reasonable. The network model presented here is based on an earlier version created by Alexander Borst (Borst, 2003a).

The analytical model was constructed by collapsing the known network into a four cell linear system. This step was taken to gain intuition about how the basic circuitry operates to amplify signals in comparison to the response to motion input alone (Fig 3.11). The system contained 4 individual units: 2 ipsilaterally projection units (IP) and 2 contralaterally projecting units (CP). The system was divided into two halves, a left and right side that contained one IP and CP unit respectively. The IP unit represented the 3 HS- and 2 CH-cells on each side of the brain, while the CP unit represented the H1-, H2-, and Hu-cells. Together, the simplified network consists of four processing units that each have first order low-pass characteristics. The IP units make inhibitory connections to one of the CP units, while the CP units project across the midline and make contact with the IP unit on the other side of the midline. The strength of the connections are represented by two variables,  $a$  and  $b$ , which are scaled between 0 and 1. In addition each unit receives motion information directly with the IP units having a PD of front-to-back, positive values of  $\bar{v}_{input}$ , and each CP unit having a back-to-front PD.

The basic system can be expressed as a set of four differential equations, which in matrix form is:

$$\begin{bmatrix} \dot{IPL} \\ \dot{IPR} \\ \dot{CPL} \\ \dot{CPR} \end{bmatrix} = \begin{bmatrix} -1 & 0 & 0 & b \\ 0 & -1 & b & 0 \\ -a & 0 & -1 & 0 \\ 0 & -a & 0 & -1 \end{bmatrix} \begin{bmatrix} IPL \\ IPR \\ CPL \\ CPR \end{bmatrix} + \begin{bmatrix} v_{input} \\ -v_{input} \\ -v_{input} \\ v_{input} \end{bmatrix}$$

Where the form of the input vectors for rotation, translation and ipsilateral input respectively are:

$$\bar{v}_{Rotation} = \begin{bmatrix} v \\ -v \\ -v \\ v \end{bmatrix}; \bar{v}_{Translation} = \begin{bmatrix} v \\ v \\ -v \\ -v \end{bmatrix} \text{ and } \bar{v}_{Ipsilateral} = \begin{bmatrix} v \\ 0 \\ -v \\ 0 \end{bmatrix}.$$

When I solve this system for its steady-state solution (i.e. the time derivative is 0) given the different ipsilateral, rotational and translation input I find that the network amplifies the



## Results

signals most for rotation. Following are the three steady-state solution for the three linear networks for the CP units:

1.  $CPL = -v \left( \frac{1+a}{1-a^2b^2} \right) \rightarrow Ipsilateral$
2.  $CPL = -v \left( \frac{1+a}{1-ab} \right) = -CPR \rightarrow Rotation$
3.  $CPL = -v \left( \frac{1+a}{1+ab} \right) = CPR \rightarrow Translation$

The gain of the system is defined as:  $gain = response/stimulus$ . As  $a$  and  $b$  are positive values between 0 and 1 then  $1+ab \geq 1-a^2b^2 \geq 1-ab$ . Also, the value of  $v$  is a constant velocity and hence the gain for rotation is always larger than that for ipsilateral

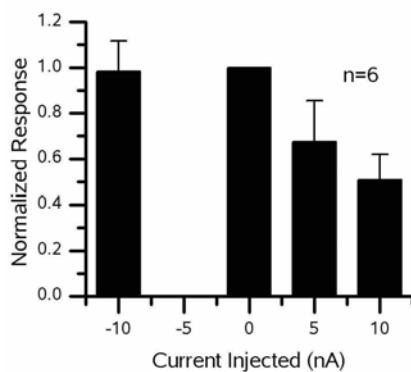


**Figure 3.12: Current Flow Rectification between CH- and H1-cells.** The response of the H1-cell to current injections into CH-cell in the same side reveals a rectification such the current of positive but not negative current is transferred.

stimulation, which is larger than for translation stimulation (Fig 3.11). In addition, this steady-state solution illustrates that during rotational stimuli the activity on each side of the network is of the same magnitude but opposite sign, while during translation the magnitude of the response will be equal on both sides of the network.

To elaborate on the analytical model a network model was constructed where each cell was represented by a single isopotential compartment with Hodgkin-Huxley like currents. The details of the model are described in the methods section. Due to the finding of the ablation experiments described above, I attempted to model the flow-field selectivity of the H1- and H2-cells and see if the combination of the basic circuitry and realistic signals present in each cell could account for the flow-field selectivity found *in vivo*.



## Results

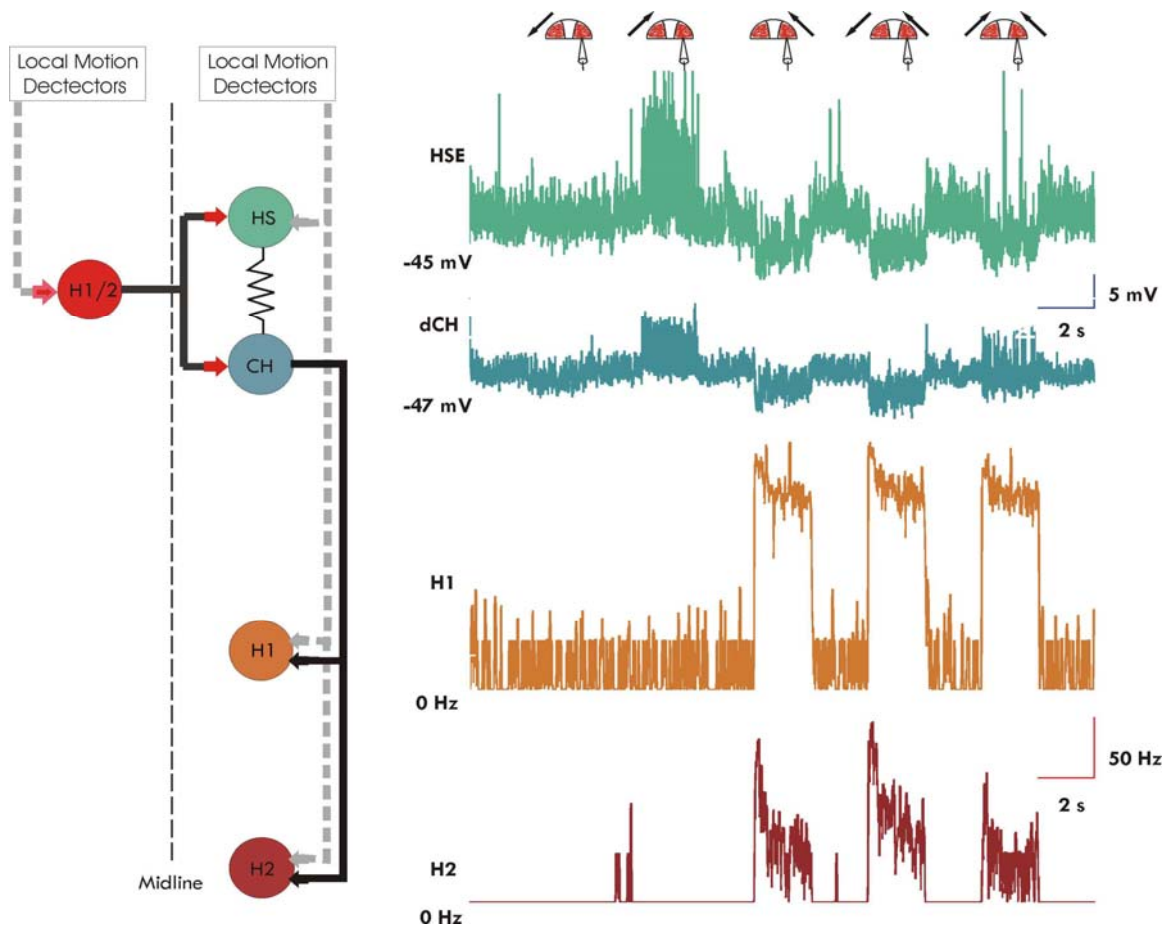


**Figure 3.13. Signals Driving H2-cell Flow-Filed Selectivity.** **Left)** Schematic diagram of the input-output pathways of HS- and CH-cells. An array of local motion detectors supplies HS, H1 and H2 cells with local motion information (grey arrows). The preferred direction for local motion input to HS-cells is front-to-back while that of H1 and H2 is back-to-front. HS- and CH-cells are connected electrically via their dendritic trees. CH-cells inhibit H1 and H2 via GABAergic synapses (black arrows). In addition HS and CH cells receive excitatory input (red arrows) from the contralateral H1 and H2 neurons. Solid lines indicate known connectivity and dashed lines indicated putative connections. **Right)** Example traces of a HS-, CH-, H1- and a H2-cell to different visual stimuli at high contrast. Note that H2 but not H1 is preferentially selective to rotational vs translation motion. Note that HS- and CH-cells respond with graded shifts in membrane potential, while H1- and H2- cells are spiking neurons. The HS- and H1-cells were recorded simultaneously, as were the CH- and H2-cells.

This model consisted of a single HS-, CH-, H1-, H2, and Hu-cell on each side of the brain. The connectivity of the cells, outlined in figure 3.14, was based in the double recordings of Haag and Borst (2001, 2002) and the ablation experiments performed here (Input Circuitry to HS- and CH-cells, pg 44). Each cell, except for the CH-cells, receives the summed input from an array of 5 motion detectors. The PD of the HS- and Hu-cells is front-to-back, while the PD of the H1- and H2-cells is back-to-front. Within a single lobula plate the HS-, and CH-cells are connected together electrically; the CH-cells supply inhibitory



## Results

input to the H1- and H2-cells and the HS-cell makes excitatory connections to the Hu-cell. The two lobula plates are connected together by the contralaterally projecting spiking cells. The H1- and H2-cells make excitatory input to both the HS- and CH-cells on the opposite side, while the Hu-cell supplies inhibitory input to the CH-cell.

The Hodgkin-Huxley currents for the HS- and CH-cells were adjusted to those measured in experiments such that each model responded as expected to current injections and visual stimulus, see methods (Borst and Haag, 1996; Haag et al., 1997; Haag et al., 1999). The synaptic characteristics were then adjusted to fit the current injection experimental data (Haag and Borst, 2001; Haag and Borst, 2002). The electrical coupling between the HS- and CH-cells was adjusted so that the response of CH-cells to ipsilateral motion was  $\sim 70\%$  that of the HS-cell. The strength of the input from H1-, H2 and Hu-cells to the contralateral HS- and CH-cells was adjusted such that the EPSP sizes evoked by the arrival of an action potential was as measured (Haag and Borst, 2001). The rectifying input from

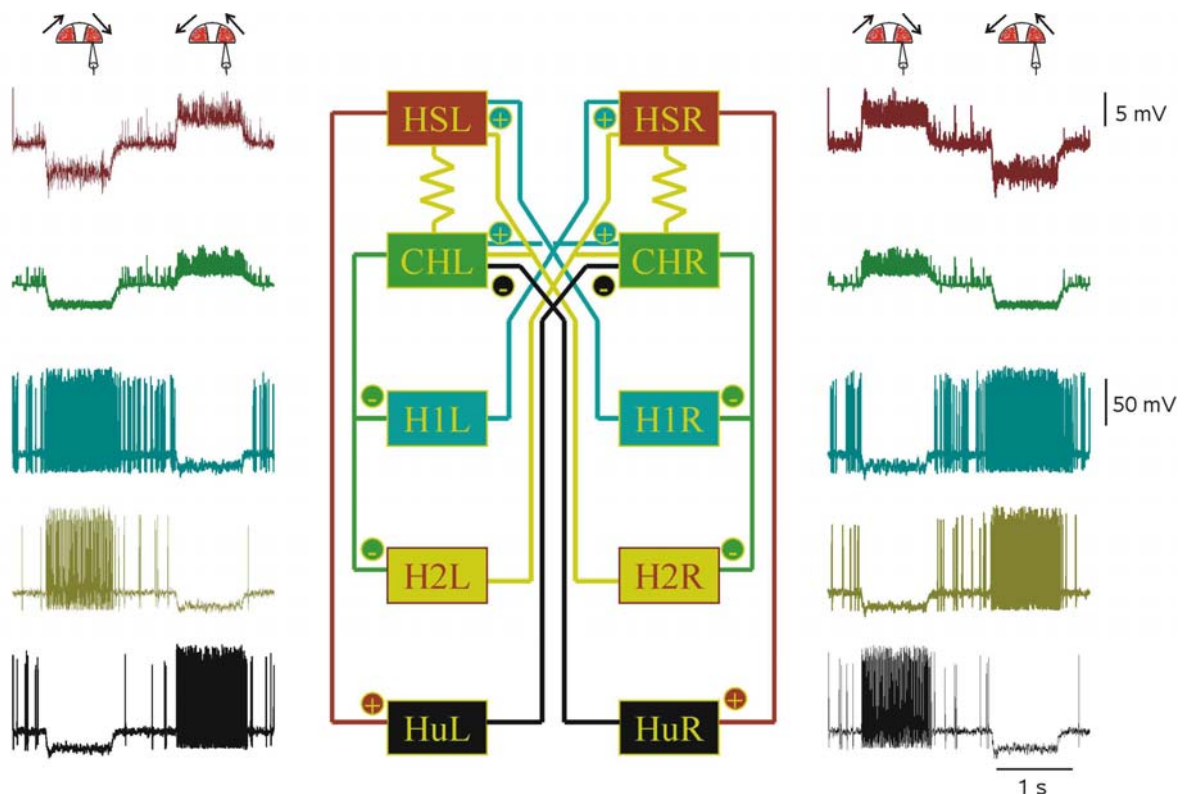


**Figure 3.14: Model Network Response to Rotation.** The model is shown in the middle without its motion detector input. The sign of the synaptic connections is indicated with a + or - for excitatory or inhibitory, respectively. The response of the 5 different LPTCs on each side sensitive to horizontal motion are displayed as a function of time around the outside. The stimulus consists of a binocular image simulating rotation, first clockwise for 1s, then counterclockwise for 1 s. Form of figure 3.14, 3.15 and 3.16 is adapted from Borst (2003)



## Results

CH-cells to H1- and H2-cell was adjusted such that current injections of positive but not negative current inhibited the H1- and H2-cells. The weights were adjusted such that +10 nA caused the H1- and H2-cells to be silenced, but current injections of  $-10$  nA had no affect. This was an amplification of the effects seen in current injection experiments performed by Haag and Borst (2001) as well as those performed here (Fig 3.12). A summary of the synaptic weights is shown in table 2.2.

After making the above adjustments the individual circuit elements responded to both monocular and binocular motion stimuli in a similar manner as the corresponding neurons in

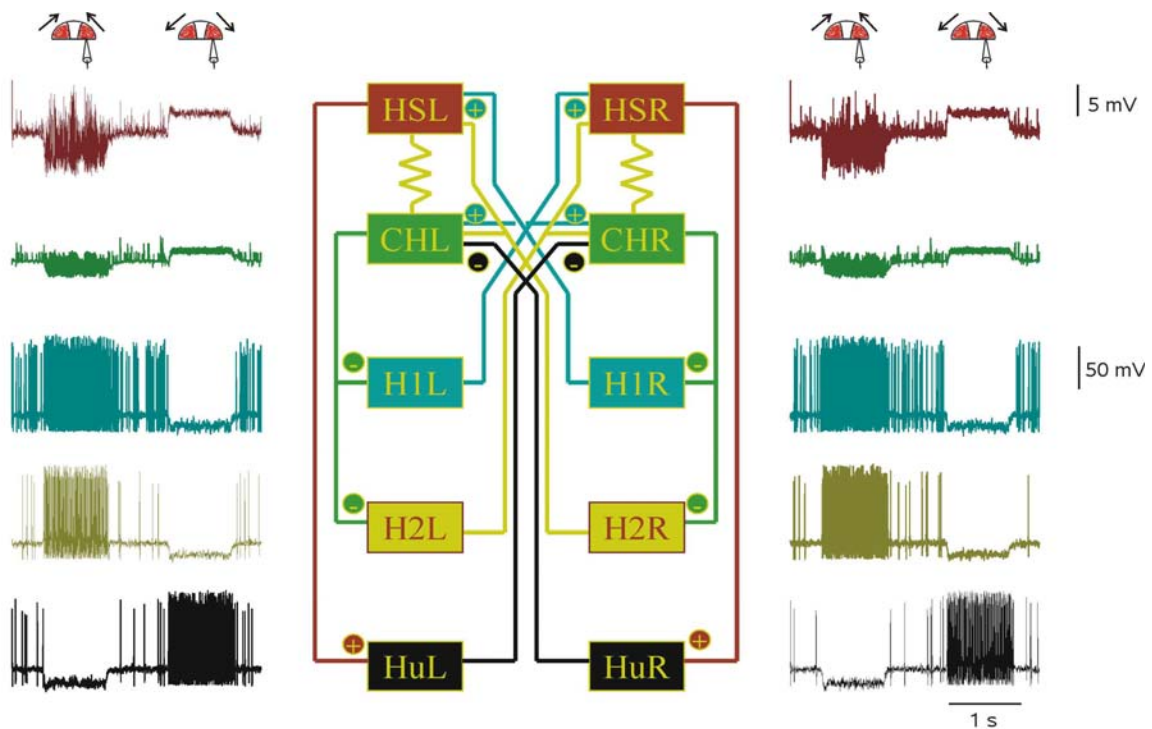


**Figure 3.15: Model Network Response to Translation.** Same as figure 3.14 except the stimulus is simulating translation, first backwards for 1 s, then forwards for 1 s.

*in vivo* (compare recording in Fig 3.13 with model results in Fig 3.14, 3.15 and 3.16). First, in response to rotational motion stimuli, all neuronal responses change polarity when the stimulus is switched from clockwise to counterclockwise (Fig 3.14). If a cell is depolarized or increased its firing rate during clockwise stimulus it hyperpolarized or decreased its firing rate during counterclockwise stimulus. In addition, the circuitry of the network amplifies the response of the two neurons that respond with graded potential shifts, the HS- and CH-cells. For example, during counterclockwise movement the left CH-cell will be excited via





## Results

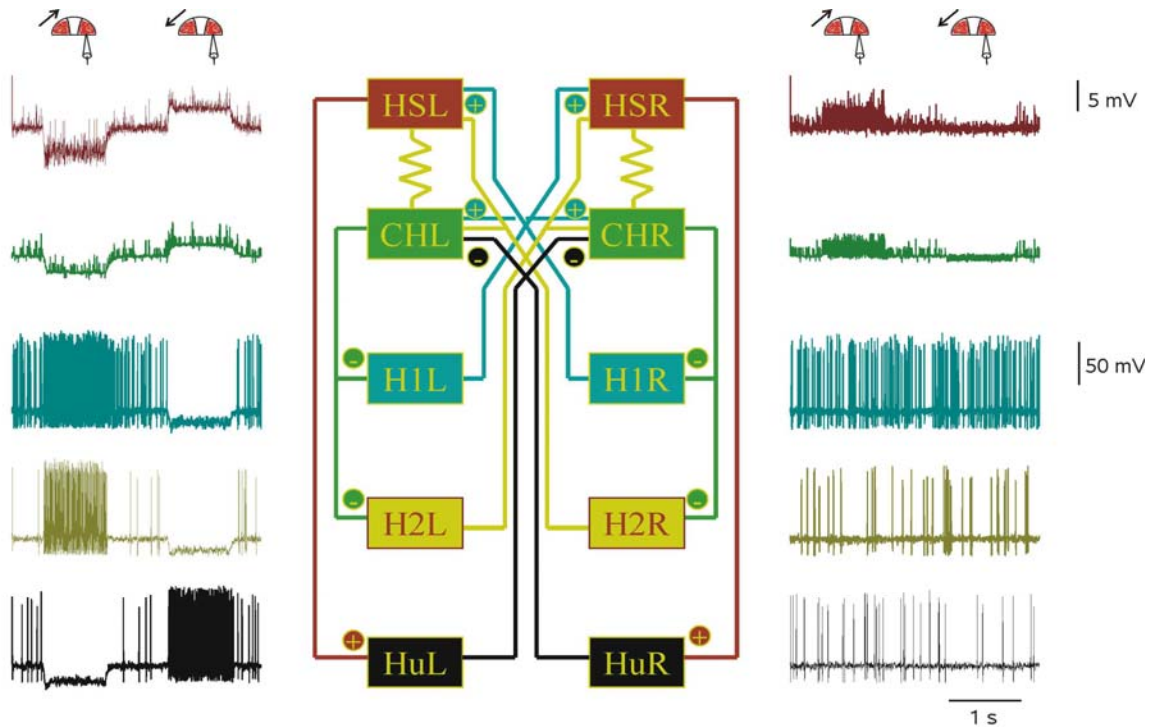


**Figure 3.16: Model Network Response to Ipsilateral Motion.** Same as figure 3.14 except the stimulus is simulating ipsilateral motion; first back-to-front for 1 s, then front-to-back for 1 s.

input from the left HS-cell causing a depolarizing shift in the membrane potential. Additionally during such stimuli, the front-to-back stimuli in front of the right eye will excite the H1- and H2-cells that make excitatory connection with the CH-cell on the left side and superimpose the depolarizing shift, caused by back-to-front motion in front of the left eye, with EPSPs. The responses of the same type of neuron in the opposite lobula plate shifts its membrane potential in the opposite direction from baseline during rotational stimuli. The amplifying effects of the circuitry seen during rotation act to reduce the neural responses during translation. Here, during contractory stimuli the CH-cells on both sides of the brain are hyperpolarized by their input from HS-cells, but the EPSP input arriving from the H1- and H2-cells from the opposite hemisphere render the final response close to zero. The individual affects of motion of the ipsilateral and contralateral eye can be seen in figure 3.16. Although, the flow-field selectivity of the HS- and CH-cells is well explained by the network presented above, the flow-field selectivity of the H2-cell is not.

The key to the flow-field selectivity of H2-cells is the difference in the signal being passed from the CH-cell during rotation and translation (Fig 3.13). In the analytic network one can



## Results

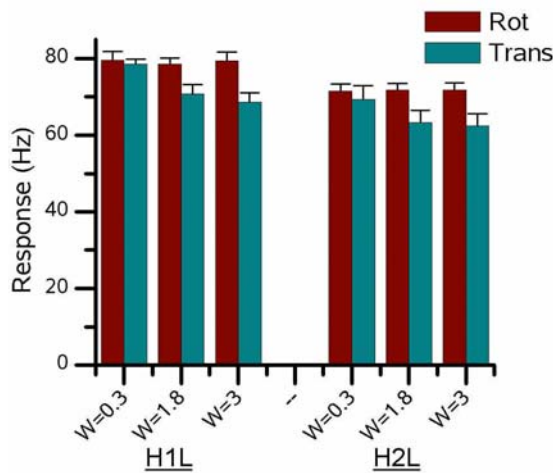


**Figure 3.17: Flow-Field Selectivity of model H1- and H2-cells.** The flow-field selectivity of the H1- and H2-cells in our network depending on the weight of the connection between the CHL and H1L/H2L cells.  $W$  is the synaptic weight between the CH- and the H1- and H2-cells. Even at a synaptic weight,  $W=3$ , ten times as big as our baseline weight, the flow-field selectivity is small. In addition the flow-field selectivity is not different for the H1- or H2-cells in the model.

see the importance of the weight of the ipsilaterally projecting unit; as  $\alpha$  is increased the separation between the gain of the CPL unit to rotation and translation separate quickly (Fig 3.11). This is analogous to examining the strength of the connection between CH-cells and the H1- or H2-cells. Also, if one examines double recording of a CH-cell and an extracellular recording of an H2-cell, one can see that they have opposite PD (Fig 3.13). Additionally, their responses during rotation and translation differ. During counterclockwise rotation the H2-cell, in the right lobula plate, is excited while the CH-cell hyperpolarizes from its resting membrane potential. During translation, a contraction, the same H2-cell is still excited but to a lesser degree than during rotation. If one looks at the signal in the axon of the CH-cell it is apparent that the mean membrane potential remains near rest but there are high frequency events that cause the signal to be depolarized for brief time periods. As the input from CH- to H2-cells only allows positive current to be passed it is the high frequency EPSP activity that has the ability to inhibit the H2-cell and could form the basis of its flow-field selectivity.

The response of H2-cells in my model exhibited almost no flow-field selectivity when the weights were set to 0.3, the weight that was determined to be most realistic (Fig 3.17). In order to test if this result was sensitive to the weight of the synapse between the CH- and H2-cells I increased the weight from 0.3 to 1.8 and 3, an increase of 6 and 10 fold respectively. I found that during simulated current injections into the CH-cell that this shut the H2-cell down even at small current injections of 1 nA (Fig 3.18). Even with such a sensitive connection the response of the H2-cell to translation was still 85 % of that found during rotational stimulus (3.16). This is in contrast to the flow-field selectivity seen *in vivo*, where the response of the H2-cell to translation is between 50 and 70 % of that seen



## Results

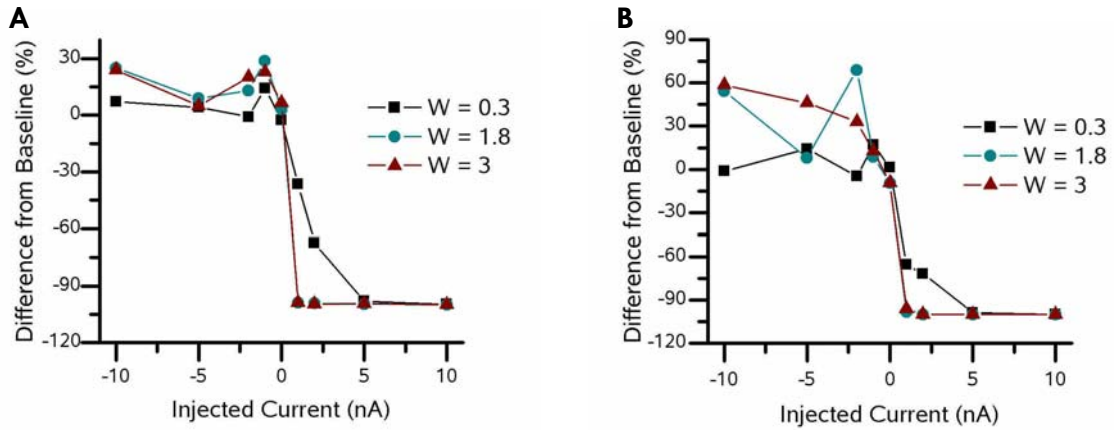


**Figure 3.18: Current Injections into Model CH-cell.** Current of varying magnitudes was injected into the model CH-cell for a period of 1s and the firing rate of the H1- (A) or H2-cell (B) was measured. The percent difference from the baseline firing rate is reported here. We find that as the weight,  $W$ , of the CH-H1 and CH-H2 connection is increased the baseline firing rate in the H1- and H2-cells are silenced by currents as small as 1 nA.

during rotation (Fig 3.7, 3.9 and 3.10). These simulations seem to suggest that the basic circuitry described here does not account for the strong flow-field selectivity of the H2-cells.

## Conclusion

The combination of ablation experiments and modeling demonstrate that the CH-cell is likely not to be responsible for the flow-field selectivity of ipsilaterally connected H2-cells. The network connections described by the Haag and Borst (2001, 2002) are not adequate to account for the flow-field selectivity found in the H2-cell. In addition, in the network model there is no difference between the flow-field selectivity in the H1- and H2-cells (Fig 3.17). Any future model should include a network architecture that allows H2-cells to be selective for rotational flow-fields but leave the H1-cell relatively unselective.



---

### Basis of the Broad Receptive Fields of VS-cells

VS-cells respond to motion presented in front of the ipsilateral eye with a graded shift in membrane potential superimposed with high frequency events that are due to either active currents or synaptic input. Active properties are present in each VS-cell and produce spikelets that are particularly prominent in the VS1-cell (Hengstenberg, 1977; Hengstenberg, 1982; Haag et al., 1997), while EPSP activity in medial VS-cells (VS7-10) is due to excitatory input, putatively from a spiking interneuron (Haag and Borst, 2004). In figure 3.20A, a schematic of the receptive fields of a VS2-, VS4- and VS6-cell is shown together with the connectivity among VS-cells as determined via double intracellular recordings (Haag and Borst, 2004). Each VS-cell has a receptive field centre (black arrows) that is attributed to the integration of local motion information across its dendrites (Borst and Egelhaaf, 1992; Haag et al., 1992; Single and Borst, 1998; Haag et al., 2004a). The location of the dendrites within the lobula plate corresponds to the position receptive field centre: as one moves laterally in the lobula plate the receptive fields of the cells shift frontally. In addition, each cell responds to motion stimuli outside its central receptive field (Krapp et al., 1998. See also Fig 1.8A). For example, all the VS-cells respond to downward motion across a much broader slice of visual space than predicted by the extent of their dendrites (grey arrows in fig 3.20).

### Neural Identification

Each VS-cell has a unique anatomy and location within the lobula plate (Hengstenberg et al., 1982; Krapp et al., 1998). However, to identify a single VS-cell can be ambiguous unless a cautious analysis of its dendritic structure is done: it helps greatly if more than one VS-cell is stained. In order to add a quantitative variable to the qualitative list defining each VS-cell I have measured the relative location of each VS-cell's main ventral dendrite in the lobula plate. To calculate the position of each cells thick ventral dendrite I used data



## Results

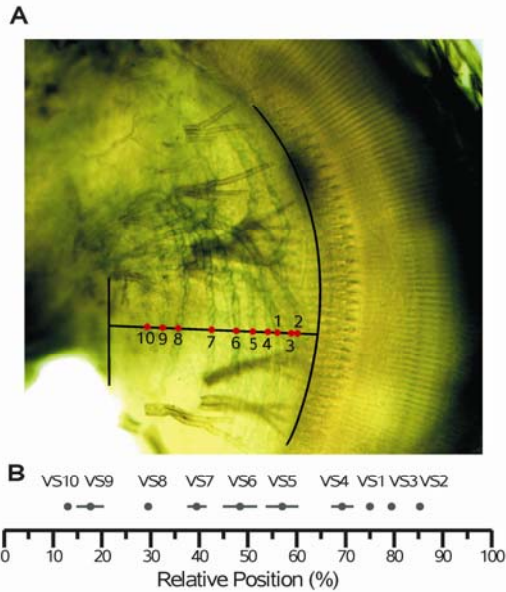


**Figure 3.19: Neural Identification.** **A)** A picture of the the lobula plate where the VS-cells have been stained with Neurobiotin. The position of each ventral dendrite is marked with a red dot. The edges of the lobula plate are marked with vertically orientated black lines. The relative position between the two edges was measured. **B)** The average position of each ventral dendrite in the lobula plate. Data was taken from 9 flies where 3 to 10 VS-cells were labels with either Neurobiotin or fluorescent dyes. Each point is the mean  $\pm$  SEM. Neurobiotin stained brains courtesy of Renate Gleich, Dietmute Buringer and Jurgen Haag.

acquired from 9 flies where a minimum of 3 VS-cells were stained. The cells were either filled with a fluorescent dye during intracellular recordings ( $n=7$ ; In 5 of the flies cells were filled by me and in 2 by Jurgen Haag), or with Neurobiotin ( $n=2$ ; filled by Renate Gleich. Data from Haag and Borst, 2005). Each thick ventral dendrite was assigned a location between 0 and 100 as determined by its relative position between the medial (0) and lateral (100) edges of the lobula plate. By assigning a relative position for each ventral branch I avoid the ambiguities caused by rotations of the pictures (Fig 3.19). I found that the order of the ventral dendrite is from lateral to medial occurs, except for the VS1-cell, as expected by the naming system. Each thick ventral branch shifts  $\sim 10\%$  across the lobula plate per cell. I marked each recorded VS-cell by dye injection and used the above measurements combined with a qualitative analysis of each cell's dendritic structure to determine the identity of each recorded cell. By combining the subjective anatomical information with a quantification of the location of each VS-cell's main ventral dendrite I could unambiguously identify each filled VS-cell.

### The Receptive Fields of VS-cells

In figure 3.20B sample traces of a VS2- and VS4-cell recorded from the same fly are shown. Notice that both cells respond to downward motion with a depolarizing shift in membrane potential. However, the azimuthal stimulus position where they are maximally responsive differs: while the maximum response of the VS2-cell is obtained at a horizontal position of  $5^\circ$ , the VS4-cell responds most strongly to pattern motion at  $52^\circ$ . In addition, both cells exhibit at least small responses at all stimulus locations.



## Results

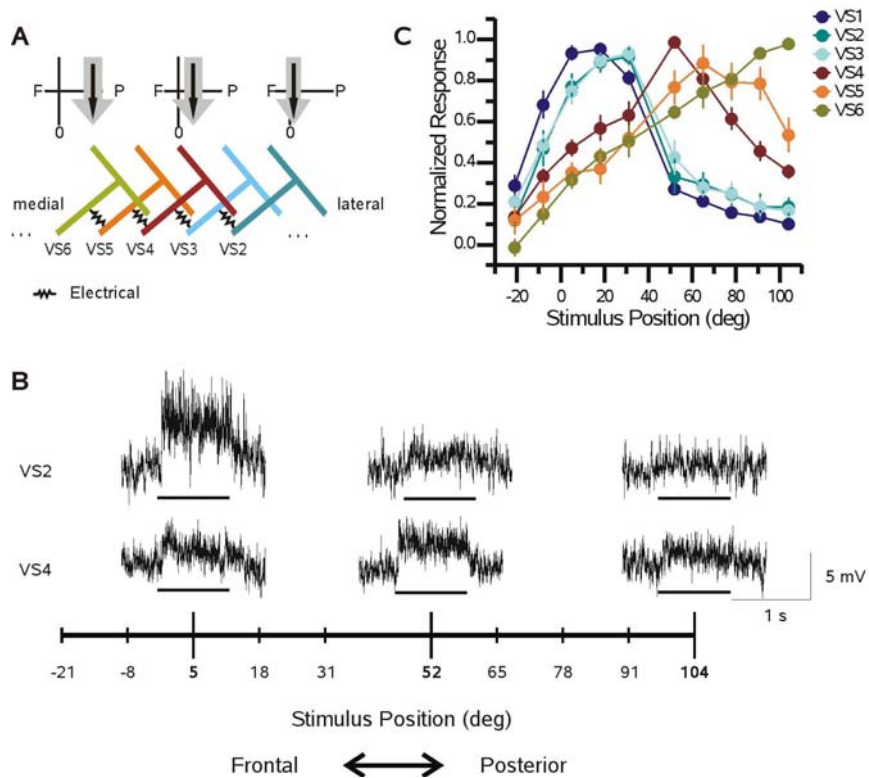


**Figure 3.20: VS-cell Network and Receptive Fields.** **A)** Schematic network of VS-cells. Above the VS6-, VS4-, and VS2-cell is a cartoon of each cell's receptive field (grey and black arrows). The black arrow indicates each cell's central receptive field, while the grey arrows illustrate its spatial extent. As one moves laterally in the lobula plate the receptive fields move frontally in visual space. **B)** Single responses of a VS2- and VS4-cell recorded from the same fly illustrate the basic response properties of VS-cells. Note that both cells respond to downward motion with a graded shift in membrane potential. The response amplitude depends on the stimulus position (see arrows). For each trace the stimulus was applied for 1s. **C)** Responses of 6 VS-cells to downward motion as a function of stimulus position. 0 deg on the x-axis represents the position directly in front of the fly, and positive numbers represent positions on the same side where the cells were recorded. Each data point is the mean response, normalized with respect to its maximum,  $\pm$  SEM. Note the strong overlap of VS1- ( $n=12$ ), VS2- ( $n=7$ ) and VS3-cells ( $n=9$ ). In addition the responses of the VS4- ( $n=13$ ), VS5- ( $n=5$ ) and VS6-cells ( $n=6$ ) shift posteriorly.

The receptive fields of VS-cells (1-6) were determined in response to thin upright stripes of horizontal grating moving vertically (fig 3.20C). Each data point is the normalized mean  $\pm$  SEM. The two most striking features of the VS-cells' receptive fields are their width and the amount of overlap between neighbouring cells. In particular, the VS1-, VS2- and VS3-cells receptive fields are almost identical. Each of these three cells shows a strong response, greater than 33% of maximum, at positions ranging from  $-8^{\circ}$  to  $52^{\circ}$ . In addition, significant responses can still be detected at the most posterior stimulus positions ( $91^{\circ}$  and  $104^{\circ}$ ). The VS4-, VS5- and VS6-cells also have highly overlapping receptive fields though not to the same extent as those of the VS1-, VS2- and VS3-cells. The



## Results

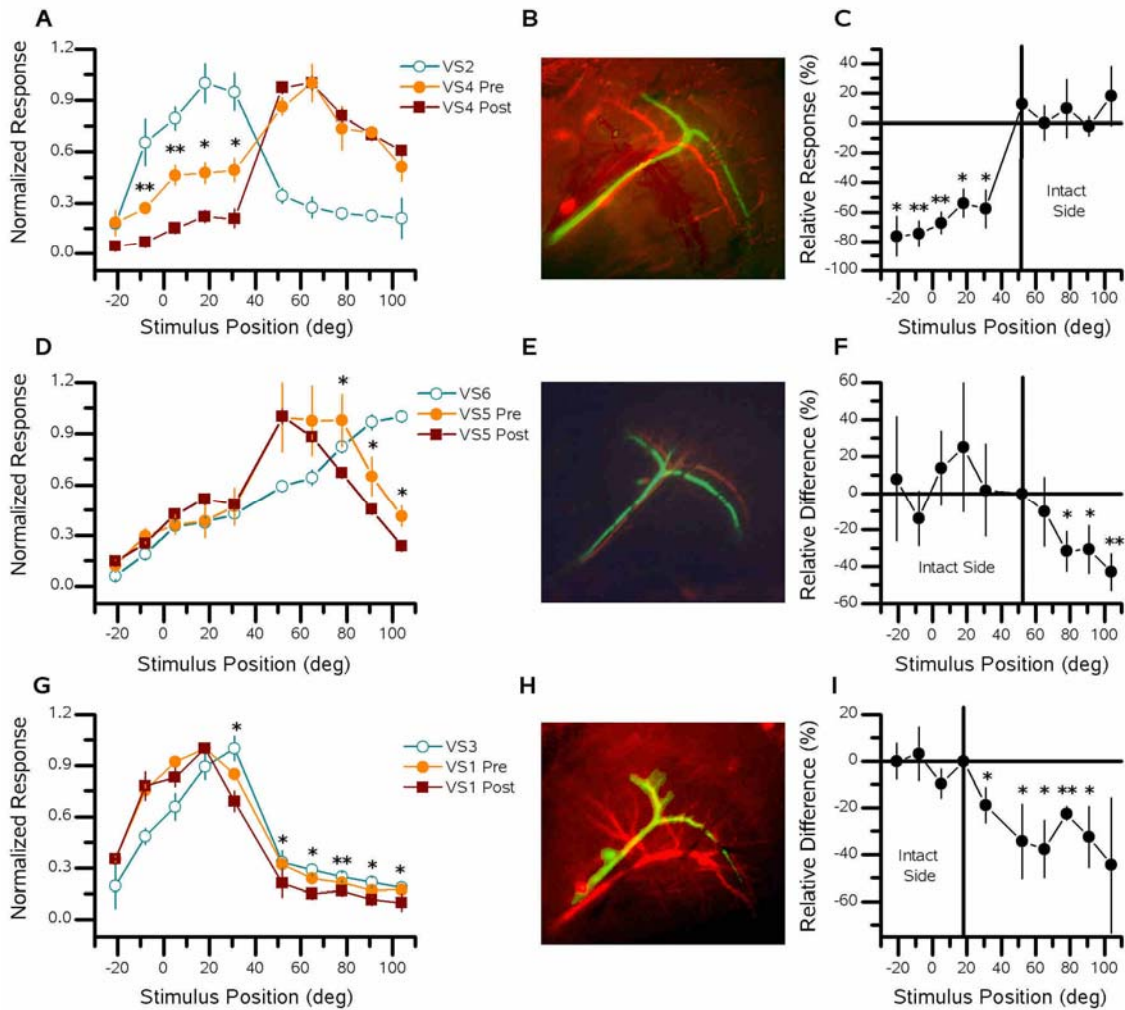


**Figure 3.21: Proximal Cell Ablations.** Three examples of the effect of ablating individual VS-cells (blue cell in B, E and H) on the receptive field of a neighbour or next-of-neighbour VS-cell (red cell in B, E and H). In A, D and G the open circles connected with the dotted blue line is the receptive field of the ablated cell (blue cell in picture), the filled orange circles is the receptive field of the VS-cell in the intact animal (red cell in picture), and the dark red filled squares is the receptive field after the blue cell has been ablated. The x-axis shows the horizontal position at which the stimulus was applied. The receptive field for each set of recordings was normalized to the maximum response. The stars indicate positions at which significant changes between the pre vs post responses of the recorded VS-cell occurred (\*  $p < 0.05$ ; \*\*  $p < 0.001$ ). In C, F and I the relative difference  $\frac{post-pre}{pre} \times 100$  (in %) between the pre (orange) and post (dark red) responses at each stimulus location is shown. The vertical line indicates the stimulus position where the intact (red) cell had its peak response. **A)** An example of a VS4-cell's receptive field before and after the ablation of a VS2-cell. **B)** Picture of VS4- and VS2-cells. **C)** Relative difference (%) of pre vs post response of the VS4-cell after the ablation of the VS2-cell. **D)** A second example of a neighbour-neighbour ablation, demonstrating the deficit a VS5-cell (red cell) experiences after the ablation of a VS6-cell (blue cell). **E)** Picture of VS5- and VS4-cells. **F)** Relative difference (%) of pre vs post response of the VS5-cell after the ablation of the VS6-cell. **G)** A third example of a neighbouring cell ablation, demonstrating the change of a VS1-cell (red cell) after the ablation of a VS3-cell (blue cell). **H)** Picture of VS1- and VS3-cells. **I)** Relative difference (%) of pre vs post response of the VS1-cell after the ablation of the VS3-cell.



## Results

receptive field peaks of the VS4-, VS5- and VS6-cells are located, as expected from the location of each cells' dendrite, at  $52^{\circ}$ ,  $78^{\circ}$  and  $104^{\circ}$  respectively. However, these three cells have exceptionally wide receptive fields showing significant responses at every stimulus position, with responses above 33% of the peak spanning  $112^{\circ}$ ,  $99^{\circ}$  and  $86^{\circ}$ , respectively (fig 3.20C). Note that the stimulus device did not allow us to record the full extent of these cells receptive fields as our most posterior stimulus was centered at  $104^{\circ}$ . Using a different stimulation design, unambiguous responses to downward motion have been noted in the VS4-, VS5- and VS6-cells across the whole ipsilateral visual field (Krapp et al., 1998). Another interesting feature of the receptive fields is the apparent grouping of the different VS-cells. In particular, the separation between the receptive fields of the VS3- and VS4-cells is much greater than that between the receptive fields of VS2 and VS3 or VS4 and VS5, respectively.

### Proximal vs Distal Ablations

The broadening of each VS-cell's receptive field, beyond its central receptive fields, has been attributed to input from neighbouring cells via electrical synapses in the axons (Haag and Borst, 2004). These electrical connections are thought to be solely between neighbouring VS-cells. According to this view, for example, if the VS5-cell is influenced by the input to the dendrites of the VS2-cell, this information must pass through both the VS3- and VS4-cell before affecting the activity of the VS5-cell. In order to determine if the electrical coupling of neighbouring VS-cells does indeed affect the width and overlap between neighbouring VS-cell's receptive fields I ablated single VS-cells and examined the receptive field structure of a nearby cell. In each experiment I first filled a single cell with Fluorescein (green cells in Figs 3.21 and 3.26). After withdrawing the electrode I filled a second cell with Alexa568 (red cells in Figs 3.21 and 3.26). Then I recorded the response of this cell to downward motion at several positions, both before and after the ablation of the Fluorescein filled cell. Figure 3.21A shows how the ablation of a VS2-cell affects the receptive field shape of a VS4-cell. Before ablating the VS2-cell, the VS4-cell responded strongly ( $\sim 50\%$  of its peak response) to stimuli at those positions corresponding to the VS2-cell's receptive field maxima (From  $0$  to  $30^{\circ}$ ). After the ablation (of the VS2-cell) the response of the VS4-cell at the stimulus locations  $5^{\circ}$ ,  $18^{\circ}$  and  $31^{\circ}$  dropped significantly ( $P < 0.05$ ) from  $\sim 50\%$  to  $\sim 15\%$  of its peak response. This drop in response magnitude is also evident in the most frontal stimulus position where the VS2-cell's response is only  $\sim 10\%$  of the peak (figs 3.21A and C). In contrast, the relative response magnitude





## Results

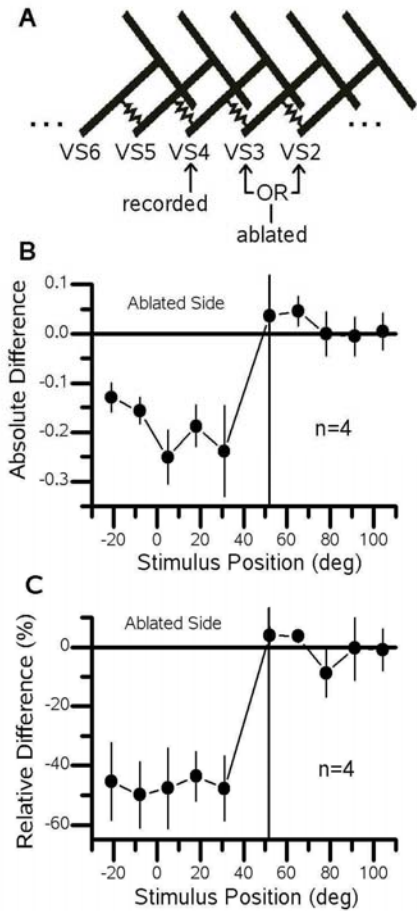


**Figure 3.22: VS4-cell's Deficit after the Ablation of Frontal Viewing VS-cells.**

**A)** Schematic of the VS-cell network showing the relationship between the recorded cell (VS4) and the ablated cells (VS2 or 3). **B)** Mean difference ( $\pm$  SEM) of the receptive fields (post minus the pre response) for a group of 4 VS4-cells where either a VS2- ( $n=1$ ) or VS3-cell ( $n=3$ ) was ablated. **C)** Relative difference ( $\frac{\text{post-pre}}{\text{pre}} \times 100$ , in %) for the data shown in B. Note that at each stimulus location frontal to the peak response of the VS4-cell the response drops by approximately the same amount ( $\sim 50\%$ ).

of the VS4-cell was maintained in the posterior stimulus positions where the VS2-cell is not highly responsive and input to the VS4-cell can be both direct from local motion elements or via other VS-cells with more posteriorly located receptive fields (fig 3.21C). This example implies that the VS2-cell supplies information to the VS4-cell about its own receptive field and that of the VS1-cell, but not about cells with receptive fields more posterior than its own.

This association among nearby VS-cells is not unique to the VS4-VS2 pair. Figures 3.21D-F contain an example of a VS5-cell, both before and after the ablation of a VS6-cell. Here, the ablated cell had a more posterior receptive field. Consequently, when the VS6-cell was ablated, the VS5-cell experienced a decline of sensitivity in the posterior, but not in the frontal divisions of its receptive field (fig 3.21D and F). A third example (fig 3.21G-I) clearly demonstrates how one cell can act as a conduit for passing information not only about its own activity but that of other cells further away. Figure 3.21G shows the



## Results

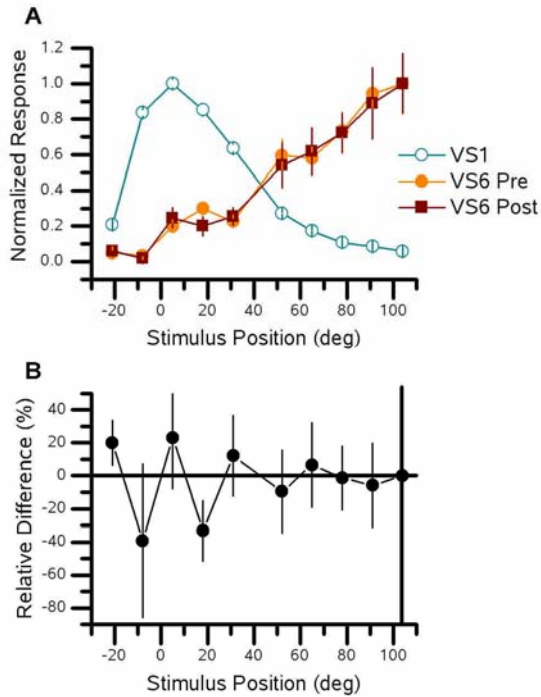


**Figure 3.23: Distal Ablation.** An example of a VS6-cell after the ablation of a distant VS1-cell. **A)** A VS6-cell's receptive field before and after the ablation of a VS1-cell. **B)** Relative difference (%) of the VS6-cell's response pre vs post ablation

receptive field of a VS1-cell both before and after the ablation of a VS3-cell. As in the previous example, the sensitivity in the VS1-cell's receptive field fell in the posterior parts of its receptive field, albeit to a lesser degree (fig 3.21G and I). Nevertheless, the percentage change was large and significantly decreased ( $p < 0.05$ ) at each stimulus position posterior to the peak response of the VS3-cell, thus demonstrating that the input to the VS1-cell about these posterior stimulus positions is relayed via the VS3-cell.

To indicate the reproducibility of the effect of ablating single VS-cells on the receptive fields of nearby neurons I grouped four experiments of VS4-cells where one of two more frontally viewing VS-cells, the VS2- or VS3-cells, was ablated (fig 3.22). Figure 3.22 shows both the absolute (fig 3.22B) and relative difference (fig 3.22C) in the responses of the VS4-cells after the ablation of single VS2- ( $n=1$ ) or VS3-cells ( $n=3$ ). Each data point is the mean difference ( $\pm$  SEM) between the normalized response after the ablation and the normalized response in the intact animal. The response of the VS4-cells at the position where the response of the VS2- and VS3-cell are largest, for stimulation at  $5^\circ$ ,  $18^\circ$  and  $31^\circ$ , dropped by 0.225 (fig 3.22B), which is a relative difference of -46 % (fig 3.22C). The mean relative difference for the two most frontal stimuli position field,  $-5^\circ$  and  $-21^\circ$ , amounted to -48 % and, thus, was almost identical to that of the other three frontal stimulus positions. These two stimulus position are located more frontally than the peak of



## Results

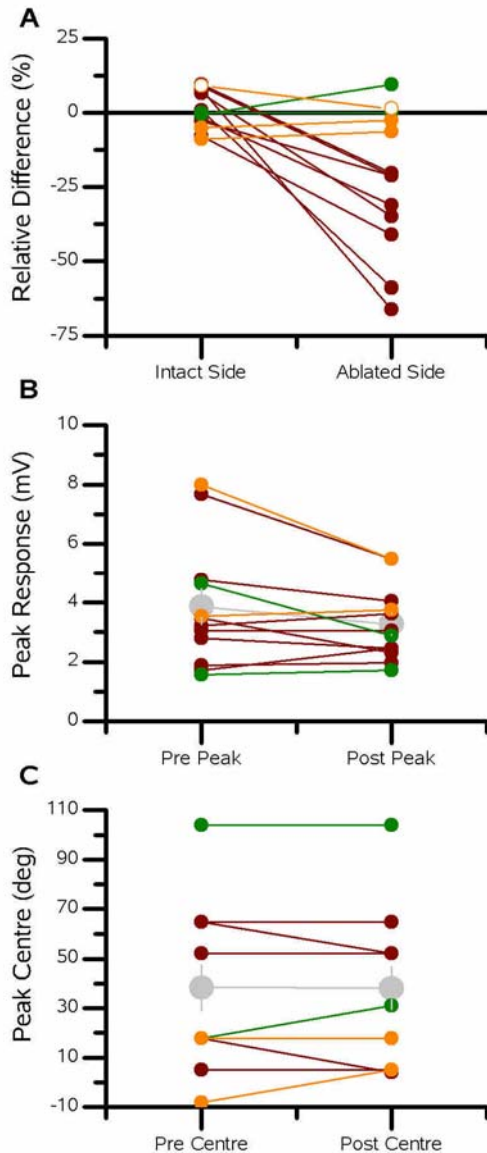


**Figure 3.24: Summary of Ablations.**

**A)** Mean relative difference between post and pre ablation response shown for both the ablated side and intact side of the recorded VS-cells' receptive fields. The ablated side consists of those stimulus positions under and beyond, from the point of view of the recorded cell, the peak of the ablated cell. The intact side comprises all other stimulus positions. In each graph the red data points represent the neighbour ablations, the green data points represent the distant ablations and the orange represent VS1-cell ablations while recording one of the medial VS-cells. **B)** Peak responses for each experiment before (Pre) and after (Post) the ablation of a single VS-cell. The grey data points represent the mean  $\pm$  SEM of all experiments. **C)** Peak response position for each cell before and after the ablation of another VS-cell. The grey data points represent the mean  $\pm$  SEM.

the VS2- and VS3-cells' receptive fields and indicate that the input from more frontal viewing cells are also interrupted when a single VS-cell is ablated. This finding is in contrast to the change in the response of the VS4-cells in the more posterior stimulus position. Here the VS4-cells' response did not change at all. These results show that the VS4-cell inherits the frontal part of its receptive field from VS2- and VS3-cells and also imply that the VS1-cell plays a role.

In order to determine if cells whose respective receptive field peaks are widely separated affect each other I performed experiments where the cell pairs were between 4 and 6



## Results

cells apart. An example of a VS6-cell with a VS1-cell ablated demonstrates that cells far apart do not influence each other (fig 3.23). After the VS1-cell was ablated there was no detectable change in the receptive field structure of the VS6-cell. Similar results were obtained with a VS3-VS7 pair (data not shown). These two examples illustrate that cells between 4 and 6 cells apart do not affect each others response.

A summary of all ablations performed is shown in figure 3.24. The mean relative change for the intact versus the ablated side is plotted for each individual experiment (fig 3.24A). I define the ablated side to include all azimuthal stimulus positions on the same side of the recorded cell's receptive field peak as the ablated cell, not including the position of the

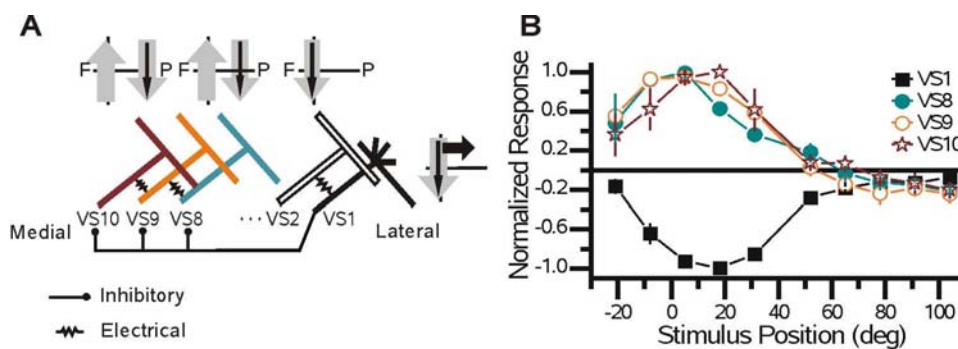


**Figure 3.25: VS1- and the Medial VS-cells' cell Receptive Fields.** **A)** Schematic network of VS-cells highlights the hypotheses of Haag and Borst (2004). It is unclear to which of the medial VS-cells the VS1-cell provides inhibitory input too. The receptive field of the VS2-, VS8-, and VS10-cell are shown above the respective cell. The format is the same as figure 1A. **B)** The receptive fields of the VS1-cell and the 3 most medial, posterior viewing, VS-cells in response to upward motion. See figure 1B for explanation. Note the overlap between the VS8- (n=2), VS9- (n=3) and VS10-cell (n=2). In addition the VS1-cell appears to mirror that of the medial VS-cells (n=5).

peak response. The intact side consists of the location of the peak response and those on the opposite side of the peak from the ablated cell. Note that for each experiment where a neighbouring, or neighbouring but one, cell was ablated the response on the ablated side dropped, whereas it remained the same on the intact side (red data points fig 3.24A).

Because of concerns that cell ablations might alter the primary visual response of VS-cells, I compared the peak response amplitude and the stimulus position at which this peak occurs for each cell (fig 3.24B and C). Before and after ablations I found no consistent effect of ablating a single neuron on the response of neighbouring cells. The mean peak response for all experiments fell from 3.9 mV to 3.3 mV, which was not significant (n=12,



## Results

$p=0.42$ ). For the set of 8 ablations where a neighbour or next of neighbour cell was ablated, the peak response also did not change. In addition, the stimulus position of the peak response remained stable. These results suggest that the observed narrowing of the receptive fields are not due to damage done to the input from the local motion detectors but rather to deficits in the input from neighbouring VS-cells.

### VS1-cell Input to the Medial VS-cells

In addition to possessing the above-mentioned broad receptive fields medial VS-cells (VS8-10) respond unexpectedly to vertical motion presented in the frontal visual field, far from their presumed local motion input (Krapp et al., 1998). Current injection into VS1-cells influenced the activity of the medial VS-cells (Haag and Borst, 2004), and this connection has been proposed to underlie the medial VS-cells' sensitivity to motion in the frontal visual field (fig 3.25A). In line with this proposal (Haag and Borst, 2004) the receptive fields of the medial VS-cells (VS8-10) and the VS1-cell have opposite polarity (fig 3.25B): upward motion in the frontal visual field hyperpolarizes the VS1-cell, but the same stimulus depolarizes the VS8- to VS10-cells. In addition, the receptive fields widths of the medial

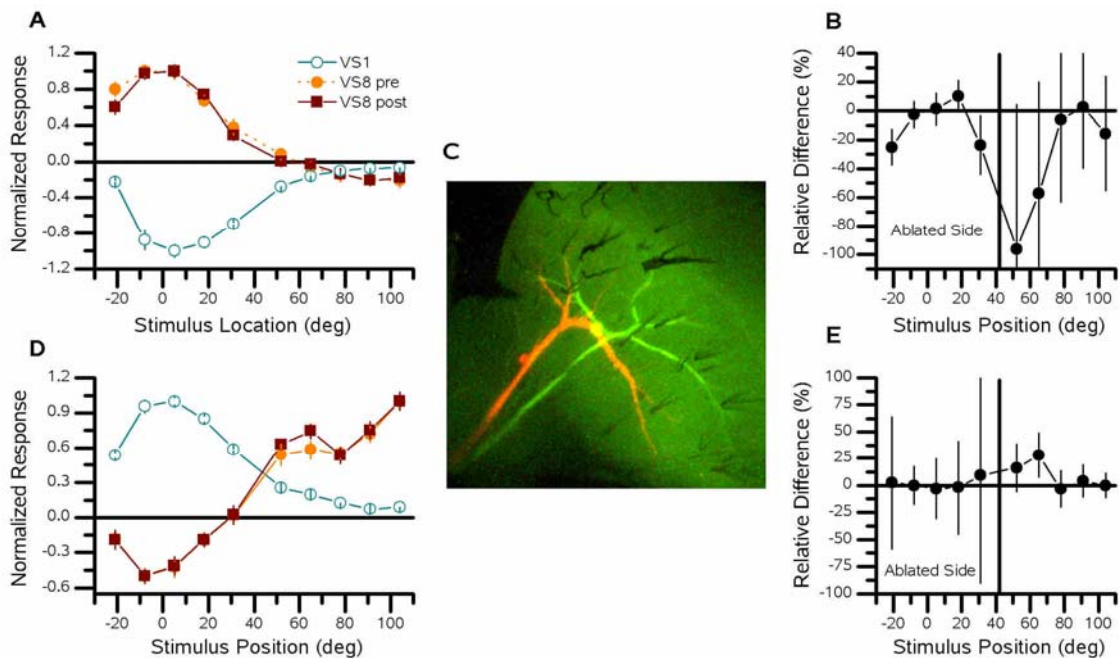


**Figure 3.26: VS1-cell Ablation.** Example recordings of a VS8-cell (red cell) before and after the ablation of a VS1-cell (green cell). The vertical line separates the five frontal stimulus positions, the ablated side, from the 5 lateral stimulus positions, the intact side. **A**) Response of a VS8-cell to upward motion before and after the ablation of a VS1-cell. **B**) Relative difference (%) of the pre versus post response of the VS8-cell to upward motion. **C**) Picture of the two recorded cells. **D**) Response of the same VS8-cell to downward



## Results

VS-cells in response to upward motion overlap, which is consistent with a common input. Each cell produced a response of greater than 33% spanning a minimum of  $50^{\circ}$  ranging from  $-21^{\circ}$  to  $31^{\circ}$ .

In order to determine whether inhibitory input to the medial VS-cells from the VS1-cell can account for their sensitivity to vertical motion in the frontal visual field I recorded the receptive fields of single medial VS-cells before and after the ablation of the VS1-cell. In figure 3.26 the receptive field to upwards (fig 3.26A) and downwards (fig 3.26D) motion of a VS8-cell (red cell in fig 3.26) is shown before and after the ablation of a VS1-cell (green cell in fig 3.26). No significant differences were found after the ablation of the VS1-cell (fig 3.26B, G). This was also true for another ablation experiment involving a VS9-cell's response to upward motion before and after the ablation of VS1-cell. Here, unlike in the proximal and distal ablations, the ablated side included the 5 most frontal stimulus positions, while the intact side included the 5 most posterior stimulus positions. The grouped average response magnitude of the five frontal and five posterior stimulus positions did not change significantly after the ablation of a VS1-cell (fig 3.26A, orange points).

In contrast to our expectations, these experiments show that input from the VS1-cell cannot be solely responsible for the sensitivity of the three medial VS-cells to vertical motion in the frontal divisions of their receptive fields.

## Conclusions

VS-cells respond to stimuli presented outside of the visual space expected from the retinotopy of the lobula plate and the extent of their dendritic arborization. The receptive fields are unexpectedly wide, and in the case of the medial VS-cells (VS8-10) include frontal sensitivity when only posterior vision was expected (Krapp et al., 1998). The results of these ablation experiments show that lateral connections among VS-cells form the basis of their unexpectedly wide receptive fields, which substantially exceed the proportion of the lobula plate covered by their dendrites. I also provide evidence that VS-cells connect sequentially in a chain like fashion beginning with the VS1-cell on the lateral edge of the lobula plate and continuing through each VS-cell to the VS10-cell on the lobula plate's medial edge. On the other hand, how the medial VS-cells acquire sensitivity in the frontal visual field remains unclear.



---

### Vertical-Horizontal Interaction

The H1- and H2-cells are spiking neurons that connect the two lobula plates, providing input to the HSN-, HSE, and both CH-cells. They respond to horizontal front-to-back motion presented in front of the ipsilateral eye with an increase in firing rate of up to 300 Hz. There exists one cell in each lobula plate. In addition to their horizontal sensitivity they have been shown to be sensitive to vertical motion in the frontal but not posterior divisions of the ipsilateral visual fields (Haag and Borst, 2003). This sensitivity to vertical motion in the frontal receptive field has been suggested to be a consequence of excitatory input from the VS1-cell (Haag and Borst, 2003). Here I elaborate on the experiments of Haag and Borst (2003) and, additionally perform single ablations of the VS1-cell in order to determine if this cell is indeed responsible for the vertical sensitivity of the H1- and H2-cells.

First, I tested how reliably I could record the H1- and H2-cells using extracellular electrodes. When recording in the known vicinity of the axonal arborizations of H1-cells I found two types of cells. Both responded to horizontal front-to-back motion with a response of 80-100 Hz. However, in response to vertical motion the cells divided into two groups: one strongly responsive to vertical motion in the frontal visual field, type A, while the other was responsive in a more lateral portion of the visual field, type B (Fig 3.27C). The type included here in the ablation and current injection experiments was type A as it responded strongly to downward motion in the frontal portion of the visual field as previously shown (Haag and Borst, 2003). When recording near the axon terminals of the H2-cell I could reliably record cells that responded to horizontal and vertical motion as expected (Fig 3.27).

In order to determine if the input from VS1-cells is a reasonable signal to drive the vertical sensitivity of H1- and H2-cells I recorded the receptive fields of the VS-, H1- and H2-cells to vertical downward motion (Fig 3.28). During a double recording of one spiking (H1 or H2) and one graded response (VS) cell I measured their receptive fields in response to thin vertically moving grating. In Fig 3.28A the relative response to the downward movement



## Results

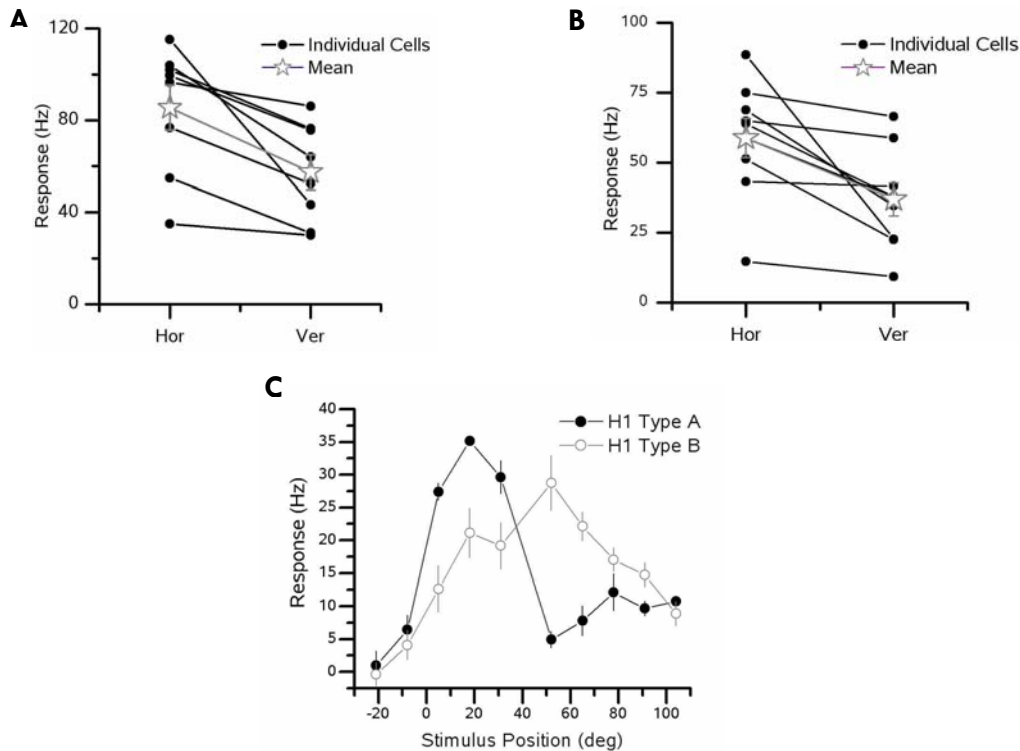


**Figure 3.27: Horizontal vs Vertical Response of H1- and H2-cells.** The response of extracellularly recorded H1- or H2 -cells to horizontal (back-to-front) and vertical (downward) motion in their frontal visual field is shown. The black circles are the response of individual cells, while the grey star is the population average. **A)** The response of H1-cells (A) to horizontal motion in the frontal visual field was compared to its response to horizontal motion. **B)** The response of H2-cells to horizontal and vertical motion was compared. **C)** The response of two cells that responded as H1-cells to horizontal motion but had different responses to vertical motion. In the ablation and current injection experiments only H1-cells that responded strongly in the frontal and not in the posterior visual fields were included.

of a VS1, VS2 and H1-cell from a single fly demonstrates clearly the overlapping nature of these cells receptive fields to vertical motion. They appear to match almost perfectly. This is also evident in the population averages (Fig 3.28B). These receptive field measurements demonstrate that either the VS1- or VS2-cell have receptive fields that could drive the vertical response of the H1-cell.

However, it has previously been demonstrated that current injected into the VS1-cell, but not the VS2-cell, causes a correlated change in the firing rate of the H1-cell (Haag and Borst, 2003). Here, in addition to checking for the sensitivity of this connection by injecting different magnitudes of current, I injected current at different locations: the VS1-cell axon near its dendrites (n=4), the VS1-cell axon near its terminal region (n=7) and the VS2-cell near its terminal region (n=3)(Fig 3.29). I found current injected into the axon near the





## Results

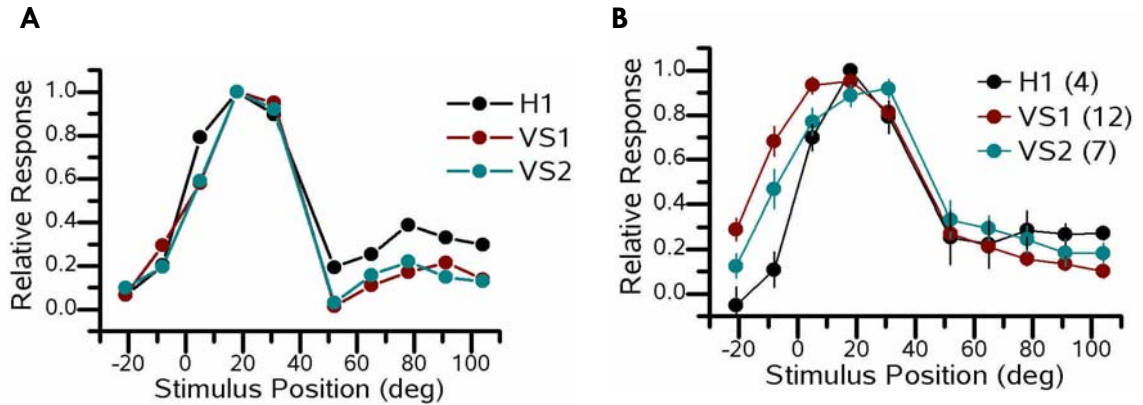


**Figure 3.28: Receptive Fields of H1 and the Frontally Viewing VS-Cells.** Each data point is the response to downward motion at the particular frontal-posterior azimuth. **A)** The receptive field of a H1-, VS1- and VS2-cell recorded from the same fly. **B)** The average receptive field as recorded from a population of flies.

dendritic end of the VS1-cell had the greatest effect while current injected near the terminal end only had a consistent influence at currents of  $\pm 10$  nA. As predicted from previous experiments the injection of current into VS2-cells had no influence on the firing rate of H1-cells. These current injection experiments provide further evidence, on top of the anatomical evidence, that VS1-cells supply input to H1-cells via dendro-dendritic connections.

### VS1-Cell Ablations

In order to test that the vertical response of the H1-cell in the frontal visual field is indeed due to input from VS1-cells, VS1-cells were selectively ablated while recording the vertical and horizontal responses of the H1-cell in the frontal visual field. In Fig 3.30A the PSTH of an H1-cell to horizontal back-to-front (black line) and vertical downward (red line) motion in an intact animal is shown. Note that the response to vertical motion, in the frontal visual field, is  $47\% \pm 0.04$  of the horizontal response, which is typical (Haag and Borst, 2003). The horizontal response is  $40.8 \text{ Hz} \pm 1.6$  while the response to vertical motion is  $19.2 \text{ Hz} \pm 1.0$ . After the ablation of the VS1-cell in this fly the vertical response disappears completely; responding at  $0.7 \text{ Hz} \pm 0.3$ . This was  $4.2\% \pm 2$  of the horizontal response of  $16.2 \text{ Hz} \pm 1.3$  (Fig 3.30C and D). On average ( $n=2$ ) the post vertical response fell from  $47.4\% \pm 3.0$  to  $10.0\% \pm 0.6$  of the horizontal response.



## Results

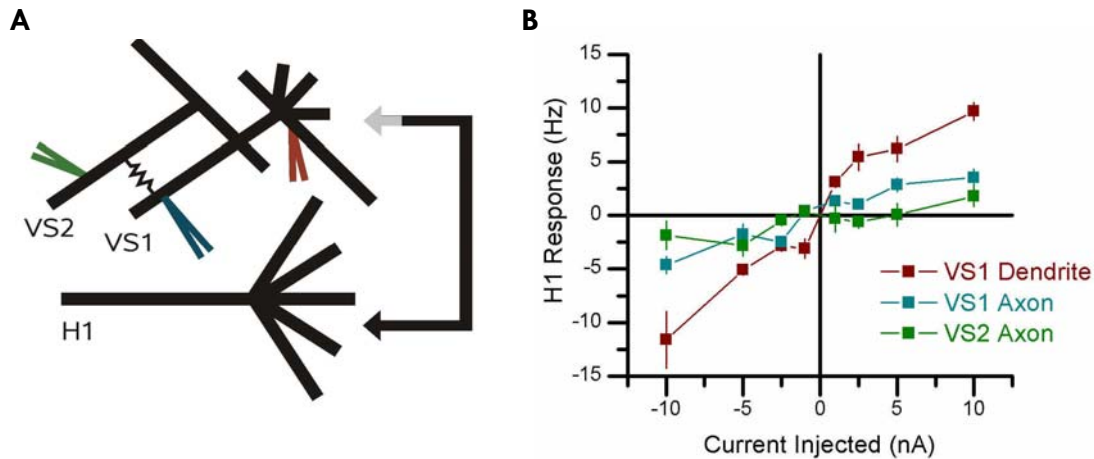


**Figure 3.29: Horizontal Vertical Interactions. A)** A schematic diagram of the interaction between the VS1- and H1-cell illustrate that aside from making lateral electrical connections with other VS-cells, the VS1-cell is also suspected to connect, via its dendrites to the H1-cell. The coloured electrodes indicate points at where we injected current while recording from the H1-cell. **B)** Current was injected into the VS2-cell axon (green, n=3), VS1-cell axon (blue, n=7) or VS1-cell thick dendritic branch (red, n=4) while recording the spiking activity of the H1-cell. The current injected is displayed on the x-axis while the resultant change in H1-cell firing rate is displayed on the y-axis.

One important caveat to these results is that after the ablation of the VS1-cell the horizontal response of the H1-cell is also compromised. In our two ablation experiments the firing rate of to horizontal motion fell from 40.8 Hz  $\pm$  1.6 to 16.2 Hz  $\pm$  1.3 after the ablation of single VS1-cells (Fig 3.30C). I found the VS1-cell more difficult to ablate than the other VS-cells and had to leave the laser on for an additional 90 second period at twice the normal power, i.e., 30 mW. As a control the affect of the extra laser illumination was measured without having the VS1-cell filled with Fluorescein. This lead to less robust spiking response in the H1-cell. In Fig 3.30G is the average response of H1-cells both before and after the application of the laser for 180s at 30 mW; the same as was used during the two ablation experiments. I found the response to horizontal motion dropped 56 Hz  $\pm$  10.4 to 31Hz  $\pm$  1.5 Hz (n=3). This was not accompanied by a significant change in the relationship between the vertical and horizontal response, which only dropped from 0.61  $\pm$  .13 to .45  $\pm$  .15 (Fig 3.30G and H).

## Conclusions

Here I demonstrate that the input to H1-cell from VS1-cell is responsible for the sensitivity of the H1-cell to vertical motion. I supply additional evidence that this input arrives via dendro-dendritic interactions with the VS1-cell.



## Results

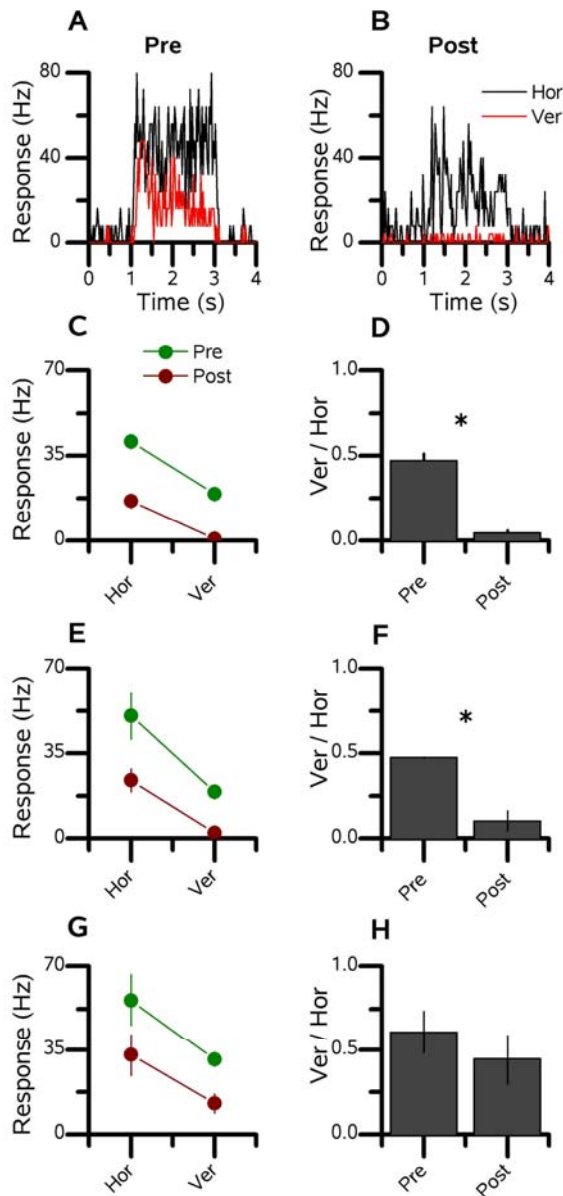


**Figure 3.30: VS1-cell Ablations.** In A and B the black line represents horizontal motion and the red line the response to vertical motion. The stimulus was applied for 1s starting at 1s. In C, E and G the green data points represent data from an intact animal and red data from a fly where a single VS1-cell was ablate (C and E) or the laser was applied for 180s at 30 mW (G). In D, F and H the normalized vertical response is shown. It vertical response was normalized to the horizontal response from the same experiment. Each bar is the mean  $\pm$  SEM. **A)** The response of the H1-cell to horizontal motion as compared to a response of to vertical downward motion. **B)** The response of the same H1-cell in A, but after the ablation of a single VS1-cell. Note that while the response to horizontal motion is still robust its response to vertical motion disappears. **C)** The mean  $\pm$  SEM response of the H1-cell shown in A and B, to horizontal motion dropped from 40.8 Hz  $\pm$  1.6 to 16.2 Hz  $\pm$  1.3; while its response to vertical motion disappeared dropping from 19.2  $\pm$  1.0 Hz to 0.7  $\pm$  0.3 Hz. **D)** The relative vertical response of the same H1-cell from A and B dropped from 47.1  $\pm$  4.1 % to 4.3  $\pm$  1.8 %. The change was significant,  $p < 0.001$  (\*). **E)** The mean response for all our experiments ( $n=2$ ) of H1-cell response before and after the ablation of the VS1-cell. The horizontal response fell from 50.4  $\pm$  9.6 Hz to 23.9  $\pm$  4.7 Hz; while the vertical response fell from 19.2  $\pm$  3.0 Hz to 2.2  $\pm$  1.5 Hz. **F)** The relative response for these two experiments dropped from 47  $\pm$  0.35 % to 10.3  $\pm$  5.9 % **G)** The response of the H1-cell to both horizontal and vertical motion drops after the application of the laser for 180s at 30 mW ( $n=3$ ). The response to horizontal motion dropped from 56  $\pm$  10.4 Hz to 33  $\pm$  8.6 Hz; while the response to vertical motion dropped from 31  $\pm$  1.5 Hz to 12.6  $\pm$  3.8 Hz. **H)** The relative vertical response stayed statistically the same. It dropped from 0.61  $\pm$  .13 to .45  $\pm$  .15 ( $p=0.44$ ).



## 4 Discussion

---

I used a single cell ablation technique to determine if the connections among LPTCs form the basis of their ability to process complex optic flow information. I found that some, but not all, of the connections between lobula plate tangential cells contributed to building their respective receptive fields. In particular the response of CH-cells is due exclusively to input from HS-cells; electrical coupling between neighbouring VS-cells forms the basis of their wide receptive fields and the input of the VS1-cell is responsible for the H1-cell's sensitivity to vertical motion in the frontal visual world. However, the inhibitory input from CH- to H1- and H2-cells is not singularly responsible for their selectivity to rotational flow-fields and the VS1-cell's input to the medial VS-cells (VS8, 9 and 10) is not sufficient to account for these cells sensitivity to vertical motion in the frontal visual field.

Below the caveats, consequences and meaning of the above results will be discussed. First the technique of laser ablations will be addressed. The results of the ablation experiments will then be dealt with as a group highlighting how the blowfly extracts useful information from the visual world. Finally, the each set of ablations will be discussed in detail, with particular emphasis on the specific consequences to visual processing of the fly.

---

### Laser Ablation Technique

The technique of photo-ablation makes it possible to assess the role of single cells within a network of neurons (Miller and Selverston, 1979). The essential principal is to fill a single cell with a fluorescent dye that breaks down easily when irradiated with the appropriate bright light. This technique was first developed by Miller and Selverston (1979) using Lucifer Yellow and a high-intensity blue light. Here I used Fluorescein and a blue laser with



## Discussion

a wavelength of 488 nm. The laser ablation technique has been successfully applied in ablating whole neurons in the lobster somatogastric ganglion (Miller and Selverston, 1979; Selverston and Miller, 1980), auditory system of the cricket (Selverston et al., 1985), cercal system of the cockroach (Mizrahi and Libersat, 2001), optic tectum of larval zebrafish (Roeser and Baier, 2003) and in the visual system of the blowfly (Warzecha et al., 1992; Warzecha et al., 1993). In addition, this technique has been shown to be useful in ablating and analyzing the function of isolated parts of neurons in the cercal system of the cricket (Jacobs and Miller, 1985), as well as in the leech (Lytton and Kristan, 1989).

One concern with this technique, however, is whether laser illumination causes unspecific damage to neurons not injected with the fluorescent dye explicitly excited by the laser. Generally, I found that the responses of both unfilled neurons (3.2) and neurons filled with Alexa568 (Fig. 3.1) were not damaged by laser illumination. Even neurons filled with Alexa488, which is selectively excited by blue light, are undamaged upon irradiation with the blue laser (data not shown). Perhaps not coincidentally, unlike Fluorescein, Alexa488 does not bleach (data not shown), suggesting a correlation between the break down of a dye and its toxicity. Warzecha et al. (1993) also found that neurons not filled with fluorescent dyes continued to function normally after laser illumination of the fly brain.

Another line of evidence suggesting that the laser does not cause unspecific damage are experiments where connected cells were ablated without having a noticeable affect on their associated cell. The best example is when CH-cells were ablated; allowing electrically connected HS-cells continued to respond normally (Fig. 3.6). In addition, the ablation of electrically coupled VS-cells did not affect the peak response of these cells to stimuli in the centre of their receptive fields (Fig 3.24), demonstrating that the individual inputs to a single cell can be assessed separately. The above is all true for ablations performed with a laser power of 15-20 mW and duration of 90-120 s.

However, when attempting to ablate the VS1-cell I had to turn the laser power up to 30-35 mW and apply it for 180 s. During such an illumination the time it took for the response of H1-cells to recover increased from 2 minutes, as seen for ablation performed at 15-20 mW, to as long as 5 minutes after exposure of 30-35 mW for 180 s. After this type of exposure I found the response of the H1-cells was decreased. They generally had a lower spontaneous firing rate and their peak firing rate during PD motion stimulus also



## Discussion

decreased (Fig 3.30G). However, similar deficits were not seen in the response of VS8-, VS9- or VS10-cells after the ablation of VS1-cell. These cells responded normally (Fig 3.26). Although it is better to use the minimum laser power necessary to ablate a neuron it is apparent that this method is relatively harmless to cells not filled with a dye that both selectively absorbs the irradiating light and breaks down easily when irradiated.

A second issue concerns the conclusions made about ablations that have no affect on the circuit. This problem is particularly acute when the input and output synapses lie close together. One clear example of the dangers of drawing conclusions from such ablation experiments is the analysis of directionally selective ganglion cells in the rabbit retina (He and Masland, 1997). They found that after the laser ablation of an amacrine cell that the directionally selective response of the connected directionally selective ganglion cell remained. Hence, it was concluded that the mechanisms for directional selectivity lie postsynaptically of the starburst amacrine cell. This was later shown to be false by ablation techniques using toxins that were either genetically expressed in starburst amacrine cells (Yoshida et al., 2001) or applied extracellularly (Amthor et al., 2002). In addition, calcium imaging showed that a directionally selective response already existed in the dendrites of starburst amacrine cells (Euler et al., 2002). The ablations of He and Masland (1997) likely caused no deficit to the process of directionally selective motion as the functionally important computations and information transfer all happen locally within single thin processes (Euler et al., 2002; Fried et al., 2002; Ozaita et al., 2004), and their laser ablation only killed the large cell bodies but left the separate processes to seal and remain functional. This is possible as other labs have purposefully only ablated parts of neurons successfully (Jacobs and Miller, 1985b; Lytton and Kristan, 1989).

Here, four sets of ablation experiments were performed where the input-output pathways were likely local dendritic processes. In two of these, i.e. the VS1-cell ablations with the medial VS-cells and the CH-cell ablations while recording the H2-cells, the ablation of the specified neurons caused no noticeable difference on the target cells. For these two cases it is not thought that the local processes remained intact. In the two other cases, i.e. the HS-cell ablation with CH-cells and the VS1-cell ablations with H1-cells, the ablations caused a significant change to the response properties of other cells in the circuit. CH-cells lost their response to ipsilateral motion stimulus after the ablation of HS-cell and the H1-cell lost its response to vertical motion after the ablation of the VS1-cell. It is unlikely that in some



## Discussion

cases I ablated the dendritic trees and in other I did not as the dendritic trees all lie in the same plane at similar depths in a thin neural tissue. In addition, in the cases where the ablation of a specific cell had an affect on its linked neighbour it occurred for each ablation. This suggests that our ablation parameters were set up correctly to ablate cells reliably. Hence, the experiments where ablations had no affect on other LPTCs suggest that I do not have a complete picture of the circuitry connecting the LPTCs together.

---

### Building Receptive Fields

The general model of how lobula plate tangential cells respond to motion has been described in great detail over the last 15 years. First anatomical evidence suggests that the arrangement of input to the lobula plate is arranged in retinal topic manner. Where the anatomy of the putative input neurons has small axonal aborizations, thus each dendritic input on a lobula plate should generally represent localized positions in the visual world. Second, it has been demonstrated that the directionally selective response of LPTCs is due to dendritic integration of local motion cues that arrive on their dendritic trees. This basic framework suggests that the receptive fields of LPTCs should then be consequence of the preferred direction of their local motion input and their dendritic architecture. However, it is clear that the whole response repertoire of many lobula plate tangential cells cannot be explained solely by dendritic integration of local motion cues.

Anatomical and physiological studies have elucidated an extensive highly organized neural network among the LPTCs that may form the basis of their often complex receptive fields. In particular, current injection experiments have revealed connections that appeared to fit with the detailed receptive field structures that have been recorded using local motion stimulus paradigm. The ablation experiments presented here along with some previous ablation studies have started to reveal which connections can account for specific response properties of individual cells. This work has clearly shown that lateral connections among LPTCs play a fundamental role in shaping their receptive fields. It is now clear that the receptive fields of the lobula plate tangential cells are a consequence of at least three variables:

1. The PD of their local motion input.
2. Their dendritic architecture



## Discussion

### 3. Their lateral connections with other LPTCs.

The lateral connections among the LPTCs appear to augment individual cells primary receptive fields that are determined by their dendritic architecture and the PD of their local motion input. In addition, dendritic integration properties, intrinsic cellular mechanisms as well as the adaptive properties of both the electrical and chemical synaptic connections are likely to play a role. Below the individual projects will be discussed.

---

## Input Structure to HS- and CH-Cells

Using the single cell laser ablation technique I have demonstrated that the response of CH-cells to visual motion presented in front of the ipsilateral eye is entirely dependent on input from electrically coupled HS-cells. In contrast, the response of HS-cells turned out to be independent of input from CH-cells. These two results provide convincing evidence that HS neurons receive local motion information directly from local motion elements and pass this information on to CH neurons (Fig. 3.3B; also see Fig 4.1). Such a connection scheme has implications for understanding the visual response properties of CH-cells including: their spatial integration properties, dendritic calcium signals during null direction motion stimuli and the spatial blurring of motion signals on their dendrites.

The fact that input from HS-cells, rather than direct input from local motion elements drives

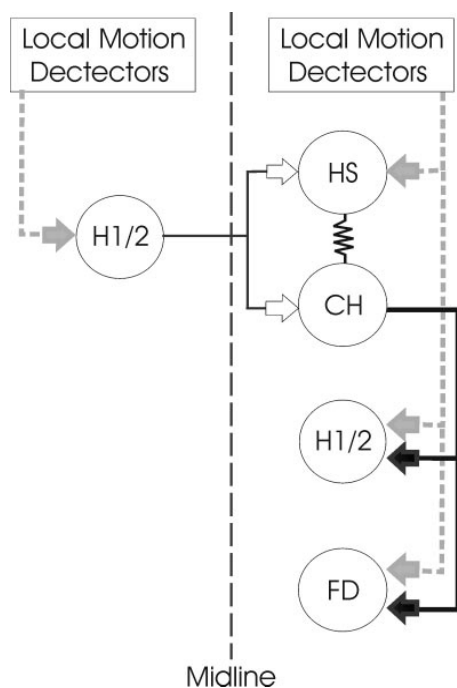


**Figure 4.1: Schematic diagram of the input-output pathways of HS- and CH-cells.** An array of local motion detectors supplies HS, H1, H2 and FD cells with local motion information (grey arrows). The preferred direction for local motion input to HS- and FD-cells is front-to-back while that of H1 and H2 is back-to-front. HS- and CH-cells are connected electrically via their dendritic trees. CH-cells inhibit H1, H2 and FD-cells GABAergic synapses (black arrows). In addition HS and CH cells receive excitatory (white arrows) from the contralateral H1 and H2 neurons. Solid lines indicate known connectivity and dashed lines indicated assumed connections. Only one half of the network is shown for clarity. The network is symmetric about the midline.





## Discussion

CH-cell activity provides an explanation for the spatial saturation properties found in these two neurons. The visual responses of CH- and HS-cells have been shown to saturate to the same degree with increasing spatial extent of the ipsilateral motion stimulus (Gauck and Borst, 1999; Haag et al., 1999). As HS-cells drive the CH-cells, one would expect that as the HS-cell response saturates so would the CH-cell.

Another important aspect resolved by the current finding refers to the dendritic calcium measurements made in tangential cells. During null direction motion an increase in calcium concentration has been observed in the small dendritic branches of VS-cells (Single and Borst, 2002; Borst and Single, 2000) and HS-cells (Haag and Borst, unpublished), but not CH-cells (Haag, Single and Borst, unpublished). This increase in calcium concentration during null direction stimuli has been assumed to be due to the low directional selectivity of the excitatory input from local motion-sensitive elements, which presumably arrive on the dendrites via calcium-permeable nicotinic acetylcholine receptors (Brotz and Borst, 1996; Oertner et al., 2001). My findings explain why the dendritic calcium in CH-cells does not rise during null direction stimulus, because ipsilateral motion information arrives via electrical coupling with HS-cells and not via chemical synapses from motion-sensitive elements. It also points to a benefit of this type of connection scheme. The outputs of a CH-cell are likely to be more directionally selective than if it received direct input from local motion elements, as the calcium signal will follow the membrane potential more closely. The effect of presynaptic calcium levels of other tangential cells, VS-cells, has been shown to be related linearly to presynaptic membrane depolarization and the firing rate of the postsynaptic V1-cell (Kurtz et al., 2001). If the VS1- and V1-cell are chemically coupled and local calcium concentrations trigger release at chemical synapses, the experiments of Kurtz et al. (2001) emphasize the importance of having a calcium concentration near output synapses that conveys information reliably. The connection scheme found here would allow for dendritic calcium signals to follow the membrane potential and thus provide a well tuned directionally selective output in CH-cells.

In addition it has been demonstrated using calcium imaging techniques that the spatial representation of motion stimuli on the dendrites of CH-cells is blurred relative to that of HS-cell dendrites (Dürr and Egelhaaf, 1999; Haag and Borst, 2002). The input blueprint to the two neuronal types described above has been shown to be sufficient to account for the blurred visual image found in CH-cells (Cuntz et al., 2003). It is likely that if CH-cells also



## Discussion

received direct input from local motion elements the relative blurring of the signals between HS- and CH-cells would be reduced.

A three neuron dendritic network has been proposed (Haag and Borst, 2002) to be important for the small field tuning of a class of tangential cells called FD (figure-detection) cells (Egelhaaf, 1985; Egelhaaf et al., 1993; Gauck and Borst, 1999; Kimmerle and Egelhaaf, 2000b; Haag and Borst, 2002). In this network the HS-CH electrical coupling allows for the creation of a blurred retinotopic image on CH dendrites (Haag and Borst, 2002; Cuntz et al., 2003), while the GABAergic connection from CH- onto FD-cells mediates the subtraction of the original retinotopic signal, putatively present on FD-cells, and the blurred signal arriving from CH-cells (Warzecha et al., 1993). The connection scheme determined here (Fig 4.1) demonstrates that the passing of motion information from the dendrites of HS- to CH-cells must be involved. However, when single HS neurons (HSE-cells) were selectively ablated the small field tuning of FD1 neurons was not affected (Warzecha et al., 1993). This might be a consequence of the large field visual stimulus used in the experiments of Warzecha et al. (1993). FD1-cells are selectively activated by front-to-back small field motion presented in the fronto-ventral part of ipsilateral visual space (Egelhaaf, 1985; Warzecha et al., 1993; Gauck and Borst, 1999; Kimmerle and Egelhaaf, 2000a). In addition FD1-cells are inhibited by back-to-front motion presented in front of the contralateral eye (Egelhaaf, 1985; Gauck and Borst, 1999; Kimmerle and Egelhaaf, 2000a; Kimmerle and Egelhaaf, 2000b). In order to determine the small field tuning of FD1-cells, Warzecha et al. (1993) compared the response of FD1-cells to a small-field stimulus presented in front of the ipsilateral eye with a stimulus that mimicked large field rotation. This stimulus consisted of an extended background moving from front-to-back on the ipsilateral side, and back-to-front on the contralateral side. vCH-cells receive excitatory input about back-to-front motion presented in front of the contralateral eye via spiking neurons (H1, H2 cells) that synapse directly on CH-cells (Hausen, 1981; Eckert and Dvorak, 1983; Gauck et al., 1997; Horstmann et al., 2000). Hence, the killing of an HSE-cell would not eliminate the activity of a vCH-cell when contralateral motion is presented. In addition, when ipsilateral stimuli are used the area of a CH-cell dendritic tree that is excited depends on the elevation at which the stimulus is presented (Egelhaaf et al., 1993; Dürr and Egelhaaf, 1999; Haag and Borst, 2002). Upper visual field stimulus will excite the more dorsal dendrites, while lower visual stimulus will stimulate the ventral dendrites. HSE- and HSS-cells are known to selectively activate



## Discussion

the dorsal and ventral halves of the vCH-cell dendritic tree respectively (Haag and Borst, 2002). This implies that after the ablation of a single HS-cell it is important to restrict the stimulus to the receptive field of this cell for the effect to become visible. Taken together, the missing effect of HS-cell ablation on the small-field tuning of FD-cells reported by Warzecha et al. (1993) can be fully explained by the large-field stimulus used in their study. This stimulus is sufficient to activate the vCH-cell through the contralateral H1 & H2 cells, as well as via the remaining ipsilateral HS-cells.

The dendritic tree of CH-cells has more than one output target. In addition to FD-cells, CH neurons have been shown to influence the activity of other tangential cells, including H1 and H2 cells (Haag and Borst, 2001). H1 and H2 cells are large field motion sensitive neurons that respond in a directionally selective way. Both cells respond best to PD stimuli moving from back-to-front. These connections appear to affect the selectivity of these neurons to rotational flow-fields.

---

### Flow-Field Selectivity of H1- and H2-cells

It has previously been demonstrated that the H2-cell shows distinct flow-field selectivity for rotational stimuli as compared to translational stimuli (Haag and Borst, 2001). It was proposed that this selectivity was due to information being passed via CH-cells onto the dendrites of the H2-cells. The ablation experiments presented here demonstrate that CH-cells are likely not a key part of the pathway that allows H2-cells to combine information arriving on both eyes. These results suggest that there are additional network connections responsible for the H2-cells flow-field selectivity.

### Review of Results of Haag and Borst (2001)

One of the key experiments of Haag and Borst (2001) was current injections into an HS- or CH-cell, while recording from the other cell type within the same lobula plate (see figure 6 Haag and Borst, 2001). It was demonstrated that current injections of -10 nA into either HS- or CH-cells reduces the number of EPSPs in the other cell by ~50 %. Haag and Borst (2001) proposed that this reduction in the number of EPSPs is due too positive feedback after the signal passes across two inhibitory and two excitatory synapses. The



## Discussion

two inhibitory synapses occur at the CH-cell input to the H1- and H2-cell dendrites located in the same hemisphere, while the excitatory synapses are the source of EPSP activity in CH- and HS-cells from H1- and H2-cell projections from the opposite side of the brain. This interpretation is in conflict with the rectifying input that CH-cells make onto both the H1- and H2-cells. Haag and Borst (2001) also showed that current injections of +10 nA but not -10 nA influence the activity of H1- and H2-cells whose dendrites are located in the same hemisphere. This means that current injections of -10 nA cannot influence the activity of the cells projecting to the other hemisphere and thus cannot provide feedback via this route. So through what connection do current injections of negative current affect the spiking activity of H2-cells whose dendrites lie in the opposite hemisphere?

### Possible Explanation

Recent double intracellular recordings of H2-cells and HS- or CH-cells (performed by Jürgen Haag, unpublished data), and Neurobiotin staining experiments (Haag and Borst, 2005) provide a possible explanation for the source of flow-field selectivity of H2-cells as well as suggest a basis for a difference between the flow-field selectivity of H1- and H2-cells (Fig 4.2). First, during double intracellular recording it was demonstrated that current can be passed of both polarities in both directions between H2-cells and either a HS- or a CH-cell (data not shown). In addition recordings from two H2-cells demonstrated that during ipsilaterally presented motion the H2-cell's spiking rate increased and decreased as seen in both extracellular recordings and recording of EPSPs from HS- and CH-cells in the opposite hemisphere (data not shown). However, during contralateral stimulus the H2-cell showed little modulation of spiking activity but demonstrated graded membrane potential shift such that front-to-back motion depolarized and back-to-front hyperpolarized the membrane potential. This graded potential input is consistent with idea that H2-cells receive electrical input from HS- and/or CH-cells, which is supported by the double recordings performed. Also, injection of Neurobiotin into HSE-, dCH- and vCH-cells illustrate that these cells are electrically coupled to the H1-cell (Haag and Borst, in press).



## Discussion

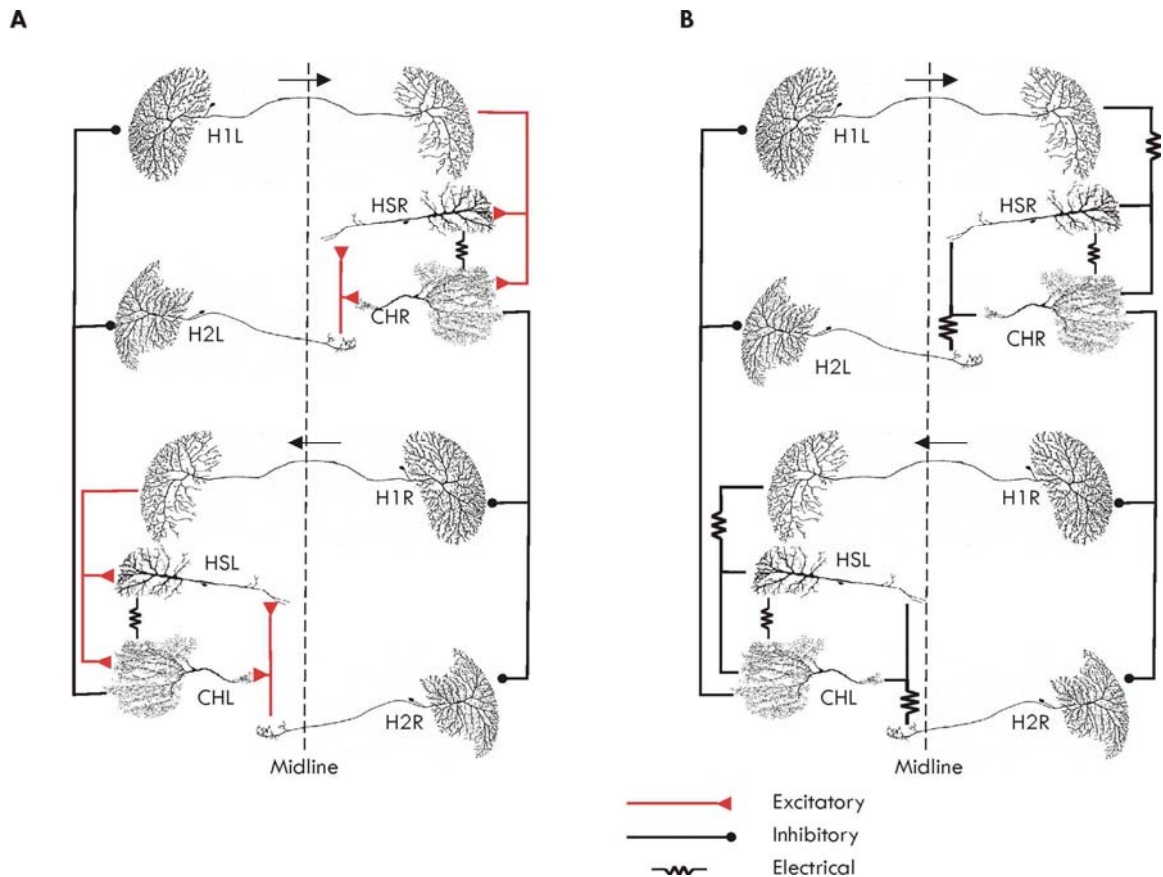


**Figure 4.2: Alternative Connectivity among the Horizontal Sensitive Cells.** A comparison of two alternative network configurations is shown that can account for the flow-field selectivity of H2-cells. Only one type of each cell is shown, where an L or R in the name indicate the left or right side of the brain, respectively. Note that the Hu cell has been omitted for simplicity (see Fig 1.9). **A)** The connectivity of horizontal sensitive cells as outlined by Haag and Borst (2001, 2002). The line around the outside indicates that the circuit should act to positively reinforce the activity of any single cell on itself. Generally, information is passed from one hemisphere to the other via the H1- and H2-cells that then provide excitatory input to the HS- and CH-cells. **B)** A new proposed network based on double recordings of Jürgen Haag and Neurobiotin staining (Haag and Borst, 2005). Here the source of excitatory input to HS- and CH-cells from H1- and H2-cells takes the form of electrical synapses. This means, signals can also pass too the H1- and H2-cells from the HS- and CH-cells, allowing for an alternative pathway for H1- and H2-cells to integrate information from both eyes.

If this is true H2-cells flow-field selectivity is easily explained as hyperpolarizing the axonal membrane potential could reduce the spiking activity of the H2-cell in the required manner that would reduce spiking activity during translation and increase spiking during rotation. In addition, Reinterpreting the double recordings of Haag and Borst (2001) suggests that H2-cells might connect directly to HS-cells, via axo-axonal connections. When negative current is injected in an HS- or CH-cell it hyperpolarizes the axon of the H2-cell and decreases the spiking activity and thus reducing the EPSP activity recorded in the



other HS- or CH-cell.

---

### Basis of the Broad Receptive Fields of VS-cells

VS-cells respond to stimuli presented outside of the visual space expected from the retinotopy of the lobula plate and the extent of their dendritic arborization. The receptive fields are unexpectedly wide, and in the case of the medial VS-cells (VS8-10) include frontal sensitivity when only posterior vision was expected (Krapp et al., 1998). The results of our ablation experiments show that lateral connections among VS-cells form the basis of their unexpectedly wide receptive fields, which substantially exceed the proportion of the lobula plate covered by their dendrites. I also provide evidence that VS-cells connect sequentially in a chain like fashion beginning with the VS1-cell on the lateral edge of the lobula plate and continuing through each VS-cell to the VS10-cell on the lobula plate's medial edge. On the other hand, how the medial VS-cells acquire sensitivity in the frontal visual field remains unclear.

### The VS-Cell Network

The serial connection scheme outlined above was suggested by Haag and Borst (2004) based on the magnitude, bi-directionality and temporal properties of the signals passing between individual VS-cells. They reported that the connection strength between the VS1- and other VS-cells monotonically decreased with increasing distance between their dendritic trees within the lobula plate, and that current could be passed bi-directionally between cell pairs. In addition, following current injection into various VS-cells, the temporal dynamics of the resulting potential in the VS1-cell revealed low-pass filter characteristics where the order of the filter increased (3rd, 4th, and 5th) with the distance to the injected cell (VS2, 3 and 4). However, the results of these current injection experiments did not exclude the possibility that the VS-cells made reciprocal contact to the VS1-cell individually with disparate properties. My experiments provide additional evidence that the VS-cells are connected in the proposed chain like manner and examine a wider set of cell pairs, suggesting that this connectivity scheme generalizes to all VS-cells.



## Discussion

Here, after the ablation of a single VS-cell, the recorded VS-cell had reduced responses to vertical motion in specific locations of their receptive field dependent on the location of the ablated cell. If the VS-cells were fully interconnected such that each cell made reciprocal recurrent connections with all other VS-cells, the response deficit would only be expected to occur at stimulus positions where the peak response of the ablated cell was located, causing a dip in the receptive field of the recorded VS-cell. However, the responses of the recorded VS-cell fell significantly not only at the stimulus positions where the ablated cell was most responsive, but also at stimulus locations further away than the peak responses of the ablated cell (e.g. fig 3.21A and G). This caused a flattening of the receptive field of the recorded cell towards zero that was dependent on the location of the ablated cell. I found that even at stimulus locations where the ablated cell was not strongly responsive the relative deficit of the recorded cell was approximately the same as the deficit at the position of the ablated cell's peak response (fig 3.22C). This was shown not just for the VS1-VS<sub>x</sub> pairs but for a range of cell pairs including: VS1-VS2, VS1-VS3, VS2-VS1, VS4-VS2, VS4-VS3 and VS5-VS6 (recorded-ablated cell). This implies that ablating a single cell breaks the chain of VS-cells, stopping the flow of information to the recorded cell from neurons beyond the ablated cell.

### Residual Responses

One caveat of our results is that the responses of the VS-cells to stimuli putatively outside their dendritic receptive field were not completely abolished. The mean relative change after the ablation of a single VS-cell dropped a maximum of 66% and a minimum of 21% (fig 3.24a). One explanation for this involves the limitations of our ablation technique. It is not exactly known whether strong illumination ablates a dye-filled cell as a whole or only a part of it. Generally, photo-ablation causes the resting membrane potential of the cell to depolarize to zero and the input resistance of the neuron to vanish (Farrow et al., 2003). However, it has been shown that selective partial ablation of a dye filled cell is possible with a focused laser beam (Miller and Selverston, 1979; Jacobs and Miller, 1985). While our laser was not focused and illuminated the entire lobula plate, it is still conceivable that laser illumination ablated large parts of the VS-cells but left electrically intact those segments where VS-cells make contact. In such a case, although the retinotopic input from the ablated cell would be abolished, the remaining segments could still function as a relay for input from cells further away.



## Discussion

### VS-cell Receptive Fields

The receptive fields I found here using long thin stripes of horizontal grating, correspond well with the receptive fields previously recorded using a local motion stimulus protocol (Krapp et al., 1998). The widths of the VS-cells, particularly the VS4-, VS5-, and VS6, span an area far exceeding the proportion of the lobula plate covered by each neurons' dendrites. In addition, I also found that the medial VS-cells (VS8, 9, 10) respond to motion presented in the frontal visual field.

One of the interesting characteristics of the VS-cell receptive field's (fig 3.20C) is the obvious grouping of cells. Most striking is the almost perfect overlap between the receptive fields of the VS1-, VS2-, and VS3-cells. This grouping is also borne out in some of the synaptic connections these cells make collectively. Specifically, all three of these cells have been shown to provide input to the V1-cell (Kurtz et al., 2001; Haag and Borst, 2003; Warzecha et al., 2003), a contralaterally projecting spiking neuron. These results suggest that common response properties may correlate with a common output.

### VS1-cell Ablation: Why No Affect?

After the ablation of the VS1-cell I found the response of the medial VS-cells to upward and downward motion unchanged (figs 3.24A, 3.26A and 3.26D). This result came as a surprise since it has been previously demonstrated that current injections into VS1-cells affect both the EPSP frequency and membrane potential of the medial VS-cells (Haag and Borst, 2004). There are two explanations for this apparent contradiction. The first involves the possible connectivity among the VS-cells. Perhaps, all three frontally viewing VS-cells provide inhibitory input to the medial VS-cells independently. This would allow the VS2-, and VS3-cells to compensate for the loss of the VS1-cell. This is plausible since, as mentioned above, these cells have highly overlapping receptive fields and have previously been shown to have a common output target, the V1-cell, independent of the other VS-cells (Kurtz et al., 2001; Haag and Borst, 2003; Warzecha et al., 2003).

The second explanation is the inconsistency between the current injections performed by Haag and Borst (2004) and the response properties of the medial VS-cells recorded here. Haag and Borst (2004) showed that positive but not negative current is passed from the VS1- to the medial VS-cells. In addition, the medial VS-cells have been reported to be





## Discussion

selective to upward motion in the frontal visual field, without an indication as to whether they depolarized or hyperpolarized in response to a particular direction of motion (Krapp et al., 1998). These two results are consistent if during downward motion the medial VS-cells hyperpolarized, while during upward motion the medial VS-cells remained at rest. However, here we find that the medial VS-cells do depolarize and hyperpolarize in response to upward and downward motion respectively (fig 3.25B, 3.26A and D). Therefore, after the ablation of the VS1-cell one would not expect a change in its response to upward motion since during such a stimulus the VS1-cell hyperpolarizes and thus its signal would not be passed onto the medial VS-cells. The results here suggest that the experiments of Haag and Borst (2004) did not reveal the complete circuitry responsible for the sensitivity of the medial VS-cells to motion in the frontal receptive field.

### Why the Broad Receptive Fields?

What is the advantage for VS-cells to import the receptive fields of their neighbours via electrical synapses? Intuitively, this appears to make the output of individual neurons more ambiguous with respect to the location of the stimulus within the visual space and consequently more difficult for downstream neurons to extract useful information. However, electrical connections among homologous cells help reduce noise due to stochastic events (photon noise, channel noise, synaptic noise) and have been described at many visual processing stages. Examples include the cones (Raviola and Gilula, 1973; Kolb and Jones, 1985; Owen, 1985; Tsukamoto et al., 1992), amacrine cells (Famiglietti and Kolb, 1975; Vaney, 1991; Stettoi et al., 1992; Feigenspan et al., 2001) and ganglion cells (Vaney, 1991; Hidaka et al., 2004) in the vertebrate retina as well as the photoreceptors (Ribi, 1978) and lobula plate tangential cells (Haag and Borst, 2002; Haag and Borst, 2004) of insects.

The effectiveness of lateral connection to aid noise reduction has been clearly demonstrated for cone photoreceptors that are electrically coupled, without greatly affecting visual signal acuity (Lamb and Simon, 1976; Tessier-Lavigne and Attwell, 1988; DeVries et al., 2002). Similarly, in the inner retina electrical coupling among All amacrine cells helps improve signal-to-noise ratios (Bloomfield and Völgyi, 2004). However, here the electrical coupling between All amacrine cells is ten times larger during twilight like light conditions (low signal-to-noise condition) than under bright light conditions, corresponding with these cells receptive field sizes under the same stimulus parameters



## Discussion

(Bloomfield and Völgyi, 2004). Analogously, the receptive field centers of alpha type retinal ganglion cells expand in darkness beyond their dendritic fields by up to 2.8-fold (Peichl and Wässle, 1983). This could be explained if the electrical coupling between alpha type retinal ganglion cells (Hidaka et al., 2004) decreases with light adaptation.

The response to motion of lobula plate tangential cells is also degraded by stochastic noise (Laughlin, 1987; de Ruyter van Steveninck and Bialek, 1995; de Ruyter van Steveninck and Laughlin, 1996; Borst and Haag, 2001; Lewen et al., 2001; Grewe et al., 2003; Borst, 2003b). In addition, my experiments demonstrate that the lateral connections between VS-cells do increase the width of their receptive fields. Whether the receptive field widths and coupling strengths between VS-cells are also sensitive to signal-to-noise levels is an open question. However, there is likely a trade off between the spatial acuity of the VS-cells and the noise present in their responses. Hence, does the low spatial acuity of these cells hinder the ability of down stream neurons in extracting useful information?

Along these lines, it has been suggested that broad receptive fields aid the extraction of information from a population of neurons. Seung and Sompolinsky (1993) found that the performance of a model that estimates the direction of motion in two dimensions by calculating a population vector from a group of neurons with various orientations is optimal for an intermediate tuning width. The amount of extracted information fell quickly to zero as the tuning width narrowed, as compared to the optimum, but fell only slowly as the tuning width increased (Seung and Sompolinsky, 1993). Hence, if the electrical coupling between VS-cells increased with decreasing signal-to-noise levels, thus increasing the width of their receptive field, the noise levels within VS-cells could be reduced without hindering the ability of downstream neurons to extract relevant flow-field information used for orientation behavior.

### Summary

Our results show that the connections among VS-cells augment the columnar input from local motion detectors. Specifically, individual VS-cells increase the width of their primary receptive fields, a result of input to their dendrites, by importing the receptive fields of their neighbours. The indirect inhibitory input of the VS1-cell to the medial VS-cells was not found to be sufficient to account for the medial VS-cells sensitivity to motion in the frontal visual field.



## Discussion

In order to explicitly address the nature of the circuit connecting the VS-cells directly future studies should include: multiple VS-cell ablations in order to clarify what an individual VS-cell views without lateral input from neighbouring VS-cells; double recordings of VS-cells receptive field where information flow in a cells axon is blocked by voltage clamp, the putative site of connection among VS-cells; and a quantitative comparison of the deficits incurred by ablating cells at different distances from a single VS-cell. Additionally, fruitful investigations into the information flow within single VS-cells could be carried out by specifically ablating small portions of individual VS-cells; thus specifying the spatial relationship of different input-output relationships within a single cell.

---

### Vertical-Horizontal Interactions

The H1- and H2-cell respond to downward motion in their frontal receptive field. Here I provide compelling evidence that the basis of this sensitivity is due to input from the VS1-cell. First, the receptive field of the H1-cell overlaps highly with that of the VS1- and VS2-cell (Fig 3.28). Second, in addition to the anatomical evidence, current injections into different regions of the VS1-cell suggest that the output region providing input to the H1-cell is located in the dendritic region of VS1-cells (Fig 3.29). Finally, the ablation of individual VS1-cells demonstrated that the input from the VS1-cell is indeed responsible for the sensitivity of the H1-cell to vertical motion (Fig 3.30). It is likely that the VS-cell is also responsible for the vertical sensitivity of H2-cells as the nature of their input from VS1-cells is similar to that of H1-cells (Haag and Borst, 2003). The form the VS1-cell to the H1- and H2-cells has been proposed to be electric as current of both polarities is passed on (Haag and Borst, 2003). However, it is also possible that VS-cells release transmitter constantly and just vary the amount that stimulates the H1- and H2-cells to different degrees. The consequence of this connectivity on the flow-field responses of other LPTCs and its possible role in behavior are discussed below.

H1 and H2 cells are heterolateral elements that project to the opposite brain hemisphere where they are presynaptic to HS- (HSN and HSE) and CH-cells (Horstmann et al., 2000; Haag and Borst, 2001). It has been shown that H1-cells make synaptic contacts to the HS- and CH-cells in their lobula-plate aborizations, while H2-cells project to the protocerebral



## Discussion

branches of HS- and CH-cells (Haag and Borst 2001). This sort of connectivity should contribute to the HS- and CH-cells sensitivity to downward vertical motion in the frontal part of the contralateral visual field. Using a local motion stimulus protocol a strong sensitivity to downward motion has only been noted in vCH-cells but not in the dCH-, HSE- or HSN-cells (Krapp et al., 2001). However, the strong downward sensitivity of vCH-cells is more likely due to input from the contralateral V1-cell (Haag and Borst, 2003). Like H1- and H2-cells the analysis of the local motion stimulus done by Krapp et al. (2001) might not reveal the dCH-, HSE- or HSN-cells sensitivity to motion in anything but its PD at any particular location as only the direction of maximum response was reported. On the other hand, Haag and Borst (2003) reported the entire tuning curves of the H1-, H2-, as well as the EPSP response in the dCH-cell. The EPSP tuning of the dCH-cell is similar to that of the tuning of the H1- and H2-cells, all responding to downward motion with a response of ~40 % of their peak response. The functional significance of these connections for behavior can only be speculated about. However, the circuitry in which these cells are embedded enhances the response of cells to rotatory horizontal motion compared to translatory motion (Haag and Borst, 2001). Since all these cells are part of this network, the vertical sensitivity of these neurons might affect the response of this network as a whole to vertical motion stimuli in the frontal visual field.

During forward flight the images move across the retina pass from front-to-back. This is the ND for the H1- and H2-cell and thus they should be silent most of the time. The only time that forward motion provides a PD stimulus to the H1/2-cell would be when it is flying close to the ground, such during a landing maneuver. In this situation the world in the frontal visual space would move from up-to-down across the frontal portion of the eye. This is putatively within the receptive field of the VS1-cell and thus would be passed onto the H1-, and H2-cells and potentially cause it to start firing. This connection scheme may then be part of the network responsible for initiating a landing response.

While the behavioral implications of this connection scheme are speculative the implications for the receptive field structure of H1- and H2-cells are clear. The connection between the VS1- and H1-cells is another example highlighting how LPTCs use lateral interactions to build up their receptive field structures. How flies use these complex receptive fields to guide behavior is not clear. In order to form good functional ideas about the benefits of the complex receptive field structures, a better understanding of the pattern of



## Discussion

connectivity of LPTCs on to descending neurons and then to the motor neurons is needed.

---

### Summary

Here I have demonstrated that many of the connections among LPTCs help increase the richness of their receptive fields. This enrichment takes on a few different forms. Specifically, the dendro-dendritic electrical coupling between HS- and CH-cells is the pathway by which local motion input drives the direction selective response of CH-cells. The lateral electrical interactions among VS-cell neighbours forms the basis of their wide receptive fields and the VS1-cell was found to provide the H1-cell with its vertical sensitivity in the frontal visual field. These findings highlight the importance of the highly interconnected network formed by the tangential cells of the lobula plate.

The lateral interactions among LPTCs appears to augment the feedforward input from local motion detectors. This allows each cell to be tuned to specific optic flow patterns. The building of these complex receptive fields occurs in two stages. First, the initial directionally selective response in each cell's primary receptive field is due to the integration of local motion information across each cell's dendritic tree. The LPTCs then pass this information on in an organized fashion to other LPTCs that enrich and enlarge each cell's receptive field, beyond that of its local motion input. This enrichment and enlargement has benefits, from a theoretical point, for each cell's ability to extract useful optic flow from the time varying brightness patterns arriving on the retina.

While all of this still needs to be further investigated, the integration of the growing knowledge about the lobula plate circuitry and free flight behavior of the fly will eventually lead us to an in-depth understanding of how such complex receptive field properties of motion-sensitive large-field neurons arise in the fly visual system and are potentially optimized to guide behavior.





## 5 References

---

- Amthor, FR, Keyser, KT, and Dmitrieva, NA. **Effects of the destruction of starburst-cholinergic amacrine cells by the toxin AF64A on rabbit retinal directional selectivity.** *Vis Neurosci.* 2002, 19: 495-509.
- Bausenwein, B, Dittrich, APM, and Fischbach, KF. **The optic lobe of *Drosophila melanogaster*. II. Sorting of retinotopic pathways in the medulla.** *Cell Tissue Res.* 1992, 267: 17-28.
- Bausenwein, B and Fischbach, K-F. **Activity labeling patterns in the medulla of *Drosophila melanogaster* caused by motion stimuli.** *Cell Tissue Res.* 1992, 270: 25-35.
- Bloomfield, S and Völgyi, B. **Function and plasticity of homologous coupling between All amacrine cells.** *Vision Res.* 2004, 44: 3297-3306.
- Borst, A. **Fly visual interneurons responsive to image expansion.** *Zool Jb Physiol.* 1991, 95: 305-313.
- Borst, A. **Modeling fly motion vision.** In *Computational Neuroscience A Comprehensive Approach*. Feng, J. Boca Raton, London, New York, Washington, DC: Chapman & Hall/CRC; 2003a: 397-429.
- Borst, A. **Noise, not stimulus entropy, determines neural information rate.** *J Comput Neurosci.* 2003b, 14: 23-31.
- Borst, A and Bahde, S. **Visual information processing in the fly's landing system.** *J Comp Physiol A.* 1988, 163: 167-173.
- Borst, A and Egelhaaf, M. **In vivo imaging of calcium accumulation in fly interneurons as elicited by visual motion stimulation.** *Proc Natl Acad Sci USA.* 1992, 89: 4139-4143.
- Borst, A and Egelhaaf, M. **Detecting visual motion: Theory and models.** In *Visual motion and its role in the stabilization of gaze*. Miles, FA and Wallman, J. Amsterdam, London, New York, Tokyo: Elsevier; 1993: 3-27.
- Borst, A, Flanagan, VL and Sompolinsky, H. **Adaptation without parameter change: Dynamic gain control in Reichardt motion detectors.** *Proc Natl Acad Sci USA.* In Press.
- Borst, A and Haag, J. **The intrinsic electrophysiological characteristics of fly lobula plate tangential cells : I. Passive membrane properties.** *J Comput Neurosci.* 1996, 3: 313-336.



## References

- Borst, A and Haag, J. **Effects of mean firing on neural information rate.** *J Comput Neurosci.* 2001, 10: 213-221.
- Borst, A and Single, S. **Local current spread in electrically compact neurons of the fly.** *Neurosci Lett.* 2000, 285: 123-126.
- Borst, A and Theunissen, FE. **Information theory and neural coding.** *Nat Neurosci.* 1999, 2: 947-957.
- Braitenberg, V. **Patterns of projection in the visual system of the fly. I. Retina-lamina projections.** *Exp Brain Res.* 1967, 3: 271-298.
- Brenner, N, Bialek, W, and de Ruyter van Steveninck, R. **Adaptive rescaling maximizes information transmission.** *Neuron.* 2000, 26: 695-702.
- Brotz, TM and Borst, A. **Cholinergic and GABAergic receptors on fly tangential cells and their role in visual motion detection.** *J Neurophysiol.* 1996, 76: 1786-1799.
- Buchner, E. **Elementary movement detectors in an insect visual system.** *Biol Cybern.* 1976, 24: 85-101.
- Buchner, E, Buchner, S, and Bülthoff, I. **Deoxyglucose mapping of nervous activity induced in *Drosophila* brain by visual movement.** *J Comp Physiol A.* 1984, 155: 471-483.
- Clifford, CWG and Ibbotson, MR. **Fundamental mechanisms of visual motion detection: Models, cells and functions.** *Prog Neuro.* 2003, 68: 409-437.
- Cuntz, H, Haag, J, and Borst, A. **Neural image processing by dendritic networks.** *Proc Natl Acad Sci USA.* 2003, 100: 11082-11085.
- de Ruyter van Steveninck, R and Bialek, W. **Reliability and statistical efficiency of a blowfly movement-sensitive neuron.** *Phil Trans R Soc Lond B.* 1995, 348: 321-340.
- de Ruyter van Steveninck, R and Laughlin, SB. **The rate of information transfer at graded-potential synapses.** *Nature.* 1996, 379: 642-645.
- DeVries, SH, Xiaofeng, Q, Robert, S, Makous, W, and Sterling, P. **Electrical coupling between mammalian cones.** *Current Biology.* 2002, 12: 1900-1907.
- Douglass, JK and Strausfeld, NJ. **Visual motion-detection circuits in flies : Parallel direction-and non-direction-sensitive pathways between the medulla and lobula plate.** *J Neurosci.* 1996, 16: 4551-4562.
- Dubs, A. **The spatial integration of signals in the retina and lamina of the fly compound eye under different conditions of luminance.** *J Comp Physiol A.* 1982, 146: 321-343.
- Dürr, V and Egelhaaf, M. **In vivo calcium accumulation in presynaptic and postsynaptic dendrites of visual interneurons.** *J Neurophysiol.* 1999, 82: 3327-3338.
- Eckert, H. **The vertical-horizontal neurone (VH) in the lobula plate of the blowfly, *Phaenicia*.** *J Comp Physiol.* 1982, 149: 195-205.
- Eckert, H and Dvorak, DR. **The centrifugal horizontal cells in the lobula plate of the blowfly *Phaenicia sericata*.** *J Insect Physiol.* 1983, 29: 547-560.
- Egelhaaf, M. **On the neuronal basis of figure-ground discrimination by relative motion in the**





## References

- visual system of the fly. II. Figure-detection cells, a new class of visual interneurons.** *Biol Cybern.* 1985, 52: 195-209.
- Egelhaaf, M and Borst, A. **Transient and steady-state response properties of movement detectors.** *J Opt Soc Am A.* 1989, 6: 116-127.
- Egelhaaf, M and Borst, A. **Are there separate ON and OFF channels in fly motion vision?** *Vis Neurosci.* 1992, 8:151-164.
- Egelhaaf, M and Borst, A. **A look into the cockpit of the fly: visual orientation, algorithms and identified neurons.** *J Neurosci.* 1993, 13: 4563-4574.
- Egelhaaf, M, Borst, A, Warzecha, AK, Flecks, S, and Wildemann, A. **Neural circuit tuning fly visual neurons to motion of small objects II. Input organization of inhibitory circuit elements revealed by electrophysiological and optical recording techniques.** *J Neurophysiol.* 1993, 69: 340-351.
- Euler, T, Detwiler, PB, and Denk, W. **Directionally selective calcium signals in dendrites of starburst amacrine cells.** *Nature.* 2002, 418: 845-852.
- Exner, S. **Experimentelle Untersuchung der einfachsten Psychischen Prozesse.** *Pfluger's Arch Physiol.* 1875, 11: 403-432.
- Fairhall, AL, Lewen, GD, Bialek, W, and de Ruyter van Steveninck R. **Efficiency and ambiguity in an adaptive neural code.** *Nature.* 2001, 412: 787-792.
- Famiglietti, EV and Kolb, H. **A bistratified amacrine cell and synaptic circuitry in the inner plexiform layer of the retina.** *Brain Res.* 1975, 84: 293-300.
- Farrow, K, Haag, J, and Borst, A. **Input organization of multifunctional motion-sensitive neurons in the blowfly.** *J Neurosci.* 2003, 23: 9805-9811.
- Feigenspan, A, Teubner, B, Willecke, K, and Weiler, R. **Expression of neuronal connexin36 in All amacrine cells of the mammalian retina.** *J Neurosci.* 2001, 21: 230-239.
- Fermi, G and Reichardt, W. **Optomotorische Reaktionen der Fliege *Musca domestica*. Abhängigkeit der Reaktion von der Wellenlänge, der Geschwindigkeit, dem Kontrast und der Mittleren Leuchtdichte Bewegter Periodischer Muster.** *Kybernetik.* 1963, 2: 15-28.
- Fischbach, KF and Dittrich, APM. **The optic lobe of *Drosophila melanogaster*. I. A Golgi analysis of wild-type structure.** *Cell Tissue Res.* 1989, 258: 441-475.
- Franceschini, N, Riehle, A, and Le Nestour, A. **Directionally selective motion detection by insect neurons.** In *Facets of vision*, ed 1. Stavenga, DG and Hardie, RC. Berlin, Heidelberg: Springer-Verlag; 1989: 360-390.
- Fried, SI, Munch, TA, and Werblin, FS. **Mechanisms and circuitry underlying directional selectivity in the retina.** *Nature.* 2002, 420: 411-414.
- Gauck, V and Borst, A. **Spatial response properties of contralateral inhibited lobula plate tangential cells in the fly visual system.** *J Comp Neurol.* 1999, 406: 51-71.
- Gauck, V, Egelhaaf, M, and Borst, A. **Synapse distribution on VCH, an inhibitory, motion-sensitive interneuron in the fly visual system.** *J Comp Neurol.* 1997, 381: 489-499.
- Geiger, G and Nässel, DR. **Visual orientation behaviour of flies after selective laser beam**



## References

**ablation of interneurons.** *Nature*. 1981, 293: 398-399.

Geiger, G and Nässel, DR. **Visual processing of moving single objects and wide-field patterns in flies: behavioural analysis after laser-surgical removal of interneurons.** *Biol Cybern*. 1982, 44: 141-149.

Götz, KG. **Optomotorische Untersuchungen des Visuellen Systems einiger Augenmutanten der Fruchtfliege *Drosophila*.** *Kybernetik*. 1964, 2: 77-92.

Grewe, J, Kretzberg, J, Warzecha, AK, and Egelhaaf, M. **Impact of photon noise on the reliability of a motion-sensitive neuron in the fly's visual system.** *J Neurosci*. 2003, 23: 10776-10783.

Haag, J and Borst, A. **Amplification of high-frequency synaptic inputs by active dendritic membrane processes.** *Nature*. 1996, 379: 639-641.

Haag, J and Borst, A. **Recurrent network interactions underlying flow-field selectivity of visual interneurons.** *J Neurosci*. 2001, 21: 5685-5692.

Haag, J and Borst, A. **Dendro-dendritic interactions between motion-sensitive large-field neurons in the fly.** *J Neurosci*. 2002, 22: 3227-3233.

Haag, J and Borst, A. **Orientation tuning of motion-sensitive neurons shaped by vertical-horizontal network interactions.** *J Comp Physiol A*. 2003, 189: 363-370.

Haag, J and Borst, A. **Neural mechanism underlying complex receptive field properties of motion-sensitive interneurons.** *Nat Neurosci*. 2004, 7: 628-634.

Haag, J and Borst, A. **Dye coupling visualizes networks of large-field motion-sensitive neurons in the fly.** *J Comp Physiol A*. In Press.

Haag, J, Denk, W, and Borst, A. **Fly motion vision is based on Reichardt detectors regardless of the signal-to-noise ratio.** *Proc Natl Acad Sci*. 2004, 16333-16338.

Haag, J, Egelhaaf, M, and Borst, A. **Dendritic integration of motion information in visual interneurons of the blowfly.** *Neurosci Lett*. 1992, 140: 173-176.

Haag, J, Theunissen, F, and Borst, A. **The intrinsic electrophysiological characteristics of fly lobula plate tangential cells: II. Active membrane properties.** *J Comput Neurosci*. 1997, 4: 349-369.

Haag, J, Vermeulen, A, and Borst, A. **The intrinsic electrophysiological characteristics of fly lobula plate tangential cells: III. Visual response properties.** *J Comput Neurosci*. 1999, 7: 213-234.

Hardie, RC. **Functional organization of the fly retina.** In *Progress in sensory physiology 5*. Autrum, H, Ottoson, D, Perl, ER, Schmidt, RF, Shimazu, H, and Willis, WD. Berlin, Heidelberg, New York, Tokyo: Springer-Verlag; 1984: 1-79.

Harris, WA, Stark, WS, and Walker, JA. **Genetic dissection of the photoreceptor system in the compound eye of *Drosophila melanogaster*.** *J Physiol (Lond)*. 1976, 256: 439-

Hausen, K. **The neural architecture of the lobula plate of the blowfly, *Calliphora erythrocephala*.** Unpublished.

Hausen, K. **Monocular and binocular computation of motion in the lobula plate of the fly.** *Verh*



## References

*Dtsch Zool Ges.* 1981, 74: 49-70.

Hausen, K. **Motion sensitive interneurons in the optomotor system of the fly. I. The horizontal cells: Structure and signals.** *Biol Cybern.* 1982, 45: 143-156.

Hausen, K. **The lobula-complex of the fly: Structure, function and significance in visual behaviour.** In *Photoreception and vision in invertebrates*. Ali, MA. New York, London: Plenum Press; 1984: 523-559.

Hausen, K and Wehrhahn, C. **Microsurgical lesion of horizontal cells changes optomotor yaw response in the blowfly *Calliphora erythrocephala*.** *Proc R Soc Lond B.* 1983, 219: 211-216.

Hausen, K and Wehrhahn, C. **Neural circuits mediating visual flight control in flies. II. Separation of two control systems by microsurgical brain lesions.** *J Neurosci.* 1990, 10: 351-360.

Hausen, K, Wolburg-Buchholz, K, and Ribi, WA. **The synaptic organization of visual interneurons in the lobula complex of flies.** *Cell Tissue Res.* 1980, 208: 371-387.

He, S and Masland, RH. **Retinal direction selectivity after targeted laser ablation of starburst amacrine cells.** *Nature.* 1997, 389: 378-383.

Heisenberg, M and Buchner, E. **The role of retinula cell types in visual behavior of *Drosophila melanogaster*.** *J Comp Physiol.* 1977, 117: 127-162.

Heisenberg, M, Wonneberger, R, and Wolf, R. **Optomotor-blind (H31)-a *Drosophila* mutant of the lobula plate giant neurons.** *J Comp Physiol.* 1978, 124: 287-296.

Hengstenberg, R. **Spike response of "non-spiking" visual interneurone.** *Nature.* 1977, 270: 338-340.

Hengstenberg, R. **Common visual response properties of giant vertical cells in the lobula plate of the blowfly *Calliphora*.** *J Comp Physiol A.* 1982, 149: 179-193.

Hengstenberg, R. **Roll-stabilization during flight of the blowfly's head and body mechanical and visual cues.** In *Localization and orientation in biology and engineering*. Varjú, D. and Schnitzler, H. Berlin, Heidelberg: Springer-Verlag; 1984: 121-134.

Hengstenberg, R, Hausen, K, and Hengstenberg, B. **The number and structure of giant vertical cells (VS) in the lobula plate of the blowfly *Calliphora erythrocephala*.** *J Comp Physiol A.* 1982, 149: 163-177.

Hengstenberg, R, Sandeman, DC, and Hengstenberg, B. **Compensatory head roll in the blowfly *Calliphora* during flight.** *Proc R Soc Lond B.* 1986, 227: 455-482.

Hidaka, S, Akahori, Y, and Kurosawa, Y. **Dendro-dendritic electrical synapses between mammalian retinal ganglion cells.** *J Neurosci.* 2004, 24: 10553-10567.

Horstmann, W, Egelhaaf, M, and Warzecha, AK. **Synaptic interaction increase optic flow specificity.** *Eur J Neurosci.* 2000, 12: 2157-2165.

Jacobs, GA and Miller, JP. **Functional properties of individual neuronal branches isolated in situ by laser photoinactivation.** *Science.* 1985, 228: 344-346.

Järvilehto, M and Zettler, F. **Electrophysiological-histological studies on some functional properties of visual cells and second order neurons of an insect retina.** *Z Zellforsch.* 1973, 136:



## References

291-306.

Karmeier, K, Krapp, HG, and Egelhaaf, M. **Robustness of the tuning of fly visual interneurons to rotatory optic flow.** *J Neurophysiol.* 2003, 90: 1626-1634.

Kern, R, Petereit, C, and Egelhaaf, M. **Neural processing of naturalistic optic flow.** *J Neurosci.* 2001, 21: RC139

Kimmerle, B and Egelhaaf, M. **Detection of object motion by a fly neuron during simulated flight.** *J Comp Physiol A.* 2000a, 186: 21-31.

Kimmerle, B and Egelhaaf, M. **Performance of fly visual interneurons during object fixation.** *J Neurosci.* 2000b, 20: 6256-6266.

Kirschfeld, K. **Die Projektion der Optischen Umwelt auf das Raster der Rhabdomere im Komplexauge von Musca.** *Exp Brain Res.* 1967, 3: 248-270.

Koenderink, JJ. **Optic flow.** *Vision Res.* 1986, 26: 161-180.

Kolb, H and Jones, J. **Electron microscopy of Golgi-impregnated photoreceptors reveals connections between red and green cones in the turtle retina.** *J Neurophysiol.* 1985, 54: 304-317.

Krapp, HG, Hengstenberg, B, and Hengstenberg, R. **Dendritic structure and receptive-field organization of optic flow processing interneurons in the fly.** *J Neurophysiol.* 1998, 79: 1902-1917.

Krapp, HG and Hengstenberg, R. **Estimation of self-motion by optic flow processing in single visual interneurons.** *Nature.* 1996, 384: 463-466.

Krapp, HG, Hengstenberg, R, and Egelhaaf, M. **Binocular contributions to optic flow processing in the fly visual system.** *J Neurophysiol.* 2001, 85: 724-734.

Kurtz, R, Warzecha, AK, and Egelhaaf, M. **Transfer of visual motion information via graded synapses operates linearly in the natural activity range.** *J Neurosci.* 2001, 21: 6957-6966.

Lamb, TD and Simon, EJ. **The relation between intercellular coupling and electrical noise in turtle photoreceptors.** *J Physiol.* 1976, 263: 257-286.

Land, MF. **Visual acuity in insects.** *Annu Rev Entomol.* 1997, 42: 147-177.

Land, MF and Eckert, H. **Maps of the acute zones of fly eyes.** *J Comp Physiol A.* 1985, 156: 525-538.

Laughlin, S. **Neural principles in the peripheral visual system.** In *Handbook of sensory physiology VII/6B.* Autrum, H. Berlin, Heidelberg, New York: Springer; 1981: 133-280.

Laughlin, S. **New views from compound eyes.** *Nature.* 1987, 328: 292-293.

Lewen, GD, Bialek, W, and de Ruyter van Steveninck RR. **Neural coding of naturalistic motion stimuli.** *Network.* 2001, 12: 317-329.

Lytton, WW and Kristan, WB. **Localization of a leech inhibitory synapse by photo-ablation of individual dendrites.** *Brain Res.* 1989, 504: 43-48.

Miller, JP and Selverston, A. **Rapid killing of single neurons by irradiation of intracellularly**



## References

**injected dye.** *Science*. 1979, 206: 702-704.

Mizrahi, A and Libersat, F. **Synaptic reorganization induced by selective photoablation of an identified neuron.** *J Neurosci*. 2001, 21: 9280-9290.

Mizutani, A, Chahl, JS, and Srinivasan, MV. **Insect behaviour: Motion camouflage in dragonflies.** *Nature*. 2003, 423: 604-

Oertner, TG, Brotz, TM, and Borst, A. **Mechanisms of dendritic calcium signaling in fly neurons.** *J Neurophysiol*. 2001, 85: 439-447.

Owen, WG. **Chemical and electrical synapses between photoreceptors in the retina of the turtle, *Chelydra serpentina*.** *J of Comp Neurol*. 1985, 240: 423-433.

Ozaita, A, Petit-Jacques, J, Völgyi, B, Ho, CS, Joho, RH, Bloomfield, SA, and Rudy, B. **A unique role for Kv3 voltage-gated potassium channels in starburst amacrine cell signaling in mouse retina.** *J Neurosci*. 2004, 24: 7335-7343.

Panzeri, S and Treves, A. **Analytical estimates of limited sampling biases in different information measures.** *Comp Neural Sys*. 1996, 7: 87-107.

Peichl, L and Wässle, H. **The structural correlate of the receptive field centre of alpha ganglion cells in the cat retina.** *J Physiol*. 1983, 341: 309-324.

Petrowitz, R, Dahmen, H, Egelhaaf, M, and Krapp, HG. **Arrangement of optical axes and spatial resolution in the compound eye of the female blowfly *Calliphora*.** *J Comp Physiol A*. 2000, 168: 737-746.

Poggio, T and Reichardt, W. **Visual control of orientation behaviour in the fly II. Towards the underlying neural interactions.** *Quart Rev Biophys*. 1976, 9: 377-438.

Raviola, E and Gilula, NB. **Gap junctions between photoreceptor cells in the vertebrate retina.** *Proc Natl Acad Sci USA*. 1973, 70: 1677-1681.

Reichardt, W. **Autocorrelation, a principle for the evaluation of sensory information by the central nervous system.** In *Sensory Communication*. Rosenblith, WA. New York, London: The M.I.T. Press and John Wiley & Sons; 1961: 303-317.

Reichardt, W. **Movement perception in insects.** In *Processing of optical data by organisms and machines*. New York: Academic; 1969: 465-493.

Reichardt, W. **Evaluation of optical motion information by movement detectors.** *J Comp Physiol A*. 1987, 161: 533-547.

Reichardt, W and Poggio, T. **Visual control of orientation behaviour in the fly I. A quantitative analysis.** *Quart Rev Biophys*. 1976, 9: 311-375.

Reisenman, C, Haag, J, and Borst, A. **Adaptation of response transients in fly motion vision. I: Experiments.** *Vision Res*. 2003, 43: 1293-1309.

Ribi, WA. **Gap junctions coupling photoreceptor axons in the first optic ganglion of the fly.** *Cell Tissue Res*. 1978, 195: 299-308.

Riehle, A and Franceschini, N. **Motion detection in flies: Parametric control over ON-OFF pathways.** *Exp Brain Res*. 1984, 54: 390-394.



## References

- Roeser, T and Baier, H. **Visuomotor behaviors in larval zebrafish after FP-guided laser ablation of the optic tectum.** *J Neurosci.* 2003, 23: 3726-3734.
- Schuling, FH, Masterbroek, HAK, Bult, R, and Lenting, BPM. **Properties of elementary movement detectors in the fly *Calliphora erythrocephala*.** *J Comp Physiol A.* 1989, 165: 179-192.
- Selverston, AI, Kleindienst, H-U, and Huber, F. **Synaptic connectivity between cricket auditory interneurons as studied by selective photoinactivation.** *J Neurosci.* 1985, 5: 1283-1292.
- Selverston, AI and Miller, JP. **Mechanisms underlying pattern generation in lobster stomatogastric ganglion as determined by selective inactivation of identified neurons. I. Pyloric system.** *J Neurophysiol.* 1980, 44: 1102-1121.
- Seung, HS and Sompolinsky, H. **Simple-models for reading neuronal population codes.** *Proc Natl Acad Sci USA.* 1993, 90: 10749-10753.
- Single, S and Borst, A. **Different mechanisms of calcium entry within different dendritic compartments.** *J Neurophysiol.* 2002, 87: 1616-1624.
- Single, S and Borst, A. **Dendritic integration and its role in computing image velocity.** *Science.* 1998, 281: 1848-1850.
- Single, S, Haag, J, and Borst, A. **Dendritic computation of direction selectivity and gain control in visual interneurons.** *J Neurosci.* 1997, 17: 6023-6030.
- Stettoj, E, Raviola, E, and Dacheux, RF. **Synaptic connections of the narrow-field, bistratified rod amacrine cell (All) in the rabbit retina.** *J Comp Neurol.* 1992, 325: 152-168.
- Strausfeld, NJ **Functional neuroanatomy of the blowfly's visual system.** In *Photoreception and vision in invertebrates.* Ali, MA Plenum Publishing Corporation; 1984: 483-522.
- Strausfeld, NJ and Lee, JK. **Neuronal basis for parallel visual processing in the fly.** *Vis Neurosci.* 1991, 7: 13-33.
- Strong, SP, Koberle, R, de Ruyter van Steveninck, RR, and Bialek, W. **Entropy and information in neural spike trains.** *Am Phys Soc.* 1998, 80: 197-200.
- Tessier-Lavigne, M and Attwell, D. **The effect of photoreceptor coupling and synapse nonlinearity on signal: Noise ratio in early visual processing.** *Proc R Soc Lond B.* 1988, 234: 171-197.
- Treves, A and Panzeri, S. **The upward bias in measures of information derived from limited data samples.** *Neural Computation.* 1995, 7: 399-407.
- Tsukamoto, Y, Masarachia, P, Schein, SJ, and Sterling, P. **Gap junctions between the pedicles of macaque foveal cones.** *Vision Res.* 1992, 32: 1809-1815.
- Vaney, DI. **Many diverse types of retinal neurons show tracer coupling when injected with biocytin or Neurobiotin.** *Neurosci Lett.* 1991, 6: 553-562.
- Warzecha, AK, Borst, A, and Egelhaaf, M. **Photo-ablation of single neurons in the fly visual system reveals neural circuit for the detection of small moving objects.** *Neurosci Lett.* 1992, 141: 119-122.
- Warzecha, AK, Egelhaaf, M, and Borst, A. **Neural circuit tuning fly visual interneurons to motion of small objects. I. Dissection of the circuit by pharmacological and photoinactivation**



## References

**techniques.** *J Neurophysiol.* 1993, 69: 329-339.

Warzecha, A-K, Kurtz, R, and Egelhaaf, M. **Synaptic transfer of dynamic motion information between identified neurons in the visual system of the blowfly.** *Neuroscience.* 2003, 119: 1103-1112.

Yoshida, K, Watanabe, D, Ishikane, H, Tachibana, M, Pastan, I, and Nakanishi, S. **A key role of starburst amacrine cells in originating retinal directional selectivity and optokinetic eye movement.** *Neuron.* 2001, 30: 771-780.



## Thanks & Acknowledgements

---

First thanks to both Axel and Bulle for being supportive and creating a great environment to work in, it has truly been a joy working with you two. Thanks also to the rest of the Borst lab for all their help along the way. In particular to Hermann for all his excellent advice regarding MATLAB and intriguing discussions about flies and their amazing capabilities. I would also like to thank Yong Choe, Dierk Reiff, Katrin Deininger and John Bailey for carefully reading this thesis and making helpful comments. Thanks to Renate Gleich for keeping the flies alive and making sure I had everything I needed.



Illustration by Leif Parsons





## Curriculum Vitae

---

Karl Farrow    February 7<sup>th</sup>, 1975    Toronto, Canada

### Education

---

- Sept 2001 – Mar 2005    Ph.D. Thesis:**  
Max-Planck-Institute of Neurobiology. Martinsried, Germany.  
Department of Systems and Computational Neurobiology.  
Supervised by Alexander Borst, PhD and Jürgen Haag, PhD.  
“Lateral Interactions and Receptive Field Structure of Lobula Plate Tangential Cells in the Blowfly.”
- Sept 1998 – May 2001    M.Sc. Thesis:**  
University of Toronto. Toronto, Canada.  
Department of Physiology and Toronto Western Research Institute.  
Supervised by Dianne M. Broussard, PhD.  
“The Neural Basis of Recovery from Unilateral Vestibular Damage: Role of the Vestibular Commissure.”
- May 2001**  
Completed Program In Neuroscience.  
University of Toronto, Toronto, Canada.
- Sept 1995 – May 1998    B.Sc. Honours:**  
University of Toronto. Toronto, Canada. McGill University. Montreal, Canada.  
Department of Physics and Zoology.  
Specialist in Physics and Biology.  
Focus: Membrane Biophysics and Neurophysiology.

### Awards

---

- 1999**                    Unilever/Upton Graduate Fellowship in Neuroscience.  
**1998**                    Dr. James A. & Connie P Dickson Scholarship In The Sciences and Mathematics.

### Publications (Parts of this thesis have previously been published)

---

Farrow, K., Borst, A. and Haag, J. (2005). **Sharing receptive fields with your neighbours: Tuning the VS-cells to wide field motion.** *J. Neurosci.* 25:3985-3993



Farrow, K., Haag, J. and Borst, A. (2003). **Input organization to multifunctional motion sensitive neurons in the blowfly.** *J. Neurosci.* 23: 9805-9811.

Farrow, K and Broussard, D.M. (2003). **Compensation for peripheral damage changes commissural inputs to interneurons of the vestibulo-ocular reflex.** *J. Neurophysiol.* 89: 3351-3353.

Farrow, K. (2001). **The neural basis of recovery from unilateral vestibular damage: Role of the vestibular commissure.** *Masters Thesis, University of Toronto.*

